NASA-CR-197183

NASw-4435

IN-05 CR
26169

Integrated Design and Manufacturing for the High Speed Civil Transport

Preliminary Design Methodology and Optimization for an HSCT Nacelle/Wing Configuration

ORIGINAL CONTAINS
COLOR ILLUSTRATIONS

Final Report

NASA USRA Advanced Design Program
Aeronautics

School of Aerospace Engieering
Georgia Institute of Technology
Atlanta, GA, June 1994

(NASA-CR-197183) INTEGRATED DESIGN AND MANUFACTURING FOR THE HIGH SPEED CIVIL TRANSPORT Final Report (Georgia Inst. of Tech.) 99 p

N95-12700

Unclas

G3/05 0026169

Abstract

In June 1992, the School of Aerospace Engineering at Georgia Tech was awarded a three year NASA University Space Research Association (USRA) Advanced Design Program (ADP) grant to address issues associated with the Integrated Design and Manufacturing of High Speed Civil Transport (HSCT) configurations in its graduate Aerospace Systems Design courses. This report provides an overview of the on-going Georgia Tech initiative to address these design/manufacturing issues during the preliminary design phases of an HSCT concept. The new design methodology presented here has been incorporated in the graduate aerospace design curriculum and is based on the concept of Integrated Product and Process Development (IPPD). The selection of the HSCT as a pilot project was motivated by its potential global transportation payoffs, its technological, environmental, and economic challenges, and its impact on U.S. global competitiveness. This pilot project was the focus of each of the five design courses that form the graduate level aerospace systems design curriculum. This year's main objective was the development of a systematic approach to preliminary design and optimization and its implementation to an HSCT wing/propulsion configuration. The new methodology, based on the Taguchi Parameter Design Optimization Method (PDOM), was established and was used to carry out a parametric study where various feasible alternative configurations were evaluated. The comparison criterion selected for this evaluation was the economic impact of this aircraft, measured in terms of average yield per Revenue Passenger Mile ($/RPM)[1].

Table of Contents

1.0 Introduction 1
2.0 Georgia Tech's IPPD Methodology 3
2.1 Implementation of IPPD Methodology 6
2.1.1 Establishing the Need 6
2.1.2 Defining the Problem 7
2.1.2.1 HSCT Customer Requirements 7
2.1.2.2 Key Product and Process Characteristics 9
2.1.2.2.1 Aerodynamics and Performance 10
2.1.2.2.2 Propulsion 12
2.1.2.2.3 Structural Analysis & Materials 14
2.1.2.2.4 Advanced Flight Systems and Control 14
2.1.2.2.5 Life Cycle Costs 15
2.1.2.2.6 Manufacturing 16
2.1.2.3 Formation of the Interrelationship Digraph and the N^2 Diagram 24
2.1.2.4 QFD - Product Planning Matrix 26
2.1.2.5 Results of Product Planning Matrix 28
2.1.3 Establishing Value Objectives 29
2.1.3.1 Feasibility Constraints 32
2.1.3.2 Life Cycle Cost Matrix 32
2.1.3.3 Average Yield per Revenue Passenger Mile ($/RPM) 35
2.1.4 Generation of Feasible Alternatives 35
2.1.4.1 Baseline Configuration 35
2.1.4.2 Stability and Control of Baseline Configuration 37
2.1.4.3 Taguchi Parameter Design Optimization Methods (PDOM) 47
2.1.4.4 Aircraft LCC Analysis and Synthesis Simulation Method 50
2.1.4.5 Test of Economic Analysis on the Baseline 51
2.1.4.5.1 Simulation Interpretation 54
2.1.4.5.2 The Experiment 55
2.1.4.5.3 Result Interpretation 57
2.1.4.5.4 Confirmation Test 61
2.1.4.6 Top Level Orthogonal Array 62
2.1.5 Evaluation of Alternatives 62
2.1.5.1 Aerodynamics Orthogonal Array 64
2.1.5.2 Aerodynamics, Structures, and Manufacturing Opt. Wing 68
2.1.5.2.1 Combined Array: Response-model/combined-array Approach to Nacelle-Wing-Fuselage Integration 68
2.1.5.2.2 Limitations of Taguchi Method 69
2.1.5.2.3 Limitations of Two-Part Experimentation Strategy 69
2.1.5.2.4 Limitations of the Loss-Model Approach 70
2.1.5.2.5 The Use of Response-Model/Combined-Array Approach 71
2.1.5.2.6 Implementation Procedure of the Combined Array Experiment for the Nacelle-Wing-Fuselage Integration ... 72
2.1.5.3 Manufacturing Implementation 76
2.1.5.4 Synthesis/ Propulsion/ Economic Analysis 78
2.1.6 Making a Decision 81
3.0 Conclusion - Future Work 83
4.0 Appendix A 85
5.0 References 88

List of Figures

Figure 1 Georgia Tech's Team Activity Network Diagram 3
Figure 2 Integrated Product and Process Development Approach 4
Figure 3 Interaction of the Four Key Elements in Concurrent Engineering 5
Figure 4 Affinity Diagram: Voice of the Customer 7
Figure 5 Customer Requirements 9
Figure 6 Key Product and Process Characteristics 10
Figure 7 CATIA Model of the Mixed Flow TurboFan 13
Figure 8 CATIA Model of a Turbine Bypass Engine 13
Figure 9 Description of Superplastic Forming Process 20
Figure 10 Powder Metallurgy Process 22
Figure 11 Interrelationship Digraph of the Key Product and Process Characteristics 25
Figure 12 NxN Diagram for Key Product and Process Characteristics 26
Figure 13 QFD Matrix Relating the Key Product and Process Characteristics to the Customer Requirements 27
Figure 14 Prioritization Matrix Showing the Influence of the Key Product and Process Characteristics on Each Other 28
Figure 15 Return on Investment Criteria 29
Figure 16 Interrelationship Digraph of the ROI Criteria 30
Figure 17 QFD Matrix Relating the ROI Criteria to the Key Product and Process Characteristics 31
Figure 18 When LCC are Rendered Unchangeable Versus When LCC are Actually Expended for a Given Design 33
Figure 19 The QFD Matrix Relating the ROI to the Cost Drivers 34
Figure 20 Baseline Mission Profile 36
Figure 21 Georgia Tech's HSCT Double-Delta Baseline Configuration 36
Figure 22 APAS HSCT Baseline Configuration 38
Figure 23 Case 1 - C_m @ Mach = 0.95 39
Figure 24 Case 1 - C_m @ Mach = 2.4 40
Figure 25 Case 1 - $C_{m\alpha}$ @ Mach = 2.4 & 0.95 40
Figure 26 Case 2 - C_m @ Mach = 0.95 41
Figure 27 Case 2 - C_m @ Mach = 2.4 41
Figure 28 Case 2 - $C_{m\alpha}$ @ Mach = 2.4 & 0.95 42
Figure 29 Case 1 - C_n @ Mach = 0.95 43
Figure 30 Case 1 - C_n @ Mach = 2.4 43
Figure 31 Case 2 - C_n @ Mach = 0.95 44
Figure 32 Case 2 - C_n @ Mach = 2.4 44
Figure 33 Case 1 - C_l @ Mach = 0.95 45
Figure 34 Case 1 - C_l @ Mach = 2.4 46
Figure 35 Case 2 - C_l @ Mach = 0.95 46
Figure 36 Case 2 - C_l @ Mach = 2.4 47
Figure 37 HSCT Economic Sensitivity Assessment Methodology 48
Figure 38 The Taguchi Method Flow Chart 49
Figure 39 ALCCA Flowchart 51
Figure 40 Complexity Factors 53
Figure 41 $/RPM Variations for All Experiments Performed Including the "Optimum" Distribution 58
Figure 42 Control Factor Influences on Average Yield / Revenue Passenger Mile ($/RPM) 59
Figure 43 Aircraft Acquisition Price Variation for the "Optimum" and "Worst" Conditions 60
Figure 44 Average Ticket Price Variation for the "Optimum" and "Worst" Conditions 60
Figure 45 $/RPM Variation for the "Optimum" and "Worst" Conditions 61

List of Figures (Cont.)

Figure 46 Feasible Alternative Evaluation Flowchart 63
Figure 47 Wing Optimization Procedure 64
Figure 48 Wing Planform Configuration 65
Figure 49 Control Factor Influences on the L/D Ratio for a Supersonic Mission 67
Figure 50 Two-Part Experimentation Strategy for Robust Design 70
Figure 51 Combined Orthogonal Array 73
Figure 52 Wing Manufacturing Consideration, Three Point Design 75
Figure 53 Significant Control Factor Influences on the System OEC, $/RPM 80
Figure 54 $/RPM Variations for the First Feasible Configuration of the Top Level Orthogonal Array Including the "Optimum" Distribution 80
Figure 55 Concept Evaluation Experimental Schematic 82

List of Tables

Table I	SPD/DB Cost Reduction Potential	21
Table II	Process Manufacturing Requirements and Costs	23
Table III	Suitability of Manufacturing Processes to Alternative Manufacturing Forms	24
Table IV	Return on Investment for Airlines and Manufacturers	33
Table V	Baseline Configuration Descriptions	37
Table VI	Economic Sensitivity Analysis Ground Rules and Assumptions	52
Table VII	Control Factors as They Relate to the ALCCA Program	54
Table VIII	Noise Factors as They Relate to the ALCCA Program	54
Table IX	The Complete Orthogonal Array for the Design of Experiments	56
Table X	The *Optimal* Configuration for the "Smaller the Better" Quality Characteristic Case	58
Table XI	Change in Average Yield per RPM from the "Optimum" Condition	61
Table XII	The "Optimum" Condition Confirmation Results	61
Table XIII	Top-Level Decision OA	62
Table XIV	Aerodynamic Experiment Control Factors	66
Table XV	Aerodynamic Experiment Noise Factors	66
Table XVI	Optimal Aerodynamic Control Factor Levels	67
Table XVII	Structure/Aerodynamics/Material/Manufacturing Combined Control and Noise Factors	73
Table XVIII	Material Selection	75
Table XIX	Manufacturing Full Factorial Experiment	77
Table XX	Propulsion/Sizing/Economic Experiment Control Factors	78
Table XXI	Propulsion/Sizing/Economic Experiment Noise Factors	79
Table XXII	"Optimal" Control Factor Settings	79

Forward

This report documents work completed during the second year for the NASA University Space Research Association (USRA) Advanced Design Program (ADP) in Aeronautics at the Georgia Institute of Technology. Professor Daniel Schrage, Professor James Craig, and Dr. Dimitri Mavris were the coordinators of this project. Various members of the Aerospace Systems Design Laboratory (ASDL) at Georgia tech provided helpful suggestions, especially Mark Hale, Peter Rohl, Bill Marx, and Dan DeLaurentis. Jason Brewer and Craig Mueller were the team leaders. The design team consisted of the following members and their corresponding areas of expertise and computational tools in parentheses used where appropriate:

Aerodynamics (BDAP)	Jae Moon Lee, Anurag Gupta
Structures (ASTROS)	Craig Mueller , Monica Morrisette
Materials	Monica Morrisette
Stability & Control (APAS)	John Dec
Propulsion (QNEP/FLOPS)	Jason Brewer, Kevin Donofrio
Manufacturing (MTT)	Hilton Sturisky and Doug Smick
Synthesis/Sizing (FLOPS)	Craig Mueller, Jason Brewer
Geometry (CADAM/CATIA)	Kevin Donofrio, Meng Lin An
Robust Design Optimization (Taguchi/MDO/QT4)	Jason Brewer, Wei Chen, Meng Lin An
Life Cycle Cost (ALCCA)	Jason Brewer

COPYRIGHT © 1994 GEORGIA INSTITUTE OF TECHNOLOGY,
SCHOOL OF AEROSPACE ENGINEERING

PERMISSION TO REPRODUCE THIS DOCUMENT OR ANY PART OF ITS CONTENTS MUST BE ACQUIRED FROM:

PROFESSOR DANIEL P. SCHRAGE
SCHOOL OF AEROSPACE ENGINEERING
GEORGIA INSTITUTE OF TECHNOLOGY
ATLANTA, GEORGIA 30332-0150

1.0 Introduction

Under the University Space Research Association (USRA) Advanced Design Program (ADP), the School of Aerospace Engineering at Georgia Tech has undertaken the initiative of integrating aircraft design and manufacturing, and incorporating it in their design curriculum at the graduate level. The faculty at Georgia Tech have felt that in order to carry out this objective, a highly focused program was needed. NASA's High Speed Research (HSR) program provided one such opportunity. Under this program, NASA and this country's aerospace industry have undertaken the challenge of developing the technology by the turn of the century which will allow the launch of a High Speed Civil Transport (HSCT) aircraft capable of cruising at a Mach number of 2.0 or greater and carrying 300 passengers to destinations in excess of 5,000 nautical miles.

A HSCT is being designed as a commercial supersonic transport vehicle that will be used in portions of the international market. This HSCT must not only be environmentally friendly (e.g. abide by FAR Stage III noise regulations, reduce or eliminate sonic boom over land associated with supersonic flight, and reduce NO_x emissions that are harmful to the ozone layer), but it must also be economically competitive with current and projected long range subsonic fleet (i.e. Boeing 747-400). Market surveys have indicated that a significant increase in ticket price will have an adverse effect on passenger demand; however, there have been indications that most passengers would be willing to pay a premium for supersonic flight (up to 30% more than subsonic transport ticket fares). A ticket price above this level will most likely reduce the total market demand to a point where airlines and aircraft manufacturers might not be willing to make a commitment to buy or to undertake the aircraft production[2]. Therefore, in order to ensure the production of a HSCT, it is essential to maintain an affordable ticket fare for the passenger, while retaining a reasonable Return on Investment (ROI) for both the airline and the airframe/engine manufacturers.

This initiative is full of technological challenges affecting each and every one of the various disciplines involved (Aerodynamics, Structures, Propulsion, Manufacturing, etc.). It is because of these challenges, as well as the overall relevance and importance of this project to our industry and nation, that this aircraft was chosen to be the focus of this investigation.

A number of graduate and senior elective courses were used to introduce the students to appropriate design and manufacturing methods. The School of Aerospace Engineering has a strong educational program in design, consisting of five graduate level courses (Concurrent Engineering, Introduction to Life Cycle Cost, Introduction to Computer Aided Design, and Aerospace Systems Design I & II)[3], that have been

continuously improved and influenced by advances made on the research side of the program. An Aerospace Systems Design Laboratory (ASDL) has been developed to support this program.

During the first year of this three year program, the overall design methodology was developed and tested (paper and report presented in USRA's 1993 ADP Summer Conference[4]). In this second year, the methodology has been applied to two of the most critical components of the aircraft - the propulsion system and the wing. This year's graduate student team identified the customer requirements and the key product and process characteristics, generated a baseline configuration, and proceeded with the implementation of Georgia Tech's preliminary design methodology.

Once the baseline was established, the team was divided into multidisciplinary groups that performed a Nacelle-Wing-Fuselage integration analysis, addressing issues related to aerodynamics, structures, and manufacturing of the wing, as well as a propulsion system down selection study. The results of all these studies were then incorporated back into a system synthesis code (FLight OPtimization System (FLOPS))[5] in order to modify the baseline configuration and generate a new "optimum" configuration. This "optimum" configuration had to be able to satisfy all design requirements and constraints and was used to assess the economic affordability of this aircraft. Furthermore, a robust design assessment of the configuration provided some indication of the risk associated with the various assumptions and decisions made throughout the design process. This analysis was based on a risk analysis/control/reduction technique called the Taguchi Parameter Design Optimization Method (PDOM). While the Taguchi PDOM has been utilized for robust design of parts, components, and some systems, it is believed that its use in this exercise is unique and offers considerable promise for Integrated Product and Process Development (IPPD). The tasks performed by the team can best be presented by an activity network diagram, one of the Seven Management and Planning Tools that will be discussed later. It is presented in Figure 1 and illustrates the sequence of events that took place over this nine month period.

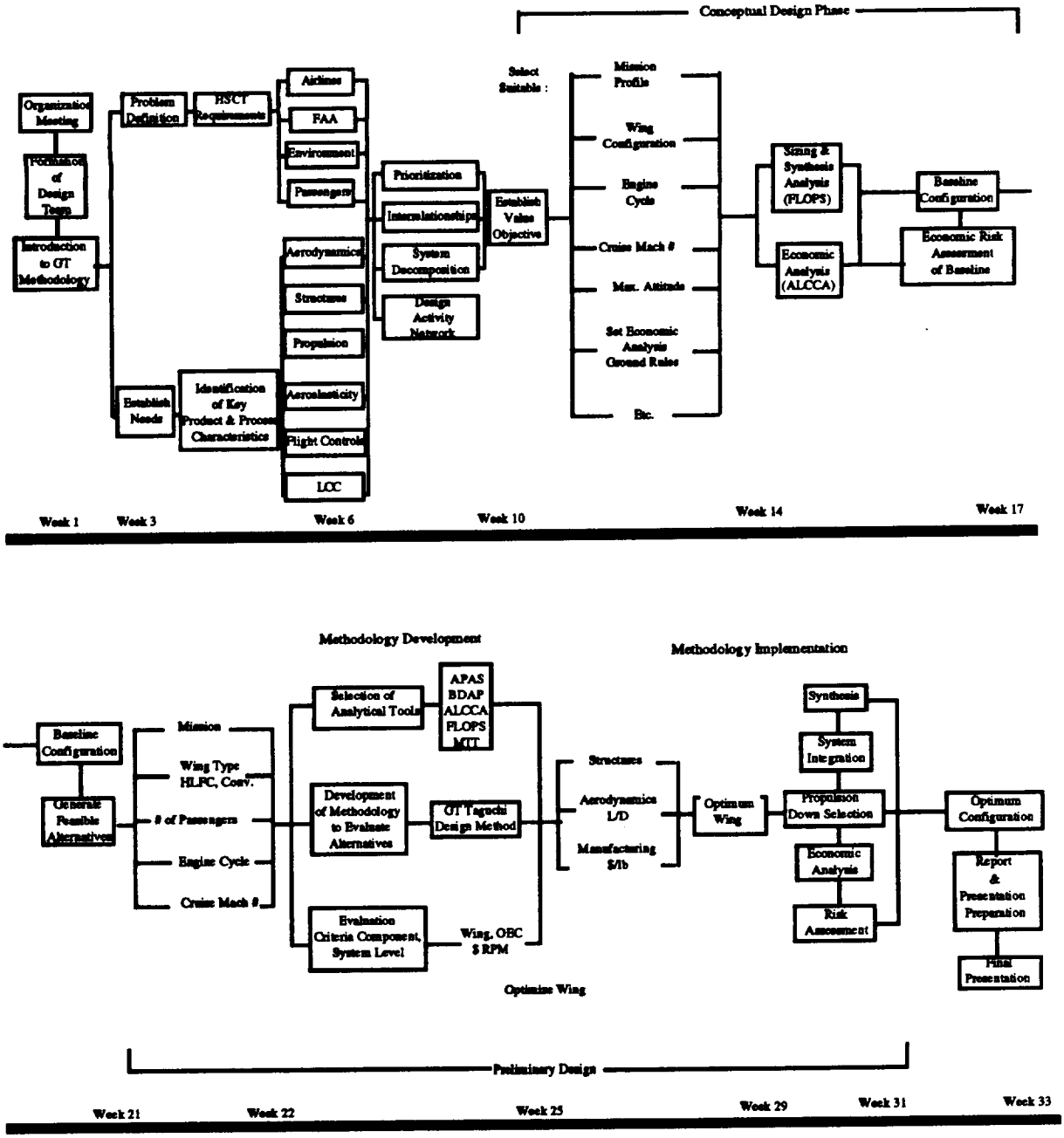

Figure 1 : Georgia Tech's Team Activity Network Diagram

2.0 Georgia Tech's IPPD Methodology

The design curriculum at Georgia Tech follows closely an Integrated Product and Process Development or Concurrent Engineering (CE) approach. Since most of the students entering the design course sequence are unaware of what Concurrent Engineering is, an entire course dedicated to the methodology and tools behind it is offered to provide them with all the necessary team building and brainstorming skills that were used throughout this investigation.

Concurrent Engineering is commonly defined as the "systematic approach to the integrated, concurrent design of products and their related processes[6]". This method provided a means for the team to brainstorm up front and understand the customer requirements. Furthermore, CE provides the tools needed to integrate manufacturing and operation support into product design, and it allows the designers to confront potential problems in the early design stages when the system is still flexible enough to be altered. This approach increases the initial effort and time needed for the early design stages, but produces significant cost and time savings in downstream activities and leads to a more efficient and effective design.

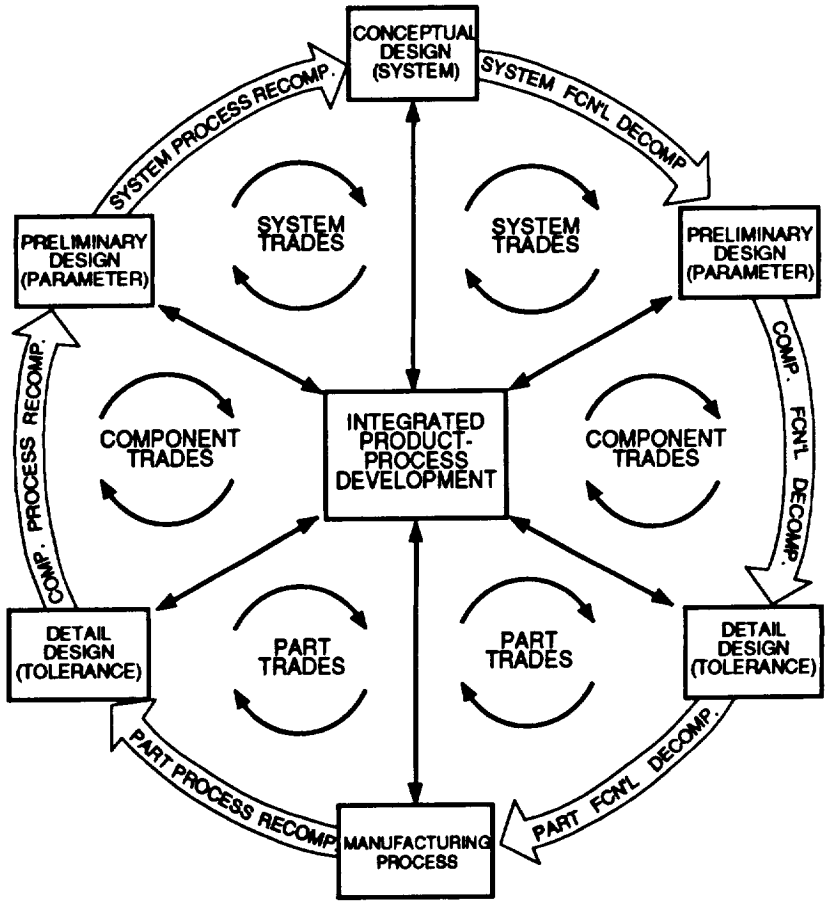

Figure 2: Integrated Product and Process Development Approach

The methodology currently used in the graduate design program is illustrated in Figures 2 and 3. The flow diagram for IPPD, presented in Fig. 2, illustrates the hierarchical decomposition activities from the conceptual design phase (system level), to preliminary design (major component/sub-system), to detailed design (part/sub-component level), and to manufacturing. The inner small loops on the right half represent the product design trade iterations. The left half shows the process recomposition activities, and the

inner loops represent the process design trades. The long outer loop iteration represents what has usually been done in the past when redesign was often required due to product design incompatibilities with manufacturing processes. What is desired with IPPD is the ability to make parallel product-process design trades at the system level, as well as the component and part level.

While Fig. 2 represents the flow process desired for IPPD, it does not provide the methodology required to implement IPPD and make the parallel product-process design trades. The methodology being developed and utilized at Georgia Tech is illustrated in Fig. 3. Industry has confirmed that, in a generic manner, this approach is very similar to the IPPD methodologies they are also trying to develop and implement.

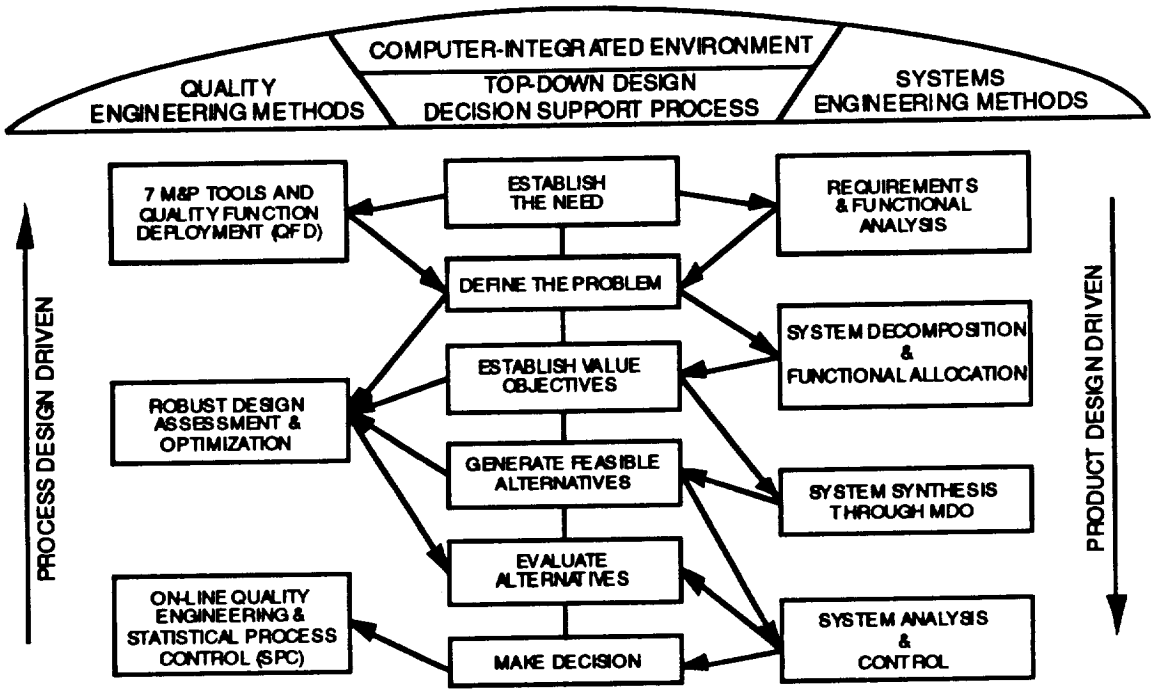

Figure 3: Interaction of the Four Key Elements in Concurrent Engineering

This methodology provides the desired systematic approach to the integrated, concurrent design of products and their related processes, including manufacturing and support. Figure 3 illustrates the interaction of the four key elements necessary for parallel product and process trades to be made at the appropriate level of system decomposition and recomposition. Depicted is an "umbrella" with the four key elements: systems engineering methods, quality engineering methods, top down design decision support process, and computer integrated environment. The interaction among these elements to make parallel product and process design trades is shown below the "umbrella". The top down design decision support process usually starts by establishing the need and proceeds by defining

the problem, establishing the value objectives, generating feasible alternatives, evaluating these alternatives, and reaching a final decision. Quality engineering methods include the use of Quality Function Deployment, Taguchi methods, and Statistical Process Control. Systems engineering methods include system decomposition, functional allocation, and system synthesis. Finally, the computer-aided environment provides a means of integrating these processes together. The methodology takes advantages of methods and tools, such as the Seven Management and Planning Tools, requirement and functional analysis, decomposition, etc. for both product and process. System synthesis is achieved through the use of Multidisciplinary Design Optimization (MDO) and robustness of design methods to evaluate the generated feasible alternatives. This way, the best alternative based on the criteria established from the value objectives is made.

2.1 Implementation of IPPD Methodology

2.1.1 Establishing the Need

The introduction of a HSCT in the long range, transcontinental air travel market is becoming increasingly more appealing to the aerospace industry as market forecasts project that world air travel will almost double by the year 2000. A need for an aircraft that could provide passengers with a significantly reduced travel time (approximately 45%) to destinations in the 5,000 - 6,500 nmi range appears to exist, provided that a fare competitive with subsonic aircraft can be achieved. This range covers the long routes of the international market including the Pacific rim where most of the travel demand increases are expected. In order for such a concept to be economically competitive with current long range subsonic aircraft similar in size to the Boeing 747-400, it is imperative that the turn-around time on the ground must be reduced so as to complete two round trips daily[2]. Therefore, only cruise speeds between Mach 2.0 and 2.6 are currently being considered, since speeds greater than Mach 2.6 would require special fuels. In addition, this HSCT will have to be able to carry 280-320 passengers in order to reduce the average yield per Revenue Passenger Mile, $/RPM. The $/RPM is a metric that captures the Return on Investment (ROI) concerns of both the airline and the manufacturer and can be easily translated to ticket price fares once the occupancy load factors are known. Finally, the aircraft must be compatible with current airports (i.e. take-off and landing field length distances, terminals, etc.).

2.1.2 Defining the Problem

Concurrent engineering techniques are implemented at this point in order to better understand the challenges faced by a HSCT. This task is achieved through the use of a series of Quality Function Deployment (QFD) matrices. Construction of a QFD matrix is accomplished using such methods as the Seven Management and Planning Tools and a functional analysis method, the N^2 diagram, which is incorporated to better organize the requirements of the different system products and their related processes. The Georgia Tech IPPD methodology employs these tools to generate a product planning matrix, establish a value objectives matrix, and identify all feasibility constraints. These Seven Management and Planning Tools include such brainstorming tools as the affinity and tree diagrams, the interrelationship digraph, and the prioritization and relationship matrices. Once a product planning matrix is developed, the remaining tools, the activity network diagram and the process decision program chart are used to layout the implementation and deployment of the product planning matrix. The affinity and tree diagrams were used extensively by the HSCT team as brainstorming techniques to identify the customer requirements and the key product and process characteristics.

2.1.2.1 HSCT Customer Requirements

A QFD approach was used to relate the customer's requirements to the key product and process characteristics. The customer requirements are established through the use of an affinity diagram by compiling a list of possible customers and attempting to define their requirements and concerns for a HSCT as seen in Figure 4. These customers included the airlines, passengers, environmental groups/agencies, and the Federal Aviation Administration (FAA).

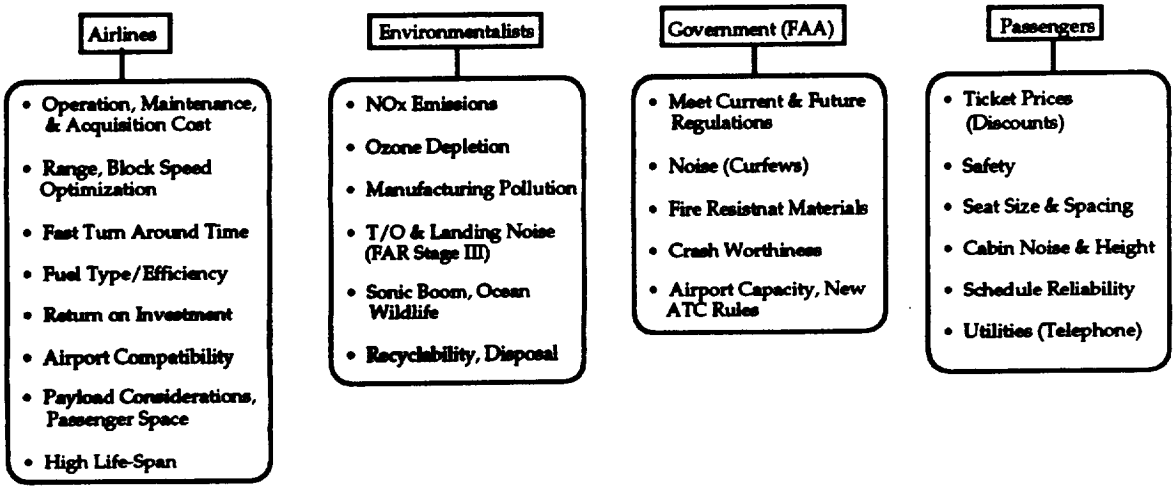

Figure 4: Affinity Diagram: Voice of the Customer

Affordability related issues pose the biggest challenge for a HSCT concept. The airlines, the HSCT's primary customer, facing serious financial problems, will be very reluctant to purchase such a vehicle if the potential for a high return on investment is not feasible. This means that the acquisition and total operating costs must be kept low, and the generated revenues must be as high as possible while maintaining low ticket fares. In order to generate significant revenues, a HSCT will need to capture a major portion of the overseas market. This can be done by reducing time on long range flights by 45% and keeping fares competitive with subsonic transports similar in size to the 747-400. The aircraft must be compatible with existing airports, have a quick turn-around time, use conventional fuels, and keep maintenance costs low.

As mentioned previously, the passenger expects fares which are comparable to subsonic transport fares. The passenger also requires a level of comfort while flying, including aspects such as low cabin noise, comfortable seating, suitable temperature, and smooth flying. Because a HSCT will be most appealing to business flyers, the aircraft must have a reliable schedule, which implies that it must have a high dispatch reliability and be easy to maintain and quick to service in case of any unexpected occurrences.

Meeting the environmental constraints imposed on a HSCT is yet another major concern. The environmental agencies require that the propulsion system for a HSCT must have reduced NO_X emissions to minimize its impact on the earth's ozone layer. These stringent requirements will definitely lead to higher development costs but must be met before a HSCT can be considered as a viable aircraft. The Federal Aviation Administration (FAA) requires that the aircraft's take-off and landing noise abide to FAR 36 Stage III requirements, the same requirements for subsonic transports. Further, if allowed to fly supersonically over land, there can be no discernible sonic boom over populated areas.

In addition to meeting the environmental constraints, a HSCT must be able to meet all current and future Federal Aviation Regulations (FAR). It must also be able to meet local airport regulations and anticipated changes in the infrastructure of the Air Traffic Control (ATC) system caused by a HSCT.

Through a series of brainstorming sessions, the design team produced a rather long list of customer requirements. This list was then narrowed down to the most important issues, as is illustrated by the tree diagram depicted in Figure 5.

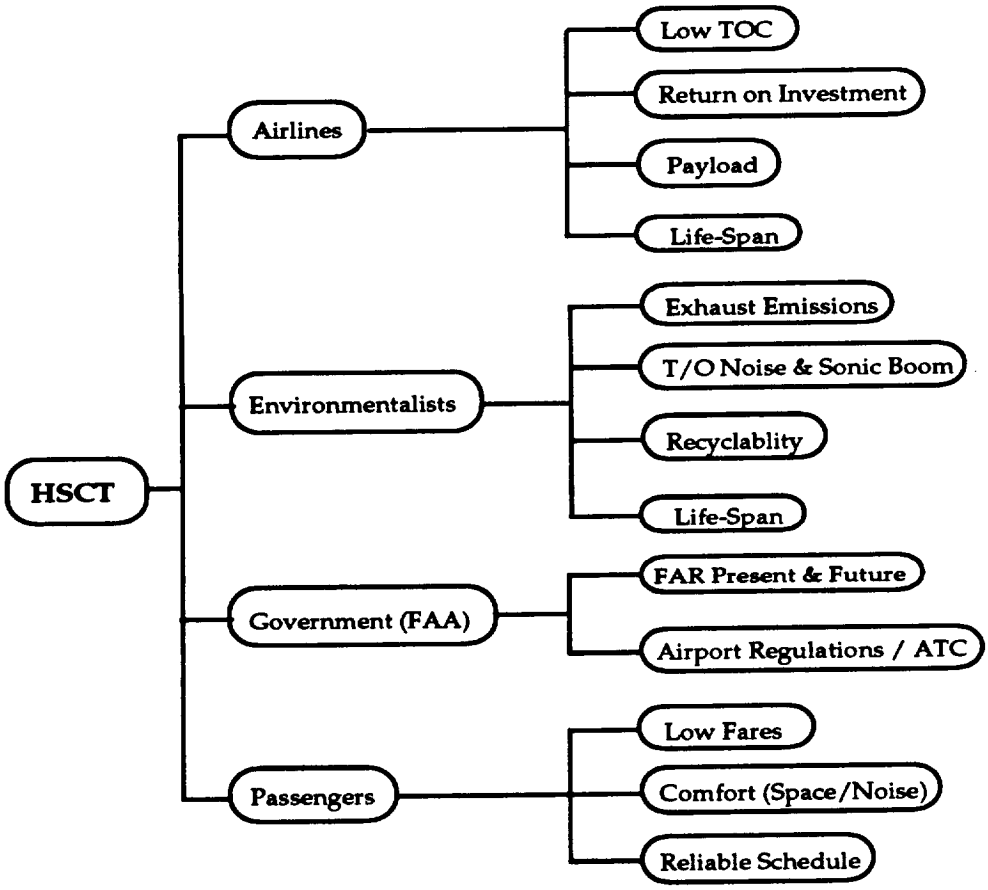

Figure 5: Customer Requirements

2.1.2.2 Key Product and Process Characteristics

Once the customer's needs are established, it is important to identify the technology which is necessary to meet these requirements. These requirements were grouped under five main categories. The disciplines selected included structures, aerodynamics and performance, propulsion, controls, and life cycle cost. Key product and process characteristics associated with each of these disciplines were subsequently identified. The tree diagram presented in Figure 6 illustrates the key product and process characteristics selected by the team.

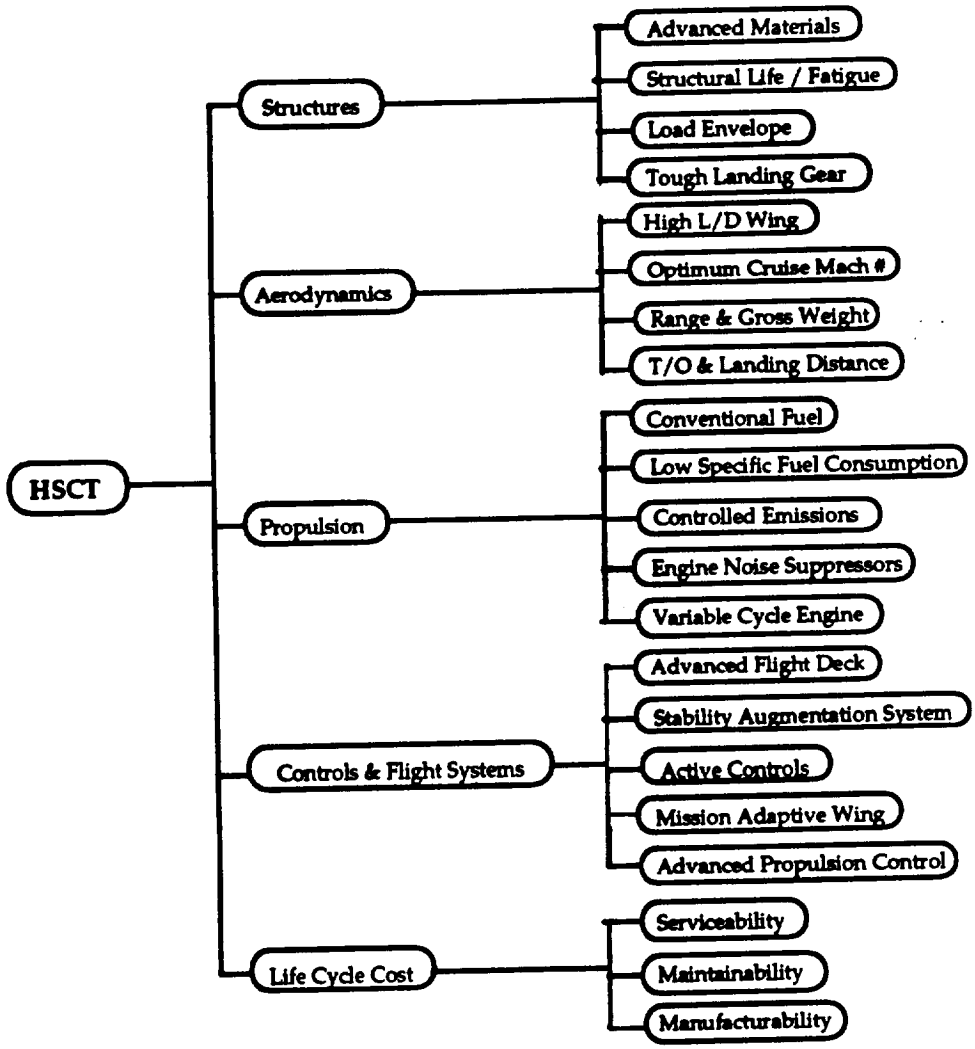

Figure 6: Key Product and Process Characteristics

2.1.2.2.1 Aerodynamics and Performance

Even under a concurrent engineering approach, aerodynamics is a very significant in the design of an aircraft. Aerodynamics establishes the requirements for structures, propulsion, and stability and control in addition to determining the performance characteristics of the aircraft.

The aerodynamic efficiency at supersonic cruise speeds is a critical factor in evaluating the performance of a HSCT. A highly swept arrow-head wing would produce the highest supersonic cruise L/D. However, a commercial supersonic transport (SST) has to operate efficiently at subsonic speeds (over-land cruise) and meet FAR noise requirements during take-off and landing. The need for high lift at low speeds to meet these requirements drives a HSCT configuration towards a moderately swept, "thick" wing. As a compromise, current research and development activity has focused on double-

delta or arrow-wing planform based wings for a HSCT. In combination with Hybrid Laminar Flow Control (HLFC), a promising technology which uses suction in conjunction with supercritical airfoils to laminarize flow over a significant portion of the wing, the wing could attain the necessary optimum (or near-optimum) cruise aerodynamic efficiencies while meeting the take-off and landing field length as well as the noise requirements. HLFC studies over subsonic commercial aircraft have shown the capability to substantially reduce the skin friction drag as well as the nacelle drag. Due to this phenomena, considerable research is currently being conducted in HLFC for a HSCT.

Another crucial factor in the aerodynamic design of a HSCT will be the integration of the engine nacelles with the wing. The nacelle pressure field interacts closely with the pressure fields over the wing and fuselage. This interaction gives rise to lift and drag interference effects that influence the lifting surface aerodynamic characteristics greatly. Any wing design optimization will have to address nacelle-wing integration.

Development of high lift technology and devices could enhance a HSCT's capability to meet runway length and take-off noise requirements. It could also enable the aircraft to reach cruise altitude faster, thus increasing the average cruise Mach number. High lift technology would also affect the take-off thrust requirements. Appropriate wing/fuselage design could reduce the sonic boom and provide comfortable cabin size without a large drag or speed penalty. Optimized propulsion-airframe integration could not only reduce drag but also accommodate stability issues during engine out conditions. The above technologies coupled with a balanced aerodynamic design for high/low speed performance will enable viable HSCT designs to meet or improve upon the set standards for required thrust, fuel efficiency, and range.

The structural, aeroelastic, and fuel volume requirements will set the design constraints on the wing size. Since an IPPD design methodology is being used, structural analysis and manufacturing will influence the choice of materials, processes, and hence the structural design of the aircraft. Therefore, in order to include the effects of manufacturing, the wing will be optimized concurrently from an aerodynamics, structures, and manufacturing point of view using a Multi-Disciplinary Optimization approach.

Under stability and control, active control technology can provide the means of reducing drag through Reduced Static Stability (RSS) and improving handling qualities and stability through the use of a Stability Augmentation System (SAS). Mission adaptive wing could optimize the wing profile through different stages of the mission. Envelope limiting, flutter suppression, and load limiting capabilities will increase safety as well as minimize the structural degradation. Furthermore, the handling qualities of the aircraft have to be such that the aircraft could be operated by a two man crew and provides an acceptable ride quality for the passengers.

The ability to meet performance requirements such as range, block time, speed, handling qualities, and airport compatibility are all dependent on the wing sizing and its integration. Thus, extensive effort has to be put into this process, especially since this is being done up front in the design process. However, the nacelle-wing integration will also set the costs, feasibility, and standards for the latter stages.

2.1.2.2.2 Propulsion

It was obvious throughout the design analysis that the propulsion system selected for a HSCT will have a major effect on the overall economic and technological viability of the aircraft. During the decomposition of this component into key product and process characteristics, several key issues had to be considered. The first issue considered was the emissions control. Emissions control is a major concern of designer due to its relation to the possible depletion of the Ozone layer. Furthermore, a HSCT will have to meet the FAR 36 Stage III noise requirements and reduce its noise footprint around the airport cites. Another question relates to the sonic boom effects when flying over populated areas and whether or not a HSCT will be allowed to fly supersonically over land. This is an issue that has yet to be resolved.

Another critical propulsion system factor is the Specific Fuel Consumption (SFC), as a supersonic aircraft requires a much larger percentage of fuel than a subsonic aircraft. Primarily, acceptable SFC levels must be achieved for not only supersonic cruise speeds, but also subsonic ones which will be necessary for overland operations (this will also determine the fuel cost which will effect the direct operating cost). In the team's final design, two separate mission profiles were flown and analyzed. The first mission profile included a 25% subsonic cruise segment and an 75% supersonic cruise segment, while the second profile consisted of an all supersonic mission (this of course does not include warm-up, taxi, takeoff, ascent, descent, and loiter). These two profiles will influence the analyses of the type of engine that will be adequate for the desired mission.

The engine type is considered as a crucial factor in analyzing the aircraft's viability. The noise of such an engine, its efficiency, and its durability are all considerations which require preliminary analysis (boosted both by environmentalist and the FAR). These factors along with the ones mentioned previously will ultimately be subject to the economic affordability of such an engine. The three types of engines under consideration for a HSCT design are a Mixed Flow Turbo-Fan (MFTF), a Turbine Bypass Engine (TBE), and a Fan in bLADE (FLADE). Only the first two engine types were examined and analyzed this year. Each of these engines have unique characteristics that are advantageous to the mission profiles under consideration. The TBE's major advantages are its capability to

generate a high specific thrust along with maintaining better performance characteristics during subsonic cruise segments. The major disadvantage of the TBE is that it tends to be more of a risk to produce if a mixer ejector nozzle with adequate jet noise suppression cannot be developed. The advantages of the MFTF include exhibiting a lower takeoff gross weight of a HSCT, a quieter engine, low jet velocities, and low SFC levels due to its bypass ratio. However, the MFTF is a larger engine in size and could be difficult to minimize the interference drag[7]. Figures 7 and 8 depict both the MFTF and the TBE, respectively.

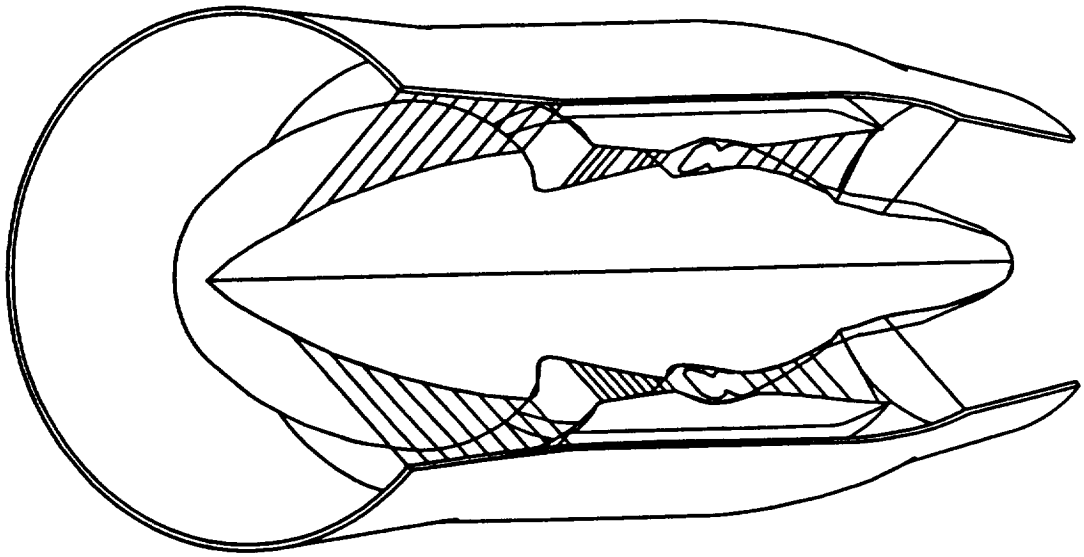

Figure 7: CATIA Model of the Mixed Flow TurboFan

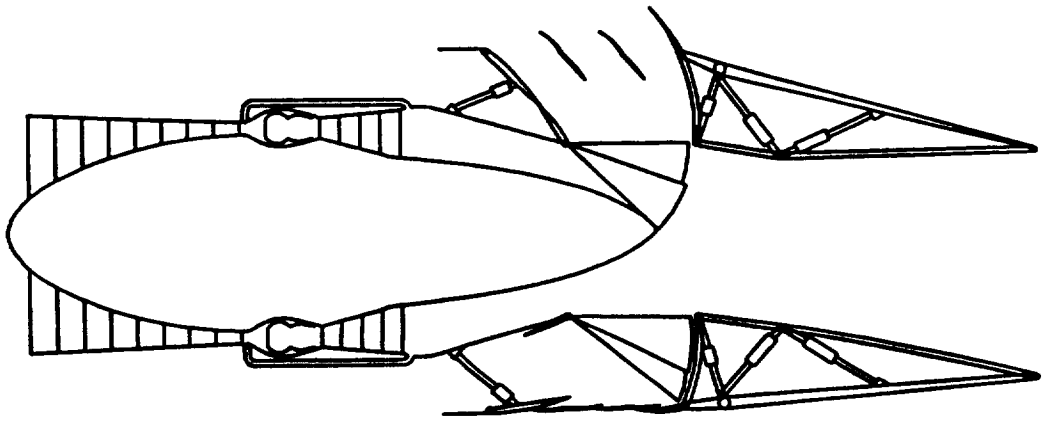

Figure 8: CATIA Model of a Turbine Bypass Engine

2.1.2.2.3 Structural Analysis & Materials

The focus of the structural design of a High Speed Civil Transport is to be made on the major areas of landing gear support, engine location, wing to body intersection, and wing sizing. The challenge is to select or develop materials which are light-weight and provide an economical solution for the meeting of strength and stiffness requirements. In the design of the structural components, safety, damage tolerance, and maintainability of the structural components for at least 60,000 hours of supersonic operations is desirable. Finite Element Analysis (FEA) and Computer Aided Engineering (CAE) tools need to be utilized to model and analyze the structures for a seven year real time accelerated testing. Technically, the structural integrity should be analyzed for operations in high temperatures at supersonic cruise speeds around Mach 2.4. Both advanced metal alloys as well as composites should be considered for implementation in the design.

2.1.2.2.4 Controls and Flight Systems

The product and processes identified under advanced flight systems and advanced flight controls are redundant fly-by-light controls (FBL), power-by-wire systems (PBW), enhanced vision systems (EVS) with head up displays (HUD), electronic library systems (ELS), data links, and an integrated vehicle management system (VMS) that incorporates flight and propulsion control, 4-D navigation, aircraft condition monitoring, satellite navigation, and flight management. The subsystems characterized here are expected to have come in line replaceable modules (LRM) or supplier replaceable units (SRU).

Fly-By-Light control is proposed since it provides significant weight savings and greater capacity for data transmission using the ARINC 629 bus architecture within the subsystems involved. Furthermore, fiber optic buses can be better integrated with composite structures, and optical transmission is not affected by electromagnetic radiation which might be a problem due to the high temperatures on the skin of the aircraft and inside the engine as well as electromagnetic (EM) interference from other sources. Advanced flight control architecture provides the basis for active control, stability augmentation, performance improvements, and restructuring for fault-tolerance. Redundancy of critical systems not only improves safety but also increases the operational availability. Aircraft condition monitoring systems and data links enable faults to be detected in-flight and to alert the ground crew prior to arrival, reducing the mean time to service.

Satellite Global Positioning Systems (GPS) (satellite-based navigation), 4-D navigation, and advanced flight management systems will enable optimization of way point routing, block time, block range as well as fuel and arrival time savings. Power-by-Wire

systems not only provide further weight savings but reduce the need for engine bleed for air conditioning, thus decreasing the drag and avoiding degrading the propulsive efficiency. They also provide better reliability and maintainability of power systems on the aircraft.

The landing gear is discussed with flight systems and control due to its importance to the successful operation of the aircraft. In the case of a HSCT, the landing gear should be relatively light weight, yet be able to support the weight of the aircraft and to evenly distribute the loading on the tarmac surface. It should be high to prevent tail strike during rotation at take-off and for easy accessibility for servicing without significant aerodynamic degradation due to storage issues. A rearward retracting wing stored main landing gear is proposed.

2.1.2.2.5 Life Cycle Costs

A HSCT must be designed for lower life cycle cost, designed for fabrication, designed for assembly, and designed for reliability and maintainability. The proceeding chapters will detail concerns in these areas. A great emphasis is placed on designing for lower life cycle costs. While the conceptual, detailed, and component designs only account for about 5% of the total life systems cost, the decisions made determine 80-90% of the total life cycle cost. In addition, 70-80% of the manufacturing productivity is determined in design.

In order for designers to include this information into their designs, they need to understand a great deal about the other areas or use a quality/performance indicator. This indicator would be a potent weapon to help quantify the expert knowledge of individuals in these other areas. This would lead directly to reduced design times, shortened manufacturing lead times, increased quality and lowered cost.

There is a great deal of interrelationships between many of the key product and process characteristics and the (LCC) characteristics. The LCC of a HSCT is broken down into three sections. These are the research and development cost, manufacturing processes cost, and the cost for reliability, maintainability, testability, and supportability (RMTS).

A very important part of the LCC of a HSCT is, in fact, research and development. It is also the main driving factor for most of the key product and process characteristics as seen in the roof of the product planning matrix in Fig. 13.

Manufacturing processes are also a major concern of the LCC of a HSCT. New technologies have to be developed due to the fact that significant portions of the aircraft will include advanced composites to meet weight requirements to make a HSCT affordable. Along with the new technologies, quality manufacturing concepts must be implemented. This will cost more money up front; however, in the long run, money will be saved

because of these innovative processes. Computer-aided engineering (CAE), computer-aided design (CAD), and computer-aided manufacturing (CAM) are new technological tools that must be used and integrated to provide a successful HSCT.

A HSCT must be designed for easy repair. Making the aircraft easy to maintain and *affordable to maintain* is another difficulty that the designers face. There will be a lot of component ground and flight testing done on a HSCT. These are additional high cost activities that industry must encounter. Again, this will directly affect the LCC of a HSCT.

2.1.2.2.6 Manufacturing

Manufacturing requires transforming raw materials into finished products. The four types of primary manufacturing processes are forming, reduction, joining, and finishing[8]. Forming transforms raw materials through deposition or deformation into a desired shape or configuration. Reduction processes transform raw materials or formed shapes by removing unwanted material. Joining is a process whereby new components are created by fastening together materials or parts. Finishing processes prepare the surface of a product for subsequent final surface treatment or provide final surface treatment. Each of these processes will now be discussed in more detail.

Forming Processes include hot forging, hot extrusion, hot rolling, cold forging, cold rolling, explosive forming, and casting.

Hot Forging is the simplest of the metal working crafts. It consists of heating the material to well over the critical temperature to soften it and then compressing the material between powerful hydraulic presses to alter the shape. Hot forging may take place between either open or closed dies, depending on the complexity and size of the part to be produced. Typical values of the force between the dies of large hydraulic presses are of the order of 100 to 200 MN, while a large forging hammer can weigh up to 20 tons, applying an impact of 400 MN.

Titanium, a material that will be extensively used on a HSCT, and other sensitive alloys require a great deal of skill by the machinist to know exactly how much deformation can be given to the component before its shape is altered and when further working becomes impossible due to the part having cooled too much. There is no well defined analytical treatment for the forging process, since the conditions under which the metal can deform vary enormously.

Hot Extrusion is a process which consists of taking a round cylindrical cast billet of the metal, which has been heated above the materials critical temperature, placing it in a cylindrical container of slightly larger diameter, closed at one end by a ram or piston, and the other end by a die. The cross section of the die has opening cut into it having the shape

of the cross section of the required product. Under the influence of large pressure (up to 200 MN), the ram is forced against the billet, forcing the material to extrude through one or more of the orifices cut into the die. This process is highly favorable for the manufacture of bars and sections of non-ferrous metals and alloys.

Hot Rolling is a process in which the reduction of the material is achieved by rolling it between pairs of rollers. Once again the material must first be raised above its critical point.

In Cold Forging the process is carried out cold to produce a hardened component with a high quality surface finish. Extremely high stresses are involved and it is occasionally necessary to heat harder materials to enable them to be worked. This heating is undesirable, because it detracts from the properties of the final product and is avoided wherever possible. If the operation is carried out at very high speeds, the interior heating if the surface causes the reductions in the yield strength. With very hard alloy steels (aircraft parts), hot-hammer forging has to be employed, with the final mechanical properties being obtained by heat treatment.

Cold Rolling is a processes confined to sheet and strip, and is used to finish sheet which has previously been hot rolled. This final process confers hardness, dimensional accuracy, and good surface finish on the strip which is then used for producing the various components required in industry.

Sandwich rolling is a technique used for rolling thin hard strips such as titanium. In this situation the harder titanium is rolled between two thinner sheets of a softer material. These softer outer layers are rolled to a slightly large reduction than the inner layer so that they extend more in the rolling direction. This reduces the roll pressure required to cause yielding of the hard metal, by inducing frictional forces between the layers which cause tensile stresses in the rolling direction within the inner lay. The net result is a reduction in the roll force and power required to roll the hard metal.

Explosive Forming is a recent development which is used to form large sheet metal components. Difficult manufacturing materials, such as titanium, can be formed relatively easily with this method. The sheet been formed is placed into a rough shape to conform to a female die. The sheet is then placed in the die and the lines of contact sealed so that the spaces between the die and metal may be evacuated. This system is then placed in water where an explosive charge is detonated to force the metal to conform to the die.

The previous forming processes have dealt with the material in the solid phase; forming can also take place in the liquid phase, which is known as casting. In casting, the liquid material is poured into a die or mold corresponding to the desired geometry[9]. The resulting shape can now be stabilized, usually by solidification, and can be extracted from the die as a solid component.

The size and geometry of the final parts are only limited by the material properties, the melting temperatures, the properties of the mold material (mechanical, chemical, thermal), and the material's production characteristics. Casting process allow the production of very complex or intricate parts in nearly all types of metals with high production rates, average to good tolerance and surface roughness, and good material properties. The advantage of casting is that it eliminates the need for expensive machining. There are three main types of casting processes: sand casting, investment Casting, and die casting.

Sand casting consists of pouring molten metal into cavities formed in a mold of natural or synthetic sand. The casting is then bonded together with an agent to provide mechanical strength at room temperature and yet burn out at elevated temperatures. This causes the mold to consolidate under shrinkage which occurs when the casting cools.

In investment casting, the patterns are made of wax, by either replicating the original product, or by pouring the molten wax into metal die. The result is a fragile wax pattern that is then coated, or invested by spraying successive layers of ceramic over it, and allowing each to dry and harden[10]. Nickel "super alloy" turbine blades are made this way.

Die casting employs pressure to force the molten metal into the mold. The required pressure can vary between 2 to 300 MPa, but the usually range is 10-50 MPa. The die casting process is rapid, providing up to 1000 castings per hour, which results in smooth surfaces, good dimensional accuracy, and thin sections (particularly in aluminum).

Reduction processes are the various methods necessary to form a product by the removal of scrap material by a chemical or physical process. Metal removal methods are divided into two categories machining and shear, pressing, and stamping.

Machining is a continuous process operating on a small volume of material at any given instant, requiring low forces. Nevertheless, the local stresses and temperatures may be very high and large strains are usually induced.

Shearing, pressing, and stamping are processes whereby large discrete volumes of material are removed from the original work piece. Large forces are involved over short periods of time.

The required geometry to the workpiece is obtained by kinematic generation of energy, which gives rise to their great flexibility. Thus, with the aid of relatively inexpensive tooling, a wide variety of shapes may be generated with a relatively short lead time. Computer numerically controlled machines provide great flexibility and constitute the most developed form of this mode of manufacture. Examples of machining machines are the lathe, spindle, milling machine, planer, sharper, broaching machine, and drill.

Methods of joining or fastening different parts together fall into three groups, viz.,. mechanical, metallurgical, and chemical. The first of these consists of screwed fasteners,

rivets, spring clips, etc., the second refers to welding, brazing, soldering and diffusion bonding, and the third, adhesion. The first criterion in selecting a joining method is if the joint must be de-mountable, because welded, brazed, and glued joints are intended to be permanent.

Screwed fasteners are intended to be readily de-mountable, while rivets, once fixed, cannot be disengaged. Care must be taken that the screws and rivets intended for external use on a HSCT must be able to withstand the high loading and temperature conditions that the airframe is exposed to.

Welding processes join materials in ways in which attempt to develop the same strength of the basic interatomic, or intermolecular, bond of the materials concerned at the joint. In this respect they differ fundamentally from mechanical or adhesive methods. Welding requires energy, which may be supplied in the form of heat (fusion welding), plastic deformation (pressure welding), kinetic energy (friction welding), or from the energy of a beam (electron or laser welding). There are more than fifty distinct variants of the basic welding process, but the most important are fusion or arc welding and electric resistance pressure welding[11]. Since the aim of welding is to produce a weld with the equivalent material properties of the material been welded, the more complex the material, the harder it is to weld. Because of this some materials are considered unweldable, because the heat of welding can alter some alloys.

There are four main problems when welding aluminum alloys; production of oxide films, weld metal porosity, softening of the weld zone and solidification and cracking[11]. These can be overcome, but the costs are tremendous and not all of the material properties can be obtained in the filler material. On the other side of the spectrum, titanium and the alpha-phase alloys weld relatively easily, but it is vital to guard against contamination from the atmosphere. Alpha-beta alloys form brittle welds, and while Ti-6Al-4V can be welded by the electron beam process, the high strength alpha-beta alloys such as Ti-4Al-Mo-2Sn-0.5Si are considered unweldable[11].

In soldering and brazing the filler material is fused while the parent metal is not. Soldering refers to low temperature soft solders of the lead-tin type melting below 250 °C, while brazing refers to copper-zinc filler alloys of high melting range, usually above 850 °C. Soldered joints are also relatively weak (38-55 MPa, 5.5-8 ksi), with brazed joints strong (~ 300 MPa, 44 ksi).

Difficulty is experienced when attempting to solder or braze aluminum and its alloys, because of there high oxygen content. The brazing and soldering process for titanium is not entirely reliable, resulting in poor joints. Subsequently these joining methods have found little use in the aerospace industry.

Diffusion bonding (DB) is a form of pressure welding in which the joint is effected by atomic diffusion across the interface without the need for fluxing or significant plastic deformation. It requires high temperature, length period of time, and a controlled atmosphere or vacuum[11].

Rockwell has developed a process that combines both SPF and DB for the fabrication of titanium parts. Trade studies have shown that using this technology in actual applications can result in cost savings up to 60% when compared to conventional titanium construction methods, while also saving weight[12]. Rockwell developed these fabrication methods to improve aircraft performance and reduce ownership costs. Titanium aircraft are expensive due to their high manufacturing and assembling costs. Their advantages are that they allow severe forming and intricate joining, which allows for the possibility of many different structural forms which could not be produced with conventional methods. Savings in weight and assembly costs are realized because the SPF/DB process produces a monolithic structure that requires less tooling, less machining with sheet metal formed to very large elongation's, reduction in part count, and a decrease in the use of expensive fasteners. Titanium has the ability to superplastically form (an ability not present in all metals) allowing a large, complex, inexpensive, monolithic structure of titanium sheet metal to be produced.

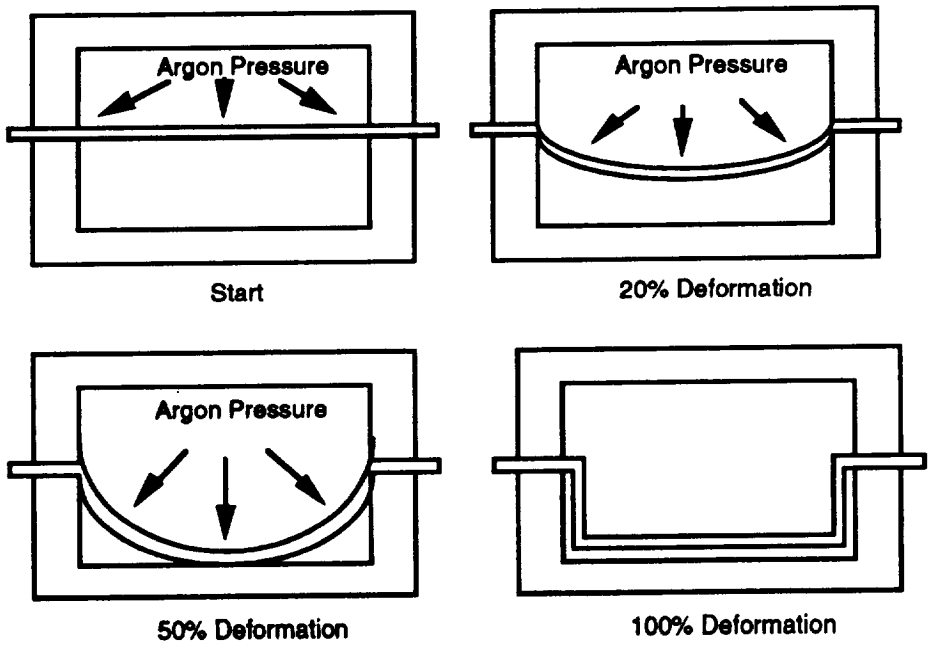

Figure 9: Description of Superplastic Forming Process

Rockwell discovered that titanium alloy 6Al-4V is normally limited to forming operations involving less than 30% elongation, but can be superplastically formed by more than 10 times this amount. Flow stresses are low in the superplastic condition; thus, metal

stock may be formed into a complex die cavity by the application of gas pressure much as nonmetallic plastic sheets are vacuum formed[12]. Rockwell's SPF/DB process can be seen in Figure 9[12]. Titanium hardware with structural efficiency that was previously unachievable may now easily designed and fabricated. The optimum temperature for superplastically forming the Ti-6Al-4V alloy is 1,700 °F (925 °C).

The capability to produce superplastically formed complex titanium metal sheets has been successfully demonstrated for a wide variety of applications. Applications include single-sheet formed parts, selectively formed and bonded hollow sections, and complex sandwich structure replacing multiple-piece assemblies and machined parts[12]. Cost and weight savings are on the order of between 30 and 50% when compared to conventional fabrication methods. Table I summaries these savings based on Rockwell's B-1 aircraft. This versatile fabrication process for titanium offers real potential for the development of the HSCT.

Table I. SPF/DB Cost Reduction Potential[12]

Part Description	Percent	
	Cost Savings	Weight Savings
Nacelle center beam frame	55	33
Nacelle frame	43	40
APU door	55	31
Windshield blast nozzle	40	50
Precooler door	60	46

Powder Metallurgy (PM) utilizes very rapid solidification of the material in powder form to produce the finished product. The consolidation techniques primarily used on aircraft structures is Hot Isostatic Pressing (HIP). The PM process for airframe structures can be broken down into three operations[12]:

- Powder production
- Containerization
- Hot Isostatic Pressing

The first of these steps is to manufacture clean powder free of any defects and contaminants. This can be achieved by using vacuum induction melting followed by inert gas atomization[12]. The next step is to fill metallic or ceramic molds defining the shape of the desired product. The PM process is so precise that tolerance levels must be built into defining molds. Care must be taken so as to prevent any contaminates from be introduced into the molds. The filled mold is now placed inside a steel container; any remaining volume in the container is filled with a granular ceramic medium that transfers external

pressure to the mold and part[12]. The steel container is then welded, outgassed, and sealed, as illustrated in Figure 10. HIP is the final step, and consists of the application of a specified cycle of heat and pressure. Duration times vary widely, but can be expected to surpass 8 hours with temperatures and pressures exceeding 2000 °F and 25000 psi respectively.

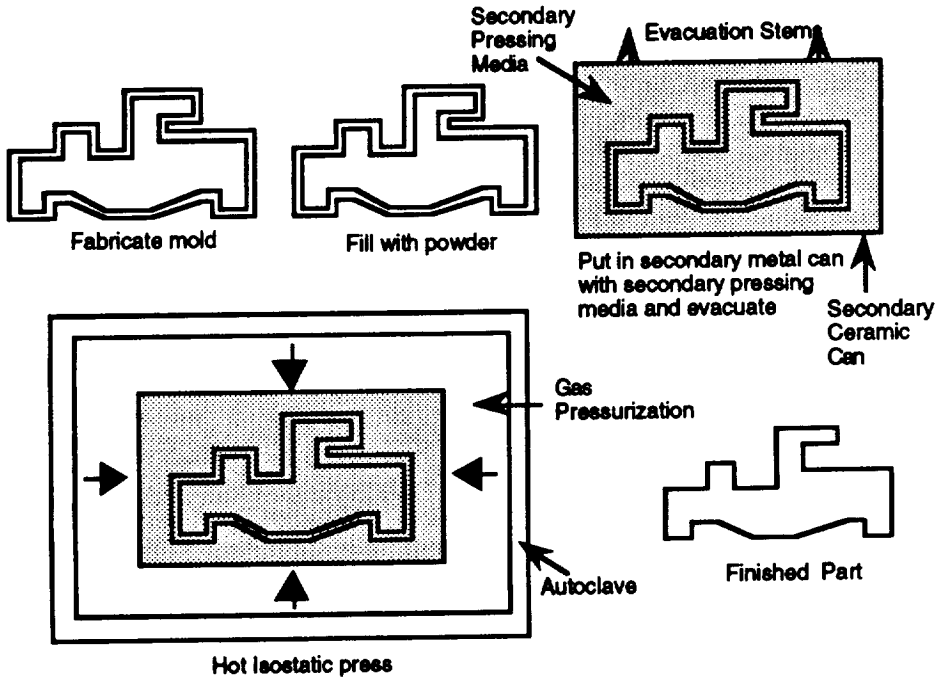

Figure 10: Powder Metallurgy Process.

The finishing process prepares the surface of the product for final surface treatment. The following methods are commonly used as finishing processes: Silk screening, cleaning, painting electroplating, and anodizing. The difference's between what finishing procedure to use on the selected material is not sufficient to change the material selection; rather the material selection should be based on the material properties and the above three fabrication processes.

Composite fabrication costs are driven by the design requirements of the structure; superior performance parts require more costly materials and fabrication processes. Primary structures, such as wing or stabilizer skins, are highly loaded, flight critical structures that must be resistant to fatigue and environmental effects, demanding high performance materials that are expensive to fabricate. On the other hand, secondary structures, which do not carry critical loads may be able to take advantage of cheaper and quicker manufacturing techniques.

Table II provides a listing of several composite manufacturing process temperature and pressure control requirements, including a relative estimate of tooling, production, and

material cost[12]. Autoclave curing, which is the most versatile, has comparatively higher tooling and production costs than the other processes. These high costs are associated with the high temperatures (600 °F) the tools and autoclave must endure. Regardless of this, autoclave curing is extensively used for its ability to easily manufacture a large range of components.

Table II. Process Manufacturing Requirements and Costs[12]

Process	Material	Close Pressure Control	Close Temp. Control	Post Cure	Tooling Costs	Production Cost	Material Cost
Autoclave Curing	Glass, Kevlar, graphite fabric; thermosets, thermoplastics	Yes	Yes	May be required with thermosets	High	High	Depends on fiber/resin choices
Elastic reservoir molding (ERM)	Glass, Kevlar, graphite fabric; forms, epoxy resins	Yes	Yes	May be required	Low	Low	"
Thermoforming - plastics	Glass, Kevlar, graphite fabric; , thermoplastics	Yes	Yes	No	Low	Low	"
Injection Molding	Glass, graphite, chopped fibers; thermosets, thermoplastics	Yes	Yes	No	Dependes on part complexity	Low	"
Hot Stamping	Glass, graphite, Kevlar fibers; thermosets, thermoplastics	Yes	Yes	No	Moderate	Low	"
Rapid Cure Thermosets	Glass, graphite, Kevlar fibers; thermoplastics	Yes	Yes	No			"
Pultrusion	Glass, graphite, Kevlar fibers; thermoplastics	No	Yes	No	Low	Low	"
Filament winding	Glass, graphite, Kevlar fibers; historically with thermosets; thermoplastics developing	No	No	Some applications	Low	Low	"

As well as the material mechanical properties, the size and shape of the desired part also places constraints on the fabrication technique. Table III presents the limitations of certain fabrication techniques to various component forms[12]. For example, large integral structures such as fuselage skins with stiffeners, wing sections with stiffeners, and bulkheads, can be manufactured using autoclave curing or filament winding. Autoclaves are expensive with the cost being proportional to the size; a single autoclave 20 feet by 50 feet can cost $7,000,000 (for use with thermosets) or $11,000,000 (for use with thermoplastics)[12].

Currently complex operations requiring great dexterity are manual procedures, but some operations, such as ply cutting and lay-up are beginning to be automated, providing substantial savings in both cost and time. These automated systems are new, and it is difficult to predict what problems will arise.

Table III. Suitability of Manufacturing Processes to Alternative Manufacturing Forms[12]

Process	Form of Manufactured Component					
	Large Integral Structure	Highly Contoured Parts	Med/Large Plain Panels	Closed Sections	Open Sections	Detailed Parts
Autoclave curing	Yes	Yes	Yes	Yes	Yes	Yes
Elastic reservoir molding (ERM)	No	No	Yes	No	Yes	Possible
Thermoforming thermoplastics	No	No	Yes	No	Yes	No
Injection molding	No	No	No	Yes	Yes	Yes
Hot stamping	No	No	Yes	No	Yes	Simple Brackets
Rapid cure thermosets	No	No	Yes	Yes	Yes	Simple Brackets
Pultrusion	No	No	No	No	Yes	No
Filament winding	Yes	Yes	No	Yes	No	No

2.1.2.3 Formation of the Interrelationship Digraph and the N^2 Diagram

After the key product and process characteristics are determined, the relationships between them are identified through a prioritization matrix to define the QFD matrix roof. The prioritization matrix was also used to identify the direction of each relationship. By using a prioritization matrix that relates the key product and process characteristics to each other, a correlation between each characteristic can be assigned. Through the use of a weighting factor, a relationship can be categorized as strong, medium, or weak. From these correlations, an interrelationship digraph is constructed that is, generally, very muddled and difficult to understand. This digraph, as depicted in Figure 11, consists of modules containing each product and process characteristic. Arrows are drawn to show how one characteristic relates to another. From this interrelationship digraph, very little can be deduced. Therefore, a tool is needed to identify in what order these characteristics can be evaluated. DeMAID (Design Manager's Aid for Intelligent Decomposition[13]) is such a tool that provides the ability to form an NxN diagram with the above characteristics. This program helps in planning, scheduling, and organizing the decomposition of a complex design problem to identify its hierarchical structure.

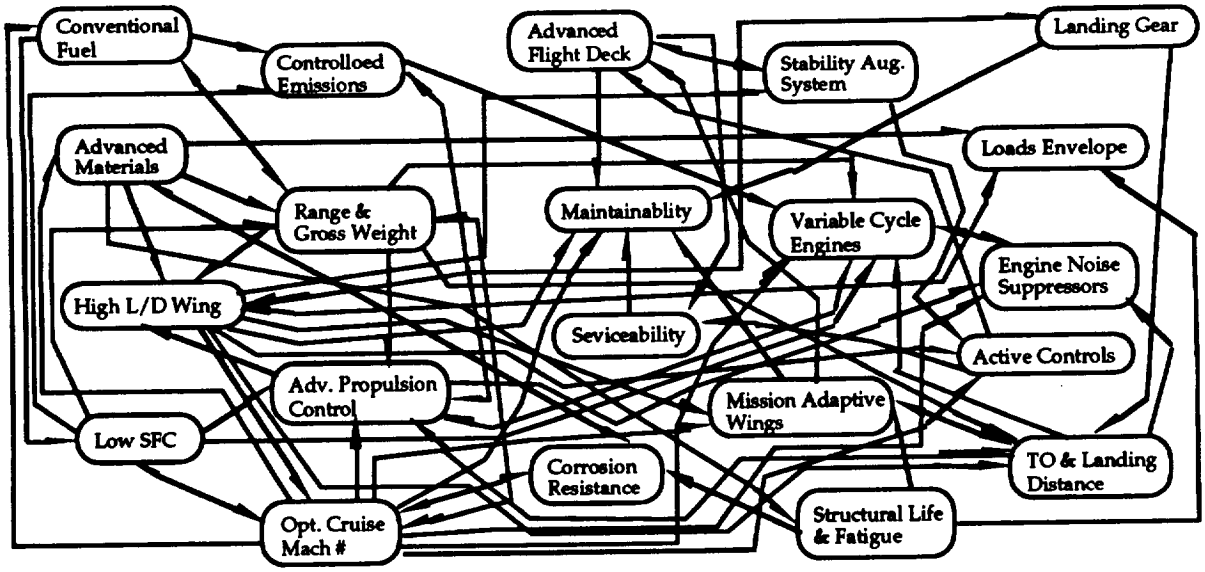

Figure 11: Interrelationship Digraph of the Key Product and Process Characteristics

DeMAID organizes system coupling data based on a knowledge base and displays the results in an NxN matrix format. It takes complex data into a set of ordered, hierarchical tasks, functions, and subsystems or modules, depending upon the level of analysis. DeMAID actually takes the information from the interrelationship digraph and translates it into a circuit of feed forward and feedback loops. Ideally, a minimum number of feedbacks is desired. Also, if smaller circuits can be modeled inside the main circuit, then the modules in the smaller circuits can be executed by themselves after they receive output from previous modules. Iteration processes can be accomplished on these mini-circuits until convergence is met. From this NxN diagram, a process order is determined. In addition, processes can also be identified that are performed in parallel with each other. The DeMAID output using the team chosen product and process characteristics identified for a HSCT is displayed in Figure 12.

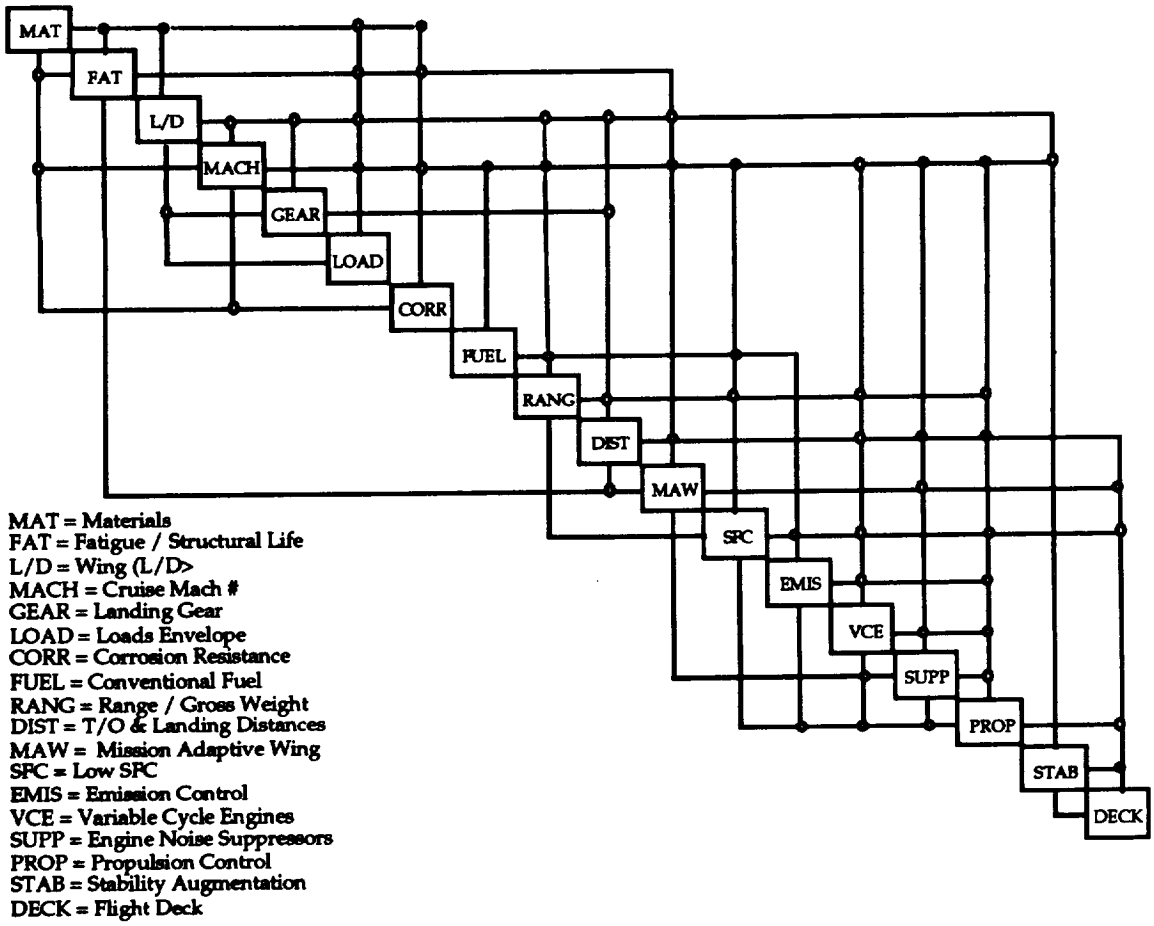

Figure 12: NxN Diagram for Key Product and Process Characteristics

2.1.2.3 QFD - Product Planning Matrix

With the help of these management and planning tools, the various requirements and characteristics were identified, a relationship matrix was constructed, and a QFD matrix was produced. Figure 13 illustrates this Product Planning Matrix, which relates the customer requirements to the key product and process characteristics. The arrows on the top of the HOWs indicate the direction of improvement for each functional requirement. The goal is to optimize, maximize, or minimize each requirement. For example, the cruise Mach number must be optimized for a HSCT.

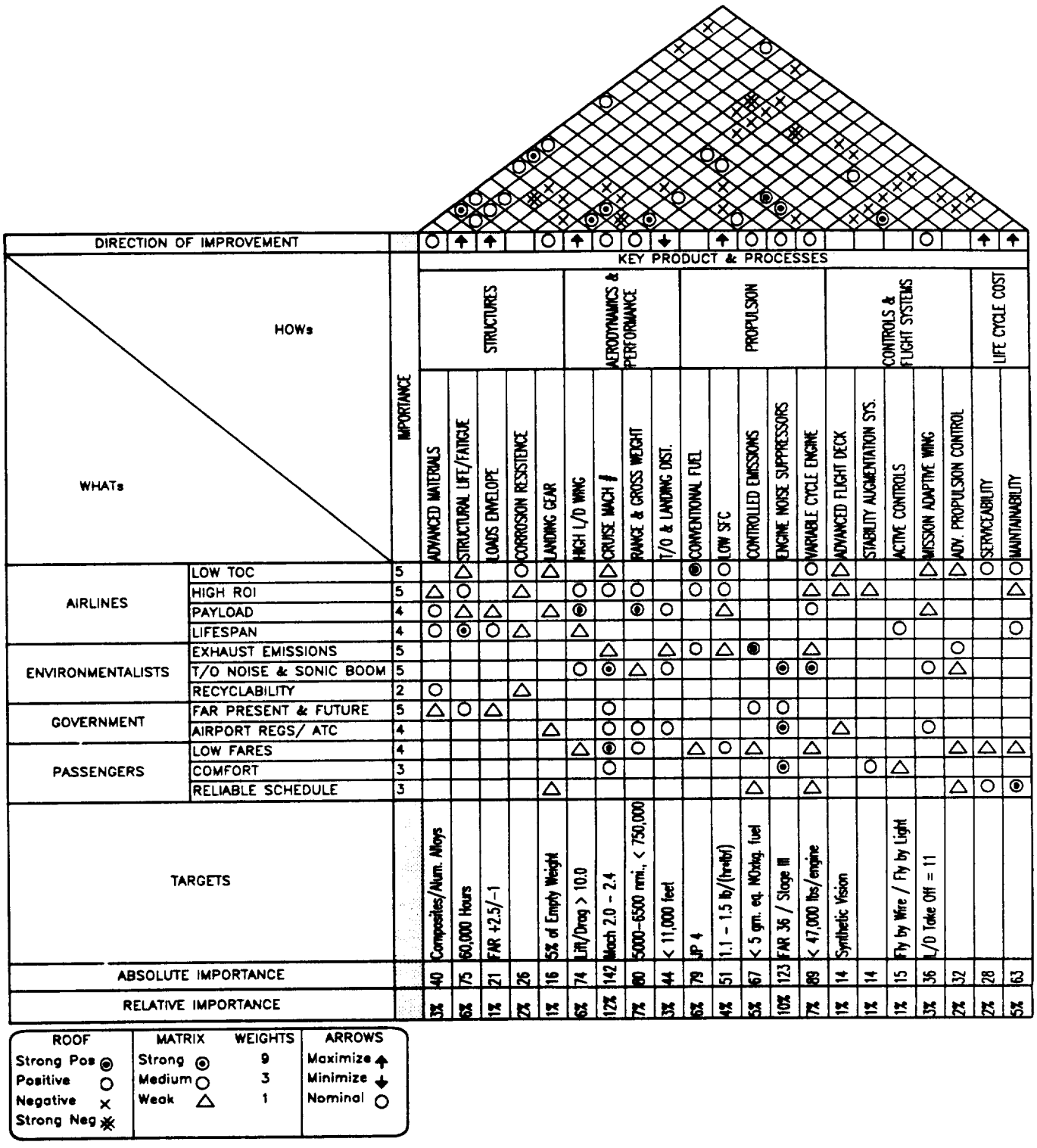

Figure 13: QFD Matrix Relating the Key Product and Process Characteristics to the Customer Requirements

2.1.2.4 Results of Product Planning Matrix

Referring to Figure 13, one can see that, for instance, strong relationships exist among the total operating cost and the fuel used. Take-off noise and sonic boom concerns strongly relate to the use of variable cycle engines. Any parameter which relates strongly to several other parameters is referred to as a driving factor. Therefore, the cruise Mach number and engine noise suppressers were identified as the driving HOWs. The relative importance ratings were instrumental in identifying the driving HOWs. The driving WHATs include such items as the payload, sonic boom, and takeoff noise.

In order to examine the type of relationship each HOW has with the others, a prioritization matrix was constructed, which can be seen in Figure 14. Notice how cruise Mach number, high lift to drag wing, and advanced flight deck have strong or medium relationships with many of the other HOWs. Appendix A contains explanations for each of the strong and medium entries in the matrix. The relationships identified by this matrix were translated into the roof of the QFD matrix. Only the strong and medium relationships were considered for the roof. Notice that some medium relationships translated as strongly positive or negative, and some strong relationships translated as only moderately positive or negative. The target values were determined by researching current literature on the HSCT project.

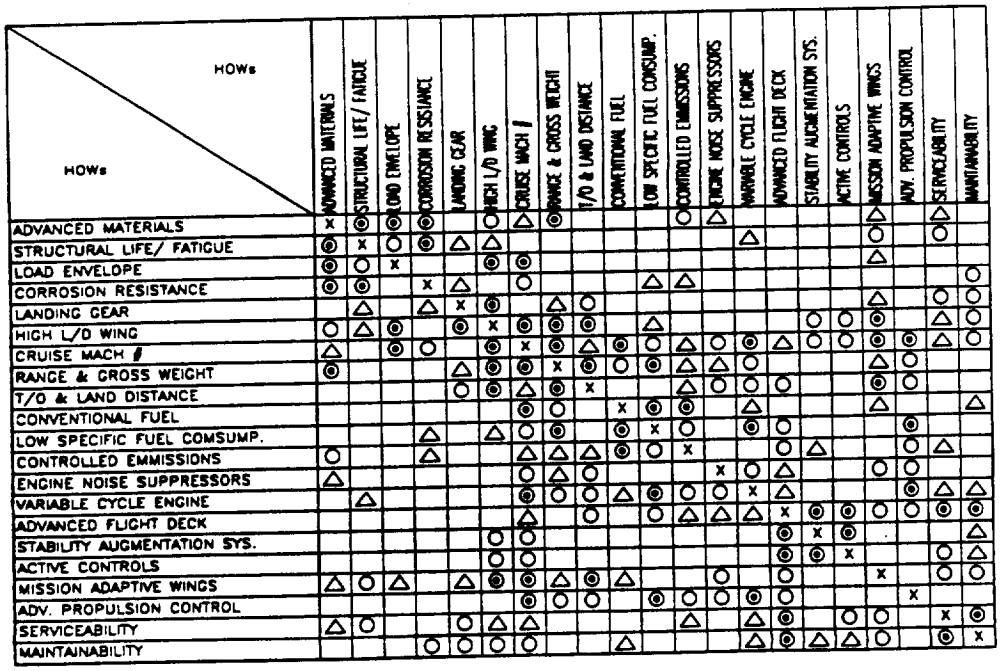

Figure 14: Prioritization Matrix Showing the Influence of the Key Product and Process Characteristics on Each Other

2.1.3 Establishing Value Objectives

Once the QFD matrix that relates the customer requirements to the key product and process characteristics is formulated, the emphasis shifts to the selection of a functional criterion. The initial system functional criterion chosen was the Return on Investment for the airlines and the manufacturers. The next generation supersonic transport needs to be a technological success, but even more important, it has to be economically viable. The Concorde, for instance, has been a technological achievement, but an economic failure never becoming capable of offering affordable ticket fares for those who want to fly supersonically.

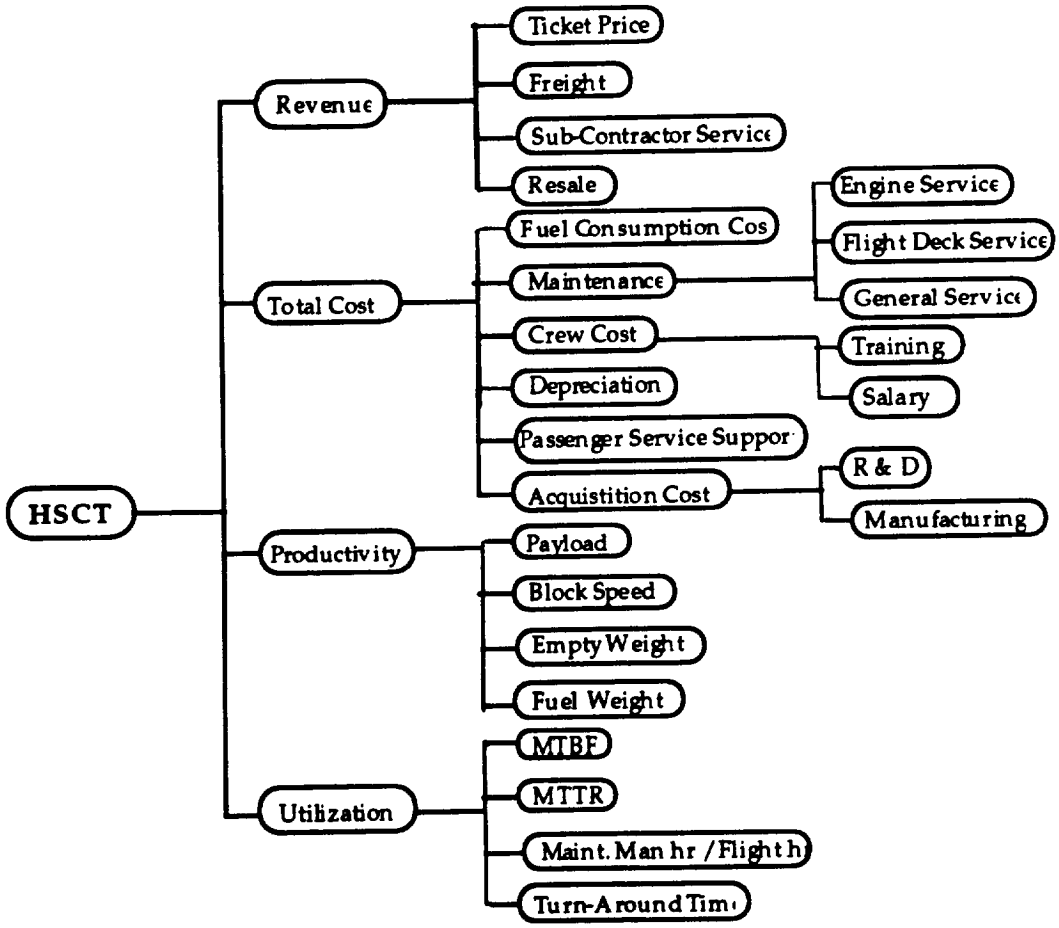

Figure 15: Return on Investment Criteria

Whether the airlines will update their future fleet with the proposed HSCT depends on their expected ROI. The main drivers of ROI are revenue, total cost, productivity, and utilization. The airlines' main source of income is through ticket sales. Total cost to the airlines include fuel cost, acquisition and crew training, and life-cycle cost including maintenance and depreciation. In addition to total cost and revenue, two other important

ROI drivers are productivity and utilization. Productivity relies solely on physical factors of the aircraft: payload, block speed, fuel, and empty weight. Utilization, on the other hand, is given by mean time between failure, maintenance man hour per flight hour, mean time to repair, and of course, turn-around time. A tree diagram identifying the ROI criteria was constructed and presented in Figure 15.

The same tasks as seen before in the development of the Product Planning Matrix were performed in the creation of an ROI QFD matrix. Once the ROI criteria have been established, another prioritization matrix was formed in order to identify the strong interrelationships between the ROI criteria. An interrelationship digraph that illustrates these relationships has been generated and presented in Figure 16.

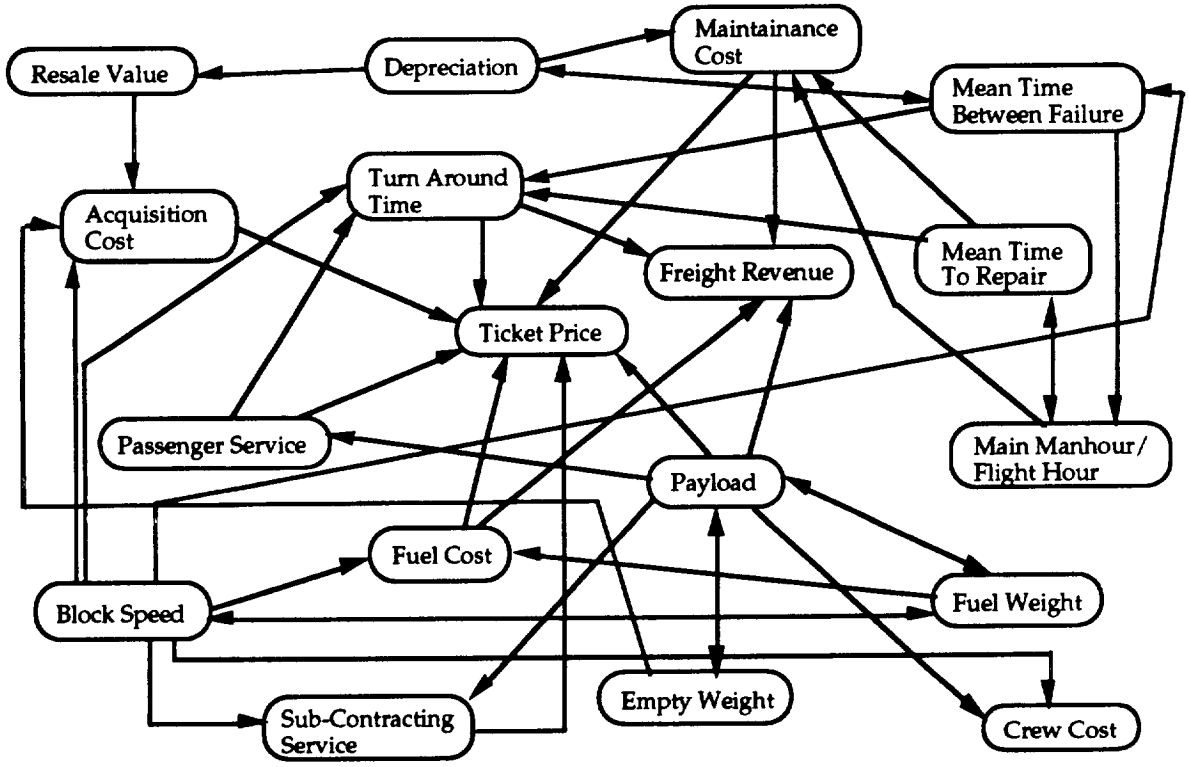

Figure 16: Interrelationship Digraph of the ROI Criteria

The next step in the process was to form the ROI QFD matrix. This matrix, displayed in Figure 17, is used to determine the criteria function of a HSCT. This QFD was used to identify all important aspects from an economics point of view.

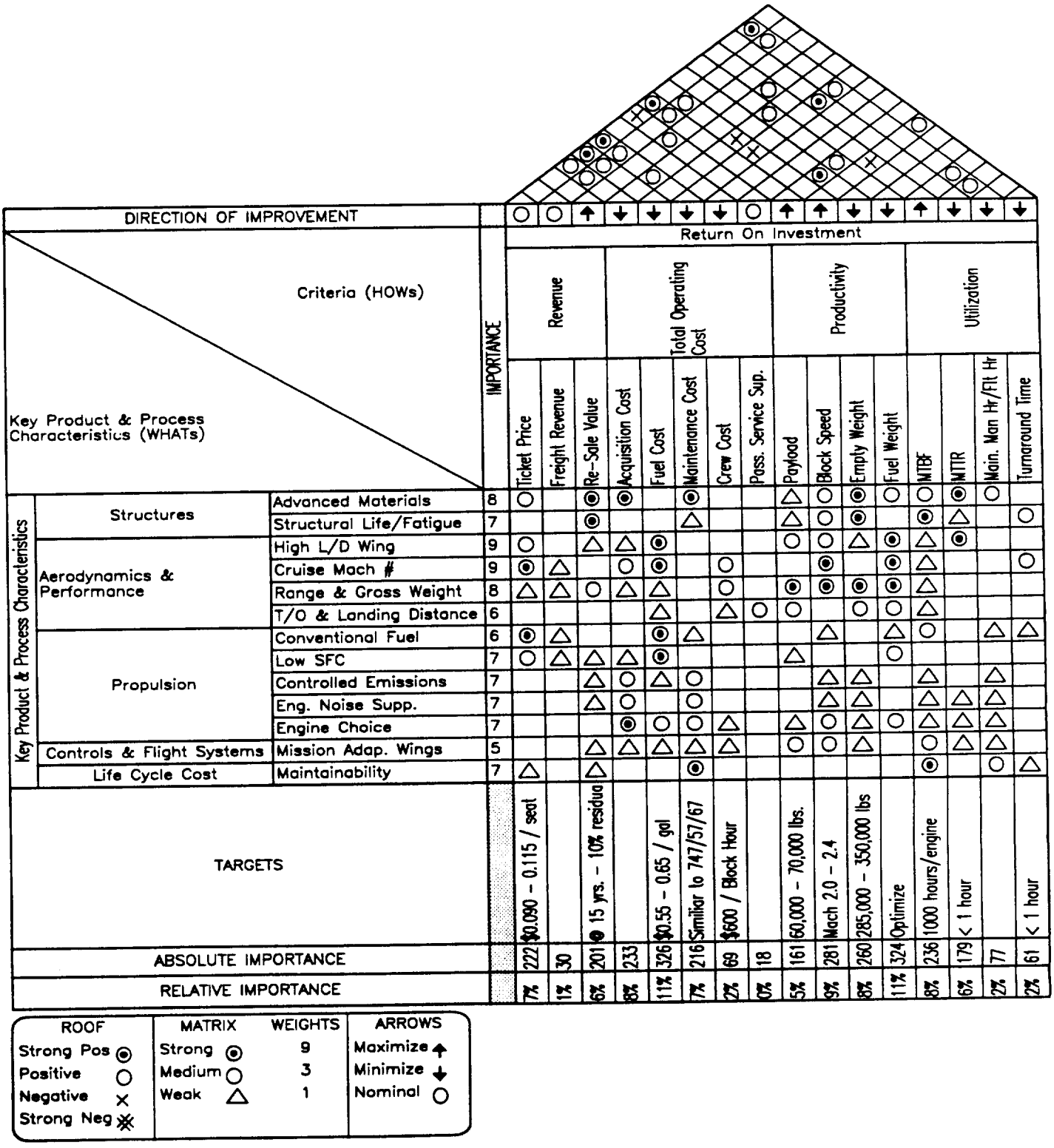

Figure 17: QFD Matrix Relating the ROI Criteria to the Key Product and Process Characteristics

2.1.3.1 Feasibility Constraints

The feasibility criteria are the economic, physical, performance, and environmental constraints which must be met in order for a design to be considered a feasible alternative. The important constraints with regards to a HSCT are shown below:

Parameter	Restriction
• Controlled Emissions	• < 5 gm NOx/Kg Fuel
• T/O & Landing Noise	• FAR 36/Stage III
• Overland Noise	• < 70 dB
• Gross Weight	• < 750,000 lbs
• T/O & Landing Distance	• <= 11.000 ft
• Cruise Mach Number	• 2.0 - 2.6
• Range	• > 5000 nm
• Structural Life	• > 60,000 hrs

2.1.3.2 Life Cycle Cost Matrix

The life cycle cost of a system is defined as the total cost to the customer comprised of acquisition and ownership of that system over its full life. It includes the cost of development, acquisition, operation, support, and disposal as seen in the equation below:

$$LCC = \sum_{t=0}^{t=n} (RDT\&E) + (PROD) + (O\&S) + (DISP), \text{ where n is in years}^{14}.$$

Approximately 60% of the life cycle cost is found in the Operations and Support area. If a company spends more on research and development to improve the reliability and maintenance access of the aircraft, a decrease will occur in the Operations and Support area. Minimizing life cycle cost requires the company to spend money and time up front in the conceptual and early design stages as seen in Figure 18. On the other hand, it is important not to lock in all of the project's finances early in the research and development stages. Decisions made in the early design stage affect the amount of LCC to be spent later in the life cycle of the aircraft.

A third QFD matrix was subsequently formulated and was dedicated to LCC where the return on investment for the airlines and manufacturing (see Table IV) were related to the cost drivers (see Figure 19). As one might notice, the ROI criteria are slightly modified from the ROI criteria as seen in the previous QFD matrix. This is due to the fact that more information is known about the product at this stage in a HSCT design than was known early in the design. Also, the major reason that the ROI criteria has been changed is to choose the ROI criteria that relates to the analysis program that was chosen to be used.

These ROI criteria can be directly modeled in the simulation code, ALCCA (Aircraft Life Cycle Cost Analysis)[15,16].

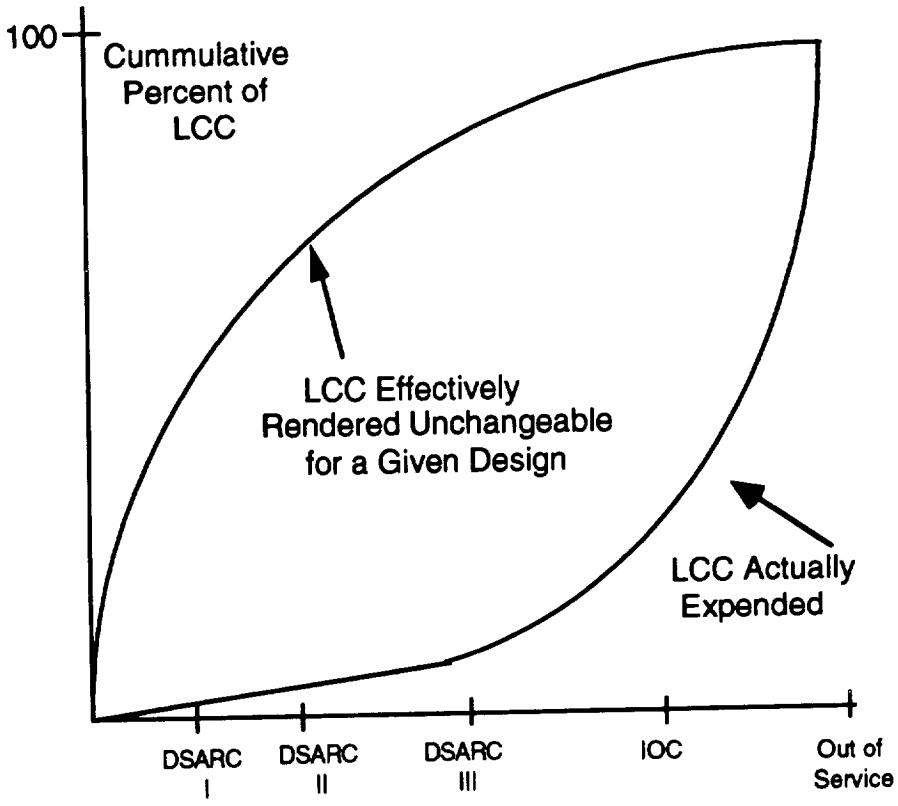

Figure 18: When LCC are Rendered Unchangeable Versus When LCC are Actually Expended for a Given Design

Table IV. Return on Investment for Airlines and Manufacturers

AIRLINES	Utilization
	Productivity
	Depreciation
	Stock
MANUFACTURERS	A/C Selling Price
	# of A/C Produced
	RDT&E Costs
	Production Cost

The factors which make up the ROI and the cost drivers were determined through brainstorming. These factors were entered into a QFD matrix, and their relationships and interrelationships were determined.

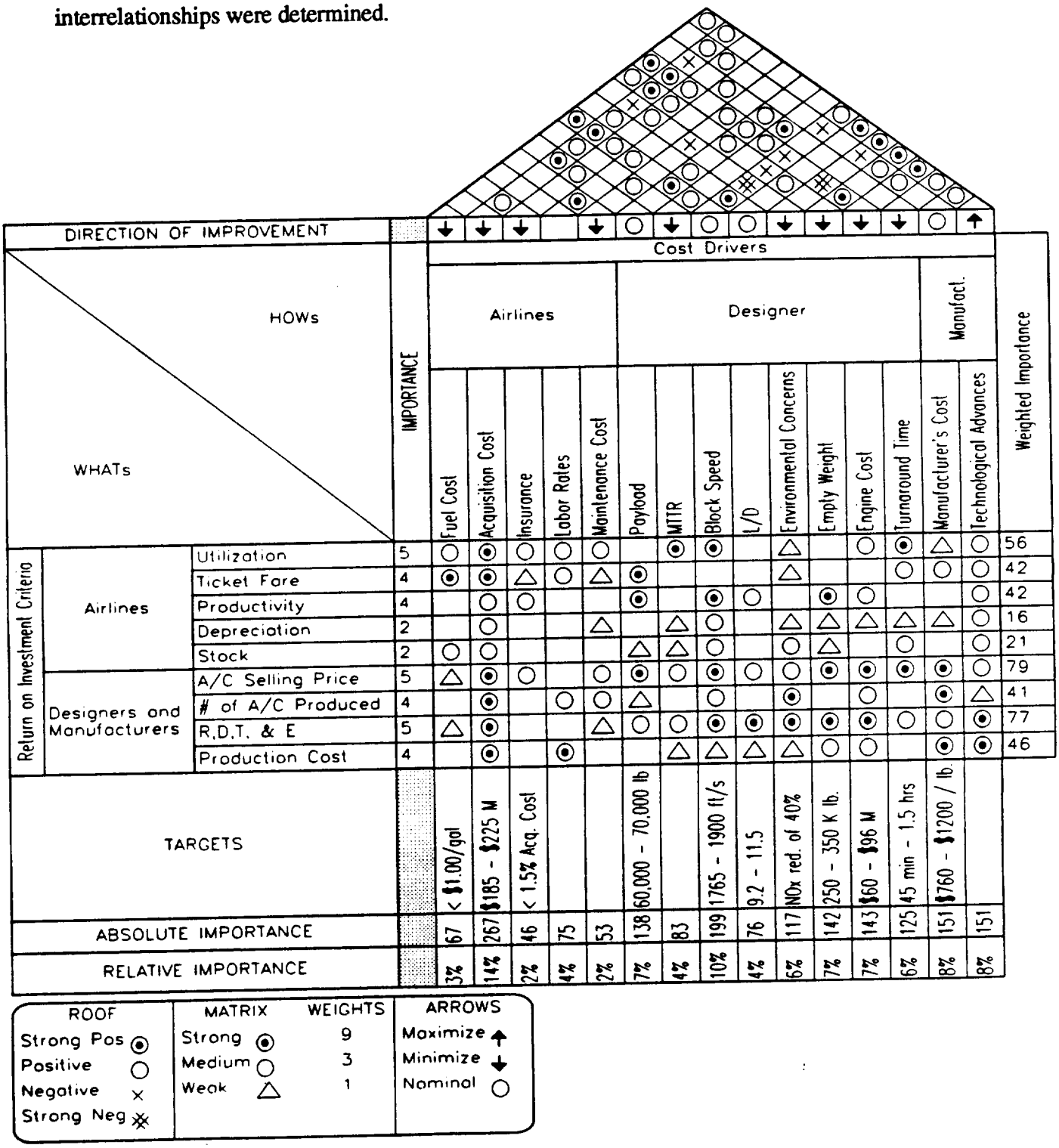

Figure 19: The QFD Matrix Relating the ROI to the Cost Drivers

2.1.3.3 Average Yield per Revenue Passenger Mile ($/RPM)

A metric that relates the concerns of both the airline and the manufacturer was needed to integrate the ROI desires of both parties. This selected metric is the average yield per Revenue Passenger Mile ($/RPM), an Overall Evaluation Criterion (OEC) that captures the concerns of all interested parties, manufacturers, airlines, and passengers[1].

In studying the economics of a HSCT, the ticket fare for a long range subsonic transport similar in size to the Boeing 747-400 is being used for comparison purposes. Since the chosen metric is the average yield per RPM, the target value for this study is based on 747-400 values of approximately $0.10/RPM. In order for a HSCT to be economically viable, economic analysts are forecasting that the target average yield for a HSCT should be between $0.10 - $0.13 per RPM. This claim is supported by several market surveys which show that most passengers are willing to pay a premium up to thirty percent more than a subsonic ticket fare[17].

2.1.4 Generation of Feasible Alternatives

2.1.4.1 Baseline Configuration

As was mentioned previously, the thrust of the effort described in this report was to set up an IPPD method to standardize and facilitate the concept evaluation process through MDO and Taguchi methods. Having established an understanding of the problem and defined value objectives in the form of $/RPM, the Georgia Tech team conducted a conceptual design study and obtained two candidate baseline configurations (a double-delta wing concept sized with today's technology (low risk), and one for development in the year 2005 (medium risk)). These two configurations were sized for an all supersonic mission, depicted in Figure 20. Figure 21 illustrates the double delta configuration which was used in this paper as a sample case for the implementation of the methodology developed. The information for these two baselines is presented in Table V.

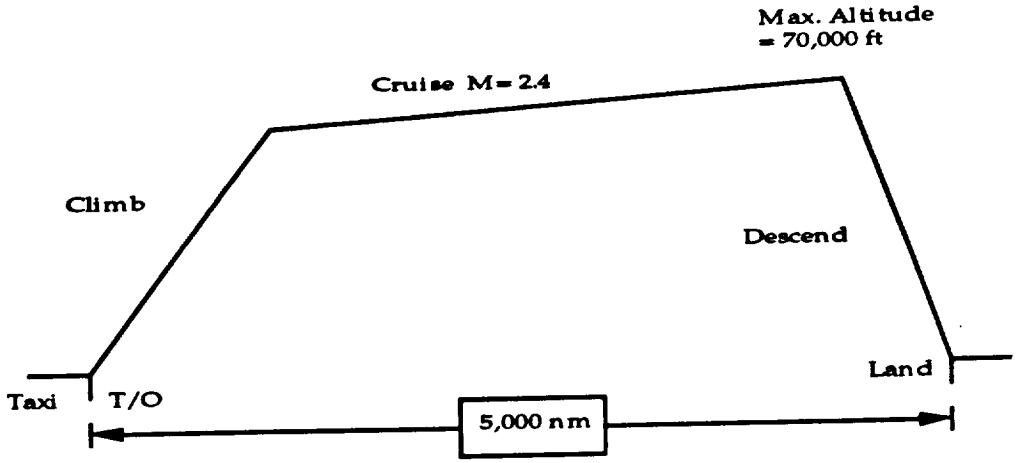

Figure 20: Baseline Mission Profile

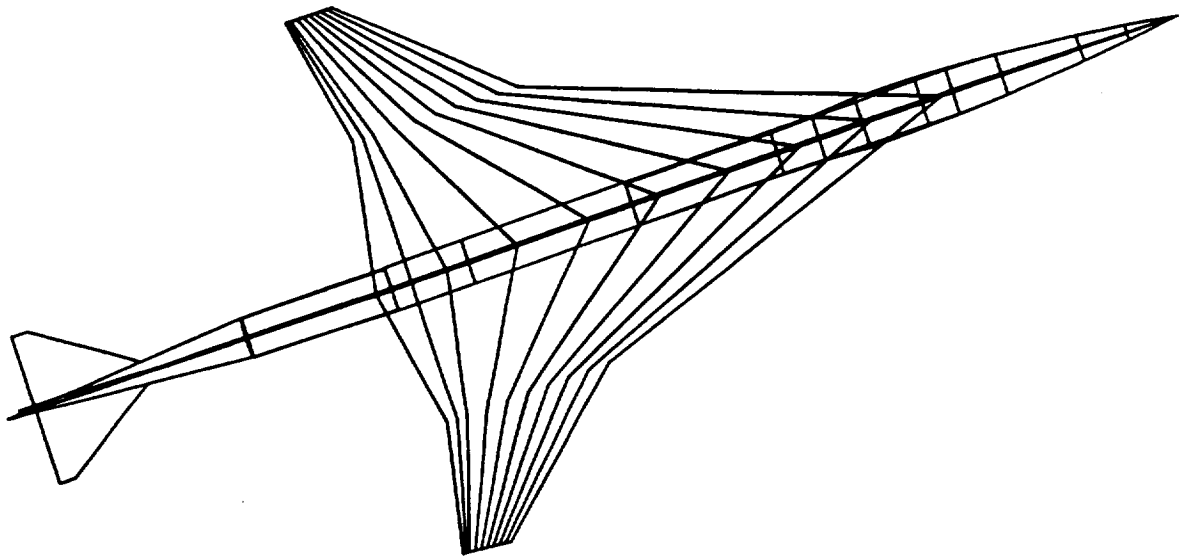

Figure 21: Georgia Tech's HSCT Double-Delta Baseline Configuration

Table V. Baseline Configuration Descriptions

	1994 (Low Risk)	2005 (Med. Risk)
• Payload	300 passengers, 62,700 lbs	
• Range	5,000 nm	
• Block Fuel	423,380 lbs	317,000 lbs
• Empty Weight	344,760 lbs	285,000 lbs
• TOGW	878,000 lbs	730,000 lbs
• Wing Area	8,500 sq. ft	8,500 sq. ft
• Span	140 ft	140 ft
• Taper Ratio	0.07	0.08
• t/c	0.03	0.03
• Thrust/Eng.	68,000 lbs	50,000 lbs
• Fuselage l.	310 ft	
• Block Time	4.44 hrs.	4.36 hrs.
• P.I.	92 knots	119 knots

2.1.4.2 Stability and Control of the Baseline Configuration

This section of the report addresses the issue of static longitudinal and directional stability of the baseline HSCT. The main tool used was a computer program called APAS, an acronym for Aerodynamic Preliminary Analysis System[18]. APAS was developed by Rockwell International for NASA Langley and is widely used throughout industry. Its purpose is to predict vehicle aerodynamics at the conceptual and preliminary design levels. The program can also determine static longitudinal and lateral stability characteristics, which is of interest here. In analyzing the stability of the baseline, the placement of the nacelles was varied along with the relative location of the wing with respect to the fuselage. To show how this was done, however, some more discussion of APAS is in order.

APAS is a program that uses a panel method to generate aerodynamic forces and moments for a given configuration. The user can create the configuration either graphically or using ASCII files called card files, which define the geometry. For simplicity, in this study the geometry was defined graphically. APAS requires that the user provide the dimensions, areas, aspect ratios, taper ratios, type of airfoil, etc. of a particular component. The code will create that particular component as it was specified. The geometry that the code creates is generic, so one may need to edit it so that the component is as close as possible to the actual geometry. Editing is done manually similar to editing a CAD drawing. A representation of a HSCT geometry is illustrated in Figure 22. Looking at the geometry, it is easily seen that the fuselage is a perfect cylinder, and a closer inspection will reveal that the wing and fuselage do not blend together nicely. Investigation into the blending issue showed that the program results are not affected by an ill-blended

configuration. The interference effects of the fuselage on the wing are accounted for through an interference shell. It is this interference that APAS uses to calculate the pressures around the wing/fuselage connected regions Once the geometry has been specified, APAS can now be run. A typical APAS run takes about five minutes. APAS generates aerodynamic data for the configuration (i.e. C_p, L, D, C_l, C_d...) based on given information such as Mach number, altitude, and angle of attack. From this data and information about the center of gravity, pitching moment, yawing moment, and rolling moment coefficients are calculated and can be plotted versus angle of attack and side slip angle. Further, the slopes of those curves can be calculated. It is those slopes that one uses to classify the aircraft's static stability. For this particular study, based on the best estimates available, the center of gravity was located at about 47% of the total aircraft length.

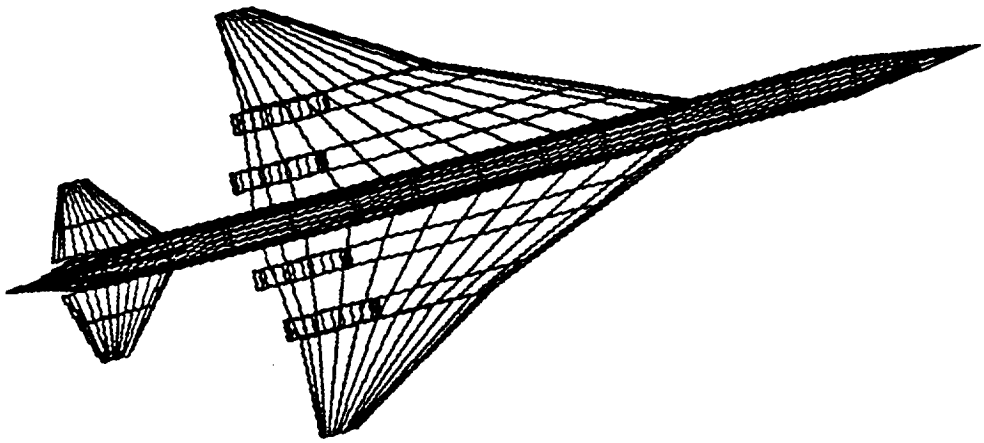

Figure 22: APAS HSCT Baseline Configuration

In analyzing the stability of the baseline, the placement of the nacelles and the location of the wing along the fuselage were varied. This was done for the investigation of both the longitudinal (α influence) and the directional (β influence) static stability. Two configuration cases were considered: Case 1 refers to the inboard nacelle being placed at 23% of the wing semi-span and the outboard nacelle being placed at 49% of the wing semi-span. Case 2 refers to the inboard nacelle being placed at 35% of the wing semi-span and the outboard nacelle being placed at 57% of the wing semi-span. "Wing @ ref." refers to the wing root leading edge being located at the baseline x-station of 91.5 feet. "Wing @ +5%" indicates that the wing has been moved forward by 5% of the fuselage length. "Wing @ -5%" indicates that the wing has been moved backward by 5% of the fuselage length. The static stability was assessed at the two cruise Mach numbers of .95 and 2.4.

Figures 23-28 contain the results of the longitudinal stability analysis. From the plots one can see that for each nacelle - wing placement combination, and at both Mach numbers, all of the "C_m versus α" curves have negative slopes. Thus, it can be concluded that for each nacelle - wing combination, the airplane is longitudinally statically stable. The magnitudes of the slopes reflect how stable each configuration is. Figure 25 shows that the aircraft appears to be more stable at subsonic cruise speeds and gets less stable when the wing is perturbed in either direction from the reference. Also, the aircraft is more stable with the nacelles placed closer to the fuselage.

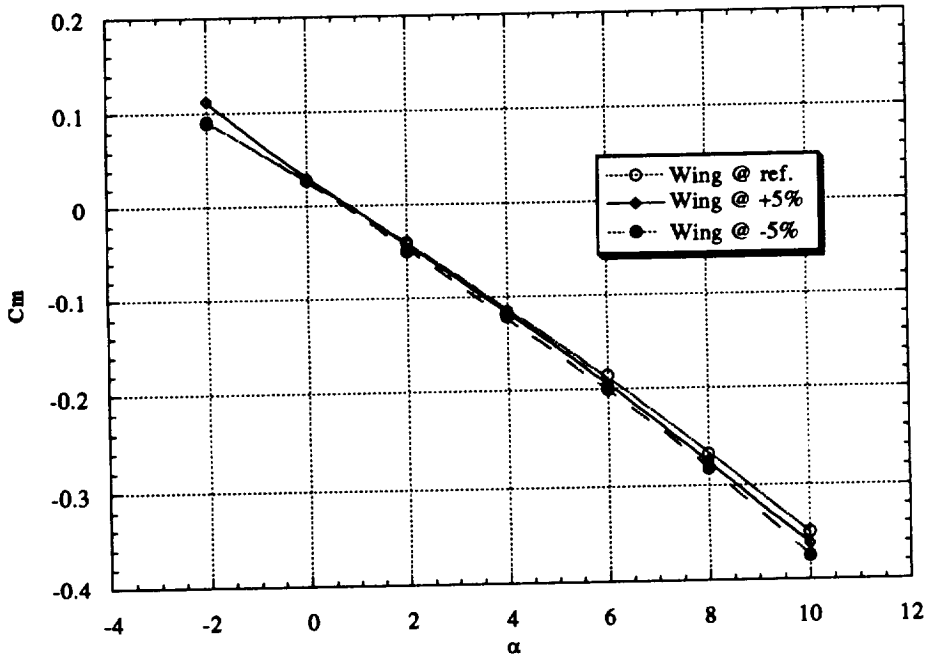

Figure 23: Case 1 - C_m Vs. α @ Mach = 0.95

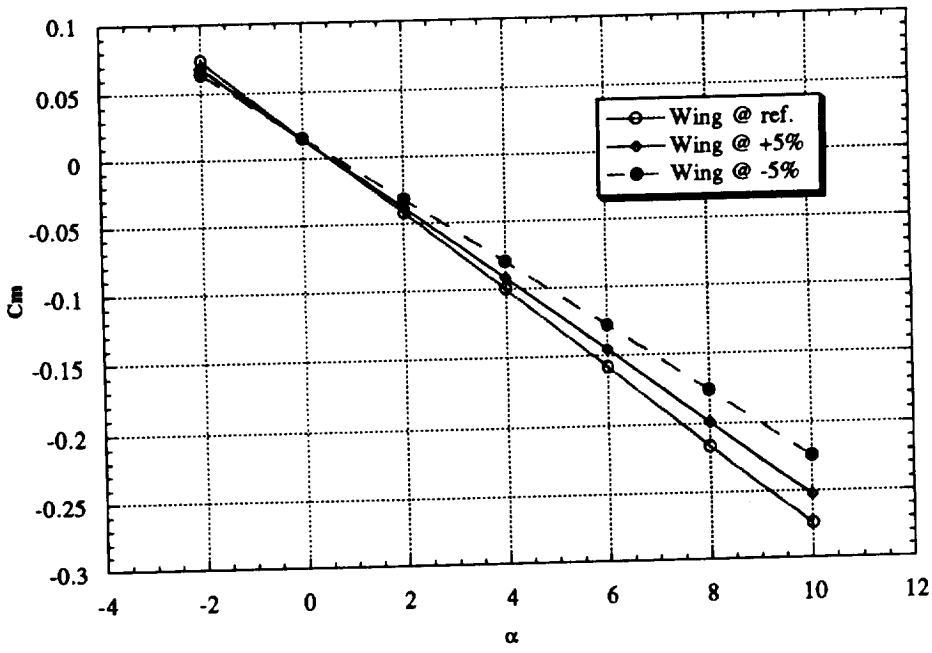

Figure 24: Case 1 - C_m Vs. α @ Mach = 2.4

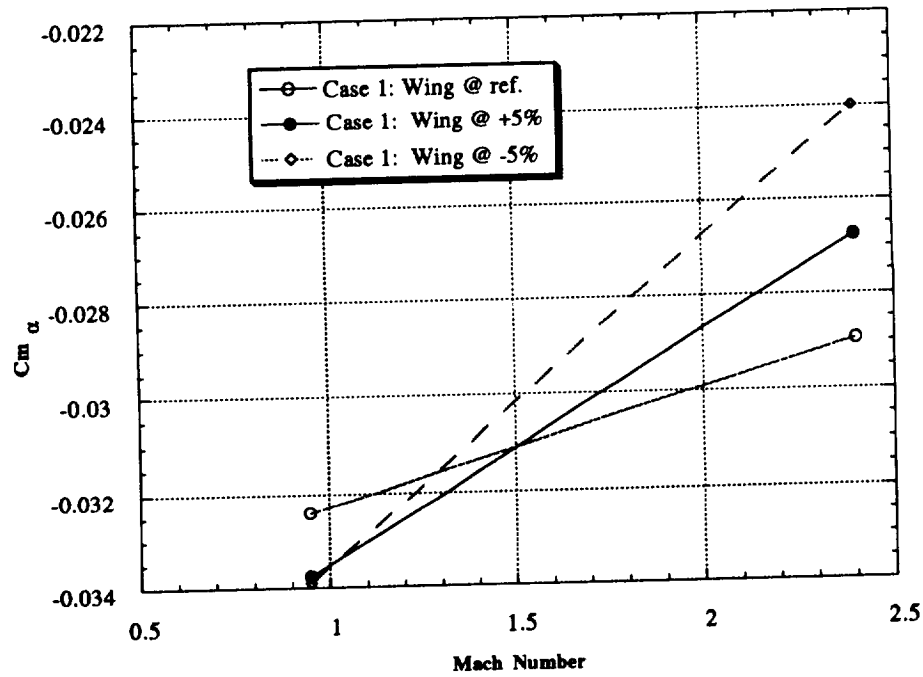

Figure 25: Case 1 - $C_{m\alpha}$ Vs. Mach = 2.4 & 0.95

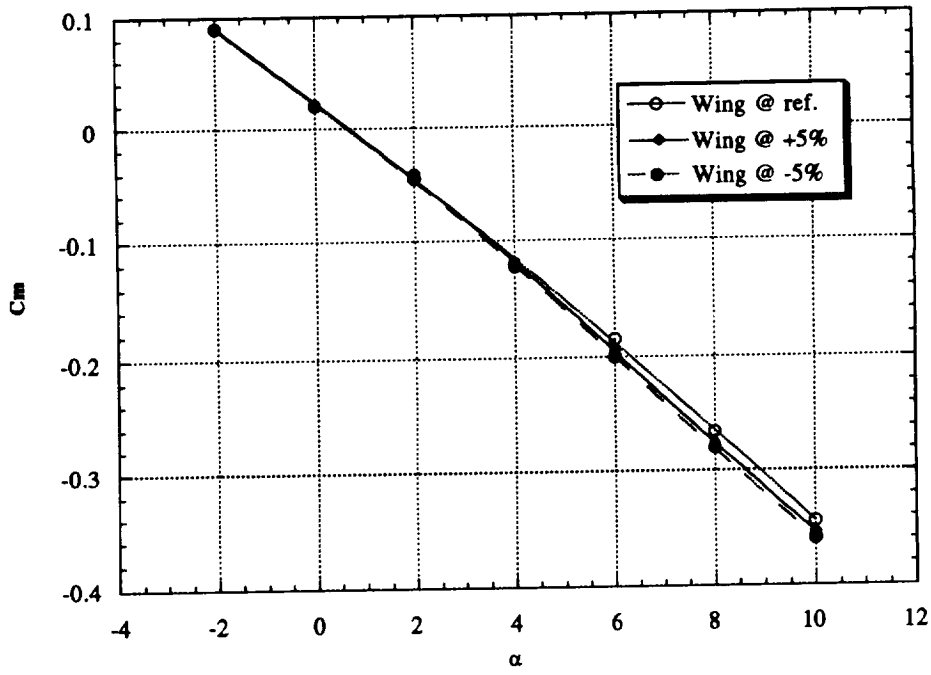

Figure 26: Case 2 - C_m Vs. α @ Mach = 0.95

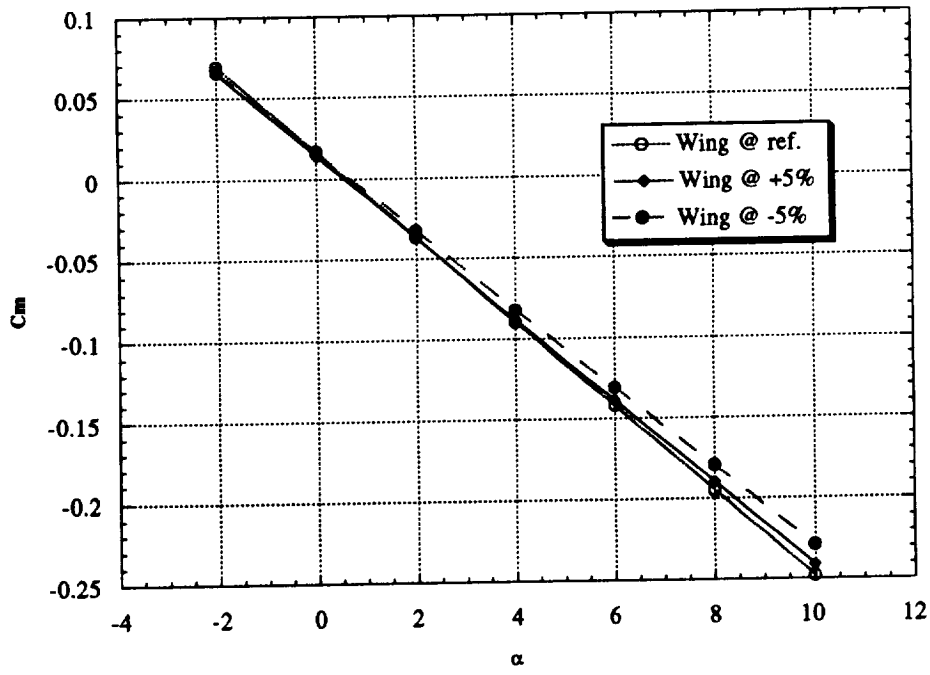

Figure 27: Case 2 - C_m Vs. α @ Mach = 2.4

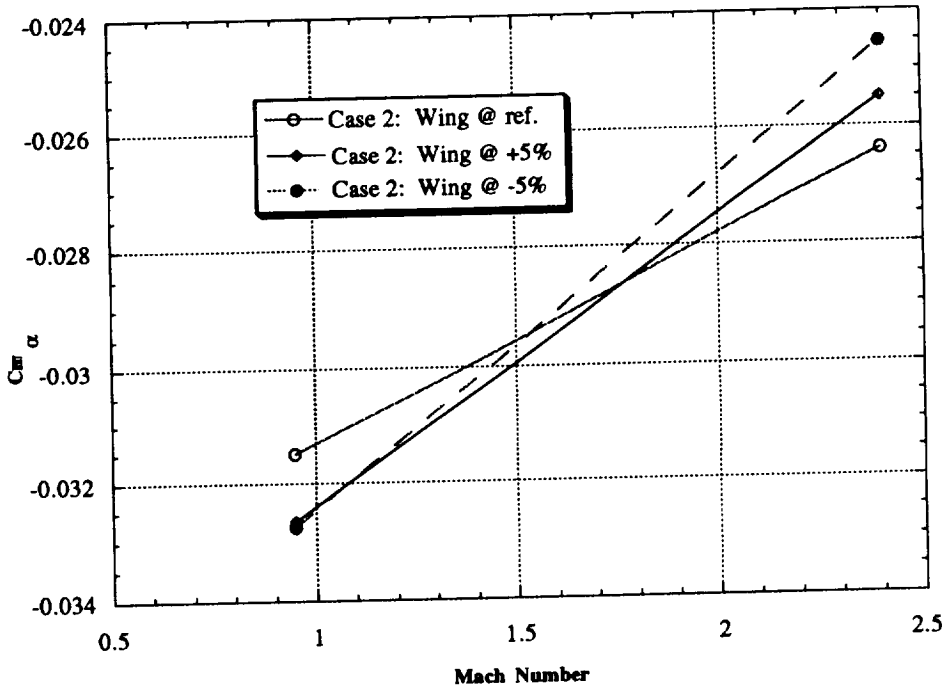

Figure 28: Case 2 - $C_{m\alpha}$ Vs. Mach = 2.4 & 0.95

Figures 29-32 show the result for directional yaw stability. From the plots of the "C_n versus β", the requirement for static directional stability (or weathercock stability) is that the slope of the "C_n versus β" curve be positive. Figs. 30 and 32 show that this configuration has neutral directional stability at Mach 2.4 (i.e. cruise). This is usually acceptable, especially since large directional damping is not needed at such speeds. Looking at the Mach .95 plots, it is seen that nonlinear results are obtained. This is due to the fact that APAS has modeling difficulties at transonic speeds. The slopes, however, are still always positive so the airplane is laterally stable, though results at transonic speeds are often suspect. It can be concluded that since $C_{n\beta}$ is positive for all nacelle wing combinations, these configurations are at best slightly stable directionally, but more probably neutrally stable, especially at cruise. Since the magnitudes of the slopes are so small it can also be concluded that the airplane has poor damping in yaw. In other words, for a small disturbance, the airplane is very slow to recover.

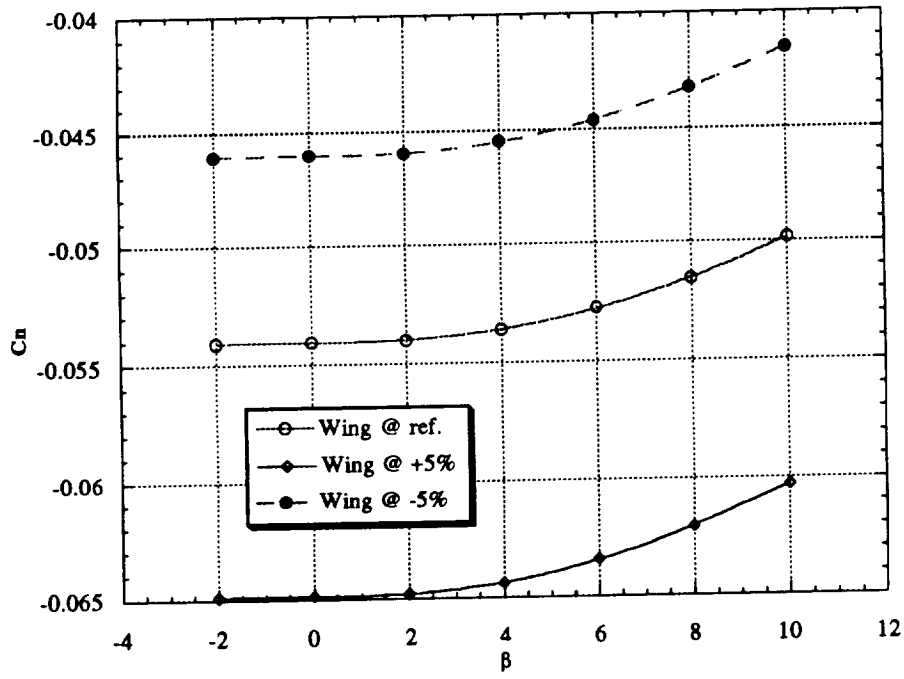

Figure 29: Case 1 - C_n Vs. β @ Mach = 0.95

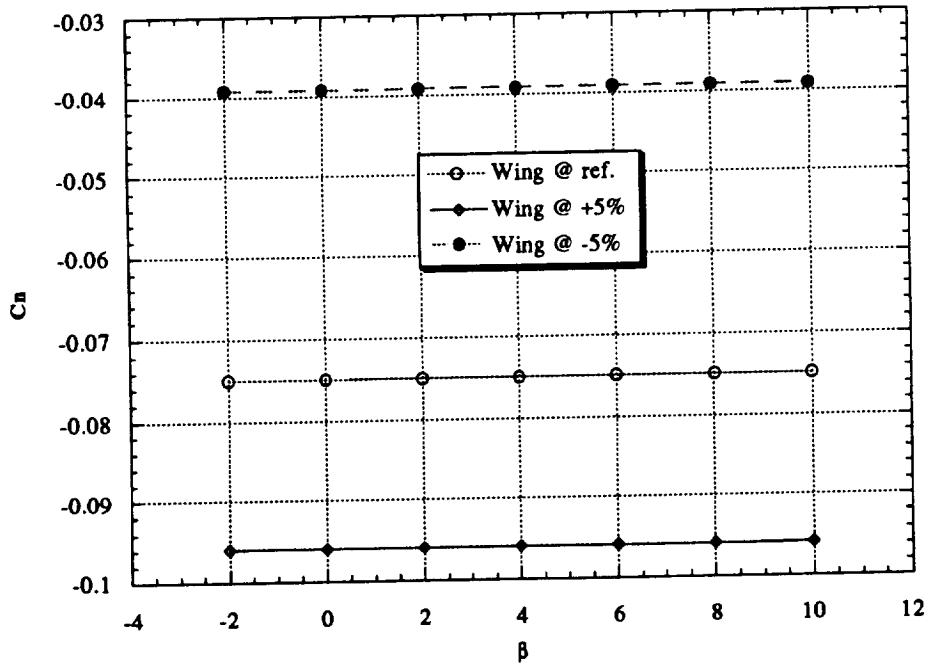

Figure 30: Case 1 - C_n Vs. β @ Mach = 2.4

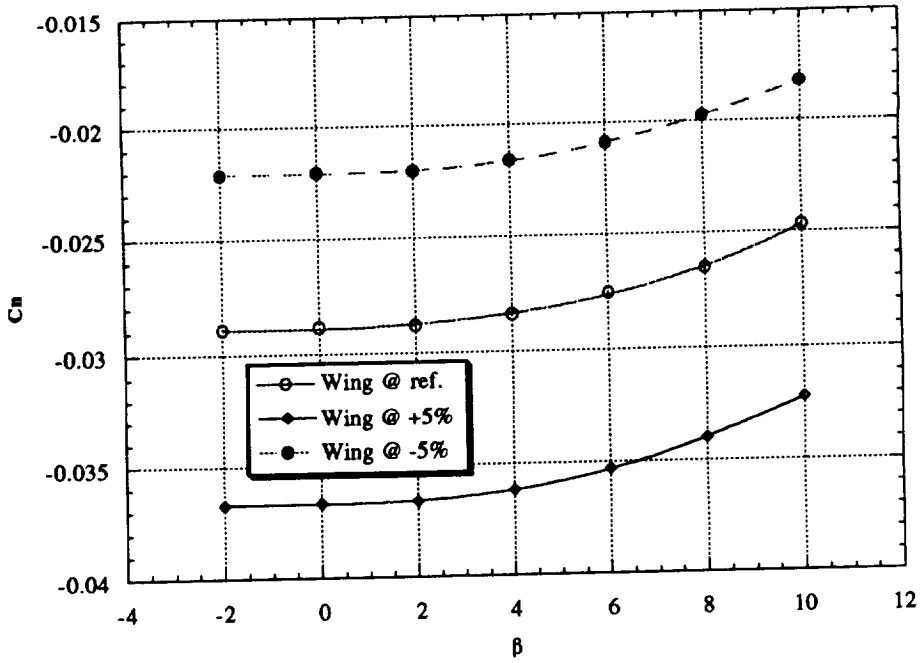

Figure 31: Case 2 - C_n Vs. β @ Mach = 0.95

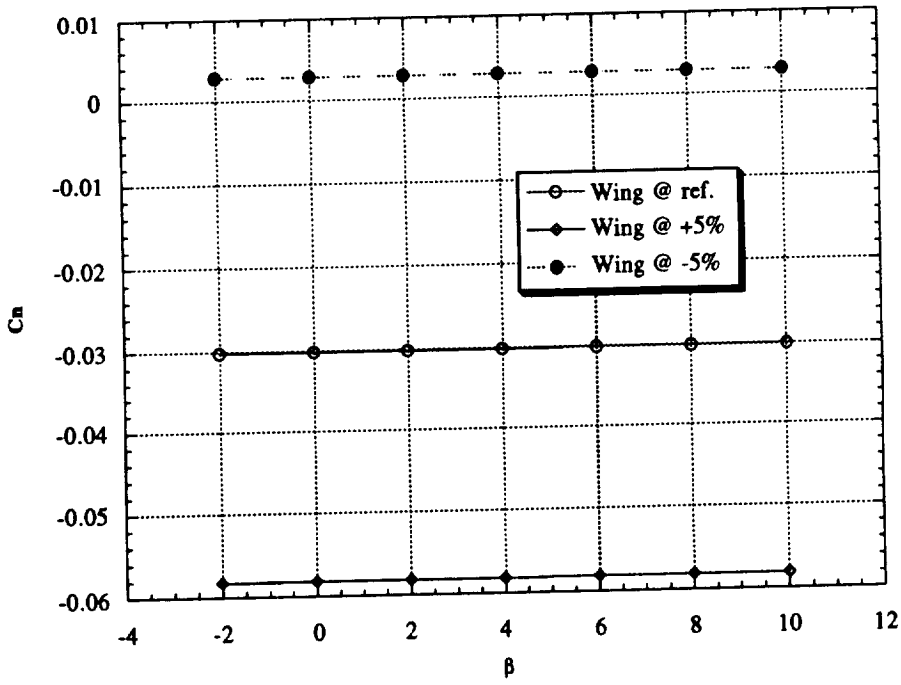

Figure 32: Case 2 - C_n Vs. β @ Mach = 2.4

The lateral roll stability results, "C_l versus β", are shown in figures 33-36. The requirement for lateral stability is that the slope of the "C_l versus β" curve be negative. Therefore, Figures 34 and 36 show that the airplane is almost neutrally stable at Mach 2.4.

At the Mach .95 cruise condition, nonlinear results are again obtained. As mentioned before this is due to the transonic speed of Mach .95. The slopes, however, are still negative; therefore, for these configurations, the airplane appears to be laterally stable. The slopes for these curves were calculated along the most linear portion of the curve and were found to be about -.000058, indicating again that the damping in roll is very weak. Again, since the magnitudes of the slopes are so small for all cases, it can also be concluded that the airplane has poor damping in roll. In other words, for a small disturbance, the airplane is very slow to recover.

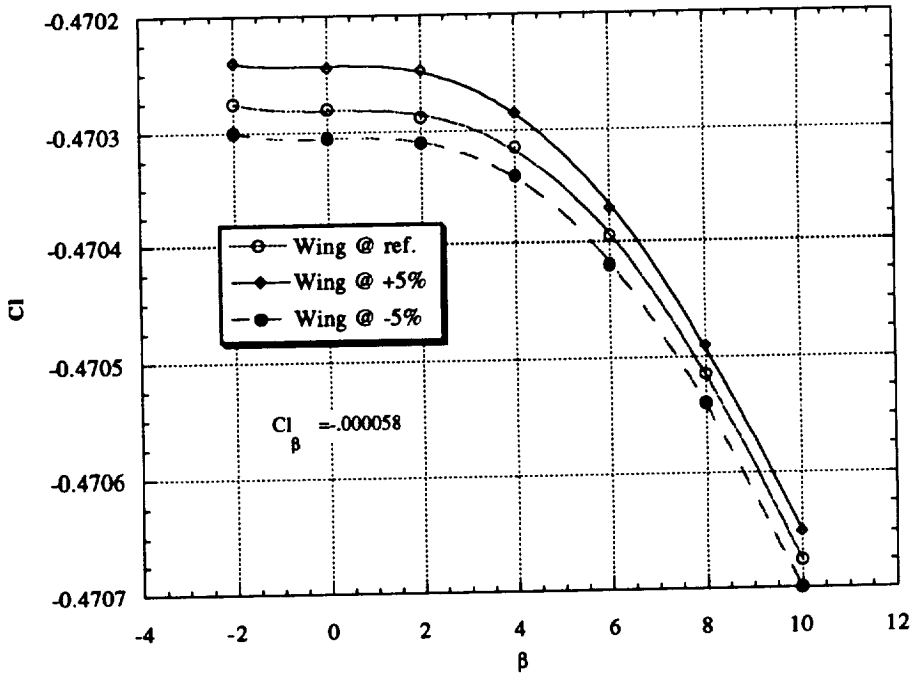

Figure 33: Case 1 - C_l Vs. β @ Mach = 0.95

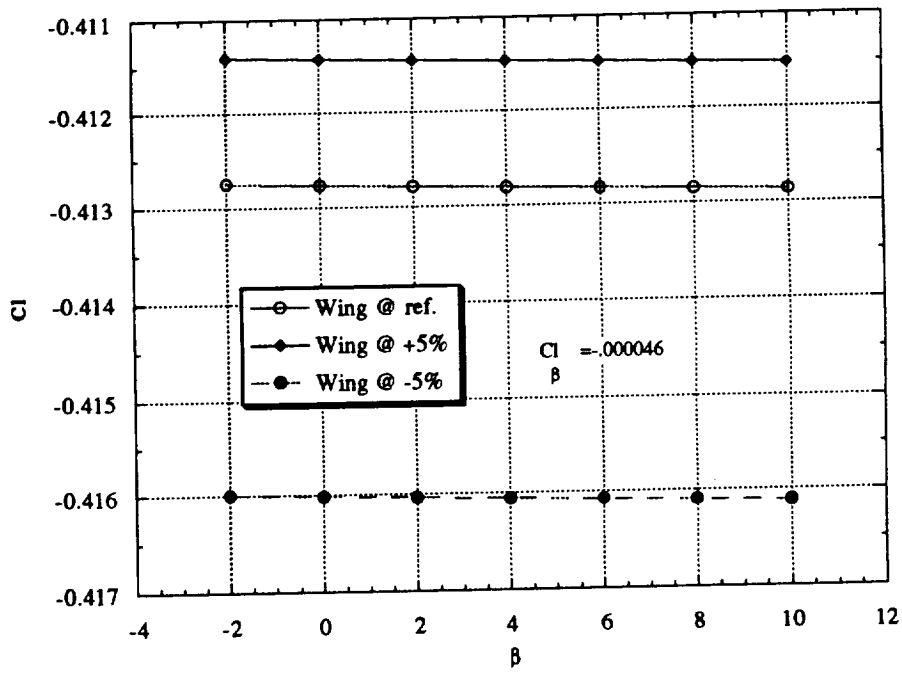

Figure 34: Case 1 - C_l Vs. β @ Mach = 2.4

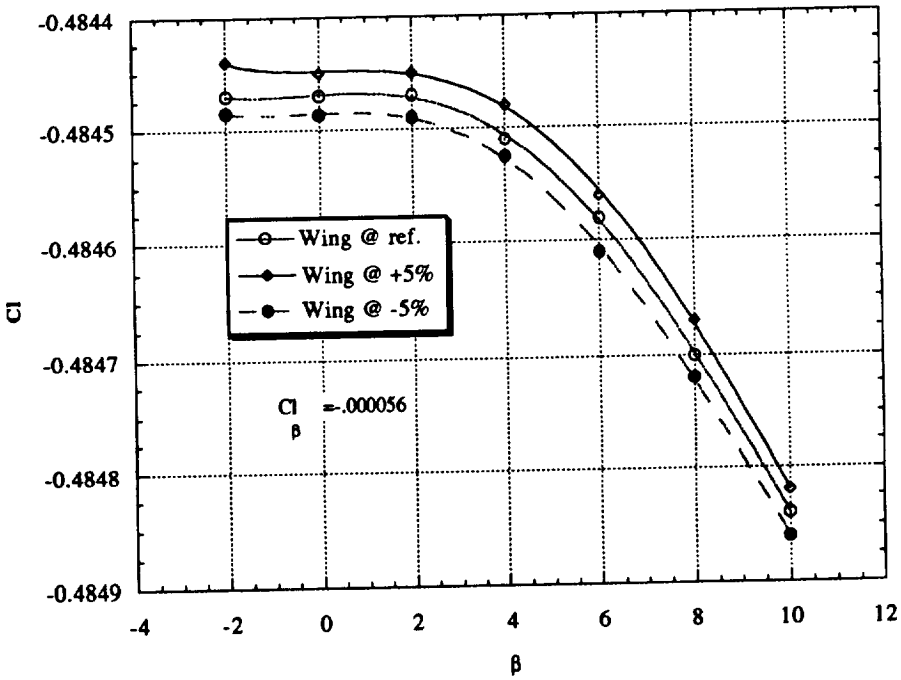

Figure 35: Case 2 - C_l Vs. β @ Mach = 0.95

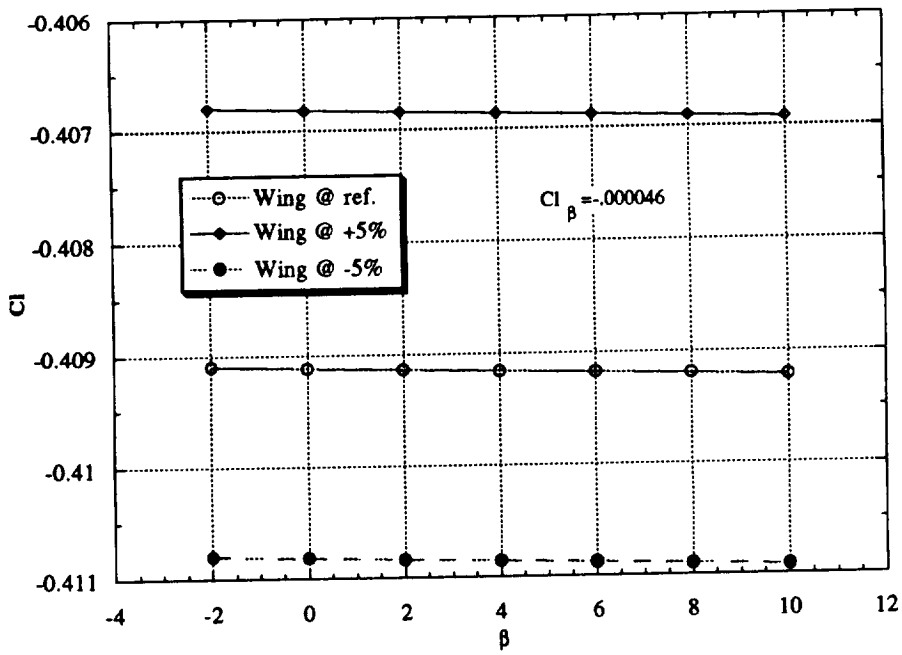

Figure 36: Case 2 - C_l Vs. β @ Mach = 2.4

A difficult task then emerged: How could these results (and stability and control issues in general) be used in the design process? One possible answer is to use stability information to rule out some of the configurations being considered. In other words, stability and control requirements can be used as a constraint that must be satisfied. In order for a particular configuration to be considered feasible it must satisfy the stability requirements. Given the fact that the average APAS run takes only about five minutes, it is obvious that if the number of configurations could be reduced by using APAS, the design process would become that much more efficient. Reduced analysis time also translates into a cost savings product, which is a very important goal in the Georgia Tech Design Methodology.

2.1.4.3 Taguchi Parameter Design Optimization Methods (PDOM)

Dr. Genichi Taguchi has been working towards the development of new methods to optimize the process of engineering experimentation for over forty years. His techniques, known as the Taguchi methods, contributed greatly to the significant changes in quality engineering methods being applied in this country[19].

Taguchi believed that the best way to improve quality was to design and build it into the product. According to his three most popular theories; quality concepts should be based upon and developed around the philosophy of prevention. The product design must

be so robust that it is immune to the influence of uncontrolled environmental factors. His second concept deals with actual methods of affecting quality. He contended that quality is directly related to deviation of a design parameter from the target value, not to conformance to some fixed specifications. Finally, his third concept calls for measuring deviations from a given design parameter in terms of the overall life cycle costs of the product[19].

The Taguchi method, as applied to aircraft design at Georgia Tech during the aerospace systems design process, is summarized in Figure 37 and is one way to optimize a chosen criterion. This technique plays a vital role in Georgia Tech's CE methodology in addressing the robustness of the design alternatives (see Fig. 3). The advantages of using Taguchi methods include:

- Increased efficiency of the simulation process
- Brings robustness into the design
- Simplification of simulation models
- Determination of "optimal" regions and reduction of the design space for optimization
- Incorporation of Risk analysis in the design process
- Generation of sensitivities of the factors

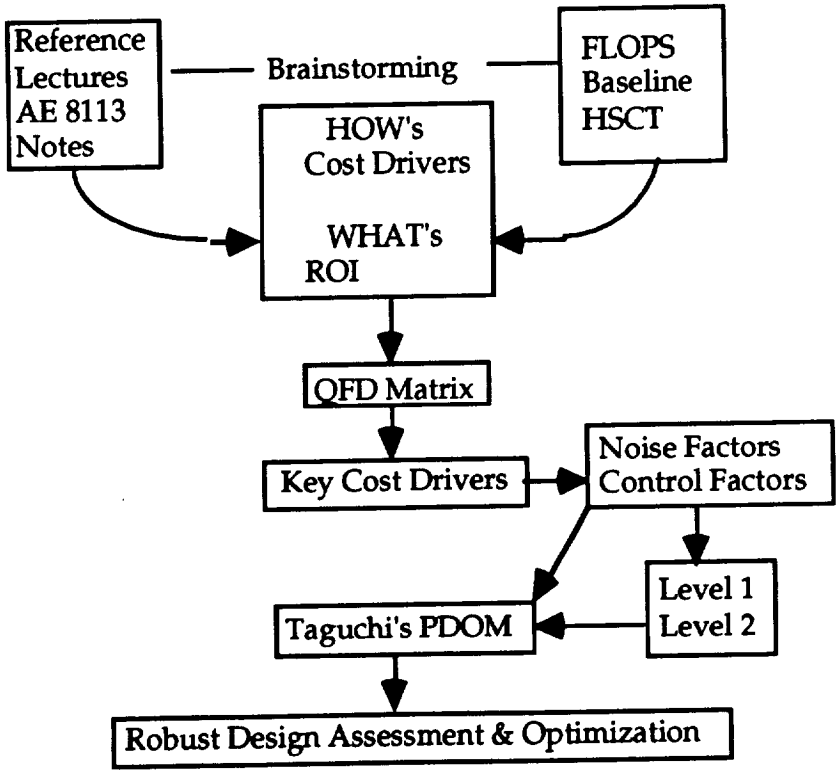

Figure 37: HSCT Economic Sensitivity Assessment Methodology

The Taguchi method implements a partial factorial design of experiment instead of a full factorial experiment to reduce the costs associated with numerous tests or simulations. The conditions for each factor in the partial factorial experiment are determined by a set of

orthogonal arrays (OA). An OA or "balanced" array is defined as a standardized, balanced table used to determine the influence that each of the control factors have on the Overall Evaluation Criterion (OEC) using the least number of experiments[19]. These OAs are then used to lay out the design of experiments. Since the emphasis of this study is to provide a way to investigate feasible alternatives in the most cost effective manner, great benefits can be achieved by the incorporation of Taguchi's techniques.

Taguchi's PDOM implementation is comprised of the following steps (see Figure 38):

- Identification of the Quality Characteristics and Design Parameters through brainstorming
- Design of Experiment(s)
- Selection of suitable simulation method(s)
- Simulation Results Interpretation
- Determination of "Optimal" Conditions
- Confirmation of the "Optimal" Conditions

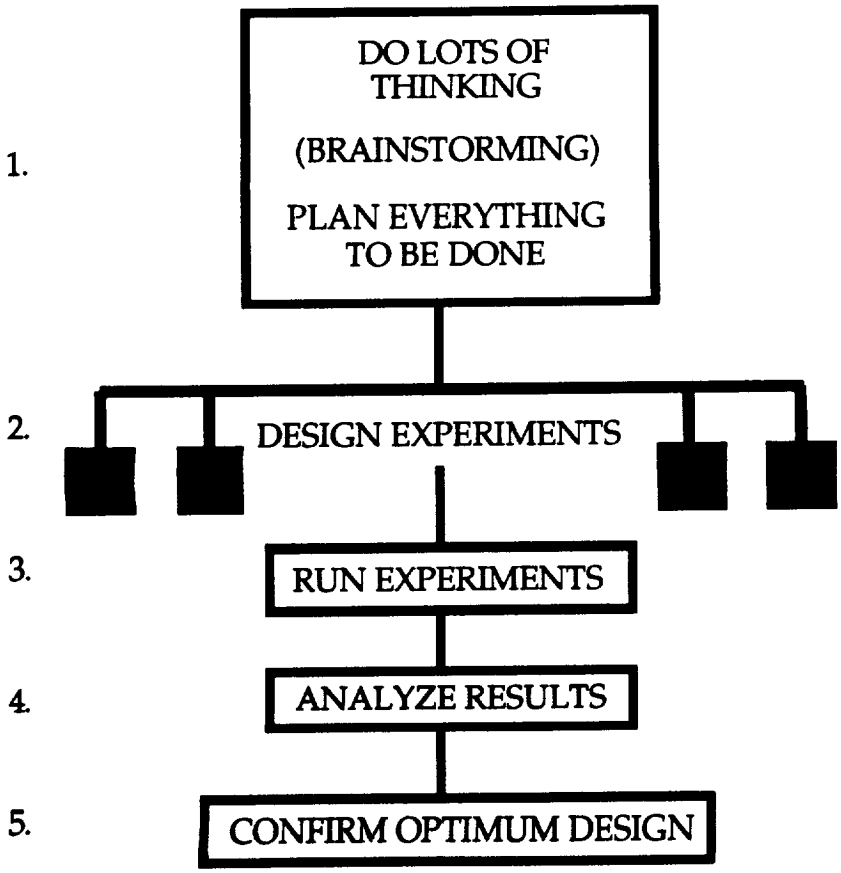

Figure 38: The Taguchi Method Flow Chart

In order to design an experiment, it is necessary to select the most suitable orthogonal array, assign the factors to the appropriate columns, and describe the trial conditions. Through a series of brainstorming sessions, the various, relevant design

variables that may be used as inputs by the selected simulation/analysis tools are determined. The next step is to design the experiments and choose the control and noise factor levels. Control factors are defined as those variables (design parameters) that can be controlled, while noise factors are those factors that are either too expensive to control or cannot be controlled but have significant impact on the results of the experiment[19]. Level 1 settings were chosen so as to represent low risk technologies, while level 2 settings corresponded to medium risk technologies.

2.1.4.4 Aircraft LCC Analysis and Synthesis Simulation Method

In order to conduct the sensitivity analysis using the Taguchi Experiment set up above, a suitable simulation model was needed. The Aircraft Life Cycle Cost Analysis (ALCCA) program provided that capability. ALCCA was developed by researchers at NASA Ames Research Center over a twenty year period, and has been enhanced in-house at Georgia Tech by Dr. Dimitri Mavris. ALCCA is capable of carrying out economic sensitivity studies for both subsonic and supersonic aircraft, while providing such information as

- Aircraft Manufacturing Costs
- Production and RDT&E Costs
- Production Cost vs. Quantity Comparisons
- Manufacturer Cumulative and Annual Cash flow
- Manufacturer Return on Investment
- Manufacturer Cost Analysis
- Airline Direct Operating Costs
- Maintenance Cost and Labor
- Airline Indirect Operating Costs
- Airline Return on Investment
- Airline ROI - Operations
- Average Yield / Available Seat Mile
- Average Yield / Revenue Passenger Mile
- Average Ticket Fare

Figure 39 displays a flowchart of the ALCCA program based on relating the airline and manufacturer ROI to the selling price of the aircraft.

Component weights and powerplant/mission information needed by ALCCA can be estimated by any aircraft sizing and synthesis code. For this study, the FLight OPtimization System (FLOPS), a synthesis code developed at NASA Langley Research Center, was selected to provide all necessary sizing information. This code is a multidisciplinary system of computer programs for conceptual and preliminary design and evaluation of advanced aircraft concepts. More specifically, the program consists of nine different modules: weights, aerodynamics, engine cycle analysis, propulsion data scaling and interpolation, mission performance, takeoff and landing, noise footprint, cost analysis,

and program control. Although FLOPS already has a built in economic analysis capability, developed by Dr. Vicki Johnson, it is only suitable for subsonic aircraft. Therefore, ALCCA was selected for the study as a more suitable cost analysis method for supersonic aircraft.

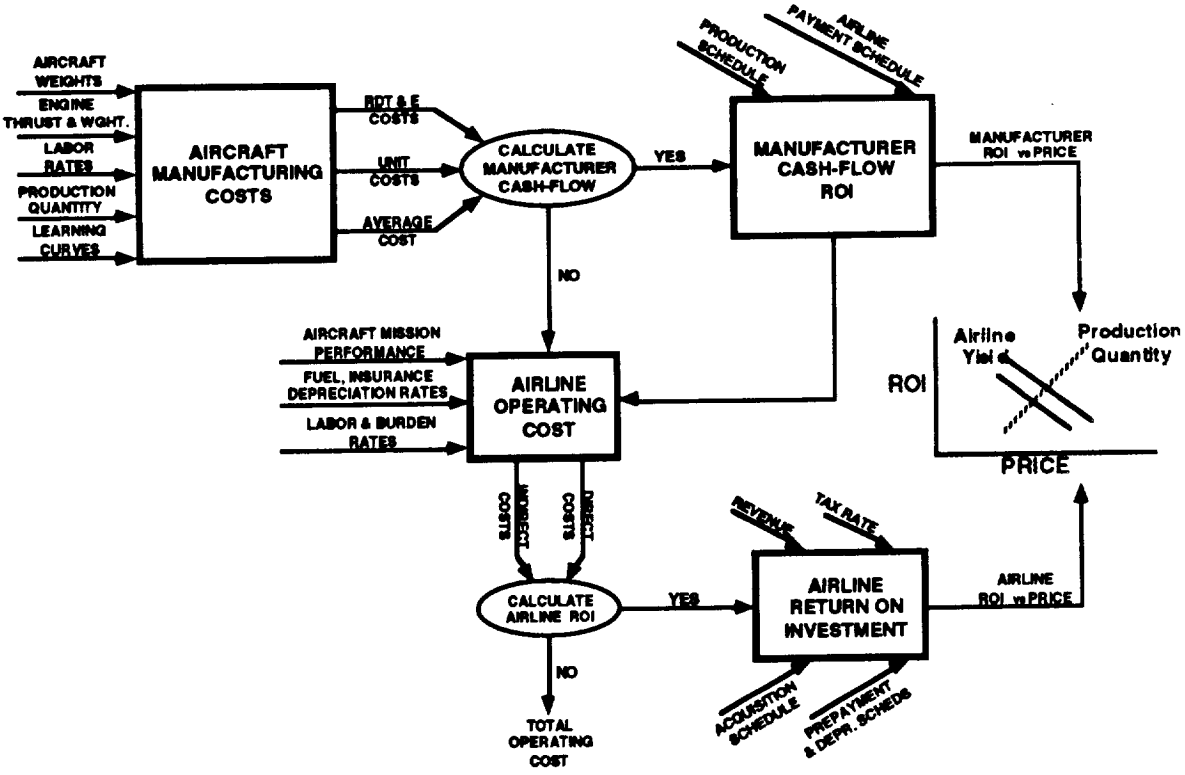

Figure 39: ALCCA Flowchart

2.1.4.5 Test of Economic Analysis on the Baseline[1]

Before embarking on the preliminary design methodology, a test case was run in order to determine if the LCC analysis program would be suitable for this experiment. A list of control and noise factors were selected to model the experiment. Four of the chosen factors were found to affect directly the various component weights and, in general, the aircraft size; Mach #, Range, Payload, % composites. Therefore, before ALCCA could be run, FLOPS had to be called upon four times to account for these variations. The total weight of the aircraft varies depending upon which level is chosen for the design range. Using FLOPS to calculate the individual component weights, the percent of advanced technology light-weight composite materials in ALCCA was also taken into account to determine their effect on the LCC of the system. ALCCA uses five different variables to identify the percent of composite material to be used: zero percent indicates conventional

materials while one hundred percent denotes the maximum use of composites. The values input into ALCCA for the two composite material levels were zero percent and sixty percent. The values for the different component weights were computed with and without composites at a range of 5,000 nmi. and 6,500 nmi. Once these values are obtained from FLOPS, they were then inserted into the ALCCA program to perform the necessary life cycle cost analysis for a HSCT.

Since in this case, the analysis was carried out from an airline's point of view, the ROI for the manufacturer was used as a noise factor, while the ROI for an airline was considered to be a factor that airlines can control or select. The ROI for the airline was allowed to vary between eight and twelve percent, while the levels for the manufacturer's ROI were chosen to be between ten and fourteen percent. Since there were concerns associated with the feasibility of a low cost, supersonic transport, the values for the ROI ranges were conservatively selected. At these levels, a corresponding average yield / RPM was calculated in order to achieve the specific ROIs for the airline and manufacturer.

Table VI. Economic Sensitivity Analysis Ground Rules and Assumptions

HSCT Production scheduled for the year 2000
Estimates are in 1994 U.S. dollars

Performance	Cruising altitude at 70,000 ft. 100% learning curve for propulsion Four engines / aircraft
Weights/Interior Crew	Three person crew Coach Passengers / Flight Attendant is 38 First Class Passengers / Flight Attendant is 11 Airline revenue is based on a load factor of 65% Aircraft component weights are estimated from a synthesis code
Spares	6% of total airframe price 30% of total engine price
Rates	Labor rate of $19.50 / hr Tax rate of 34% Inflation rate of 8%
Burden	200% of labor
Financing	100% @ 10.25% interest rate 0% down payment
Insurance	Hull insurance is 0.35% of aircraft cost
Depreciation	15 years; 10% residual

Several assumptions had to be made in order to run the ALCCA program, and a list of the most significant ground rules/assumptions is presented in Table VI. As far as the use of composites is concerned, although composites are in general lighter in weight, they are usually more expensive. Figure 40 summarizes complexity factors for various

conventional and advanced materials. For this study, a $55/lb graphite epoxy material was used that has complexity factor of 1.03 or 3% more than aluminum. In addition to this list, another simplifying assumption was made regarding the component weights. These component weights change in actuality not with respect to the percent composites used and the flight range, but also vary with respect to changes in the design cruise Mach number. If more precise results were to be obtained, then FLOPS could be run an additional four times for the different Mach numbers, and new component weights would need to be calculated before performing the cost analysis on the aircraft. ALCCA was modified in order to treat the ROI for the airline as an input. A corresponding average yield increment was also included in the program to create tables based on certain yield per RPM (i.e. $0.10 - $0.13/RPM). This approach is aimed at comparing the average yield per RPM for a HSCT to the average yield / RPM for aircraft similar in size to the Boeing 747-400.

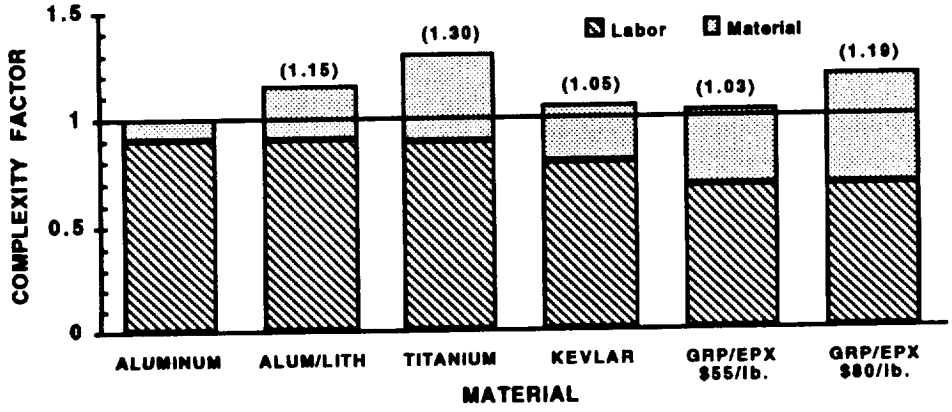

Figure 40: Complexity Factors

The finalized list of control and noise factors with respect to ALCCA are displayed in Table VII and VIII, respectively. As mentioned previously, these factors were identified with the help of the LCC QFD matrix. These variables were subsequently used to define an orthogonal array. An L_{16} matrix was used to represent the control factors in the inner array, while an L_4 was used for the noise factors in the outer array (Table IX).

Table VII. Control Factors as They Relate to the ALCCA Program

Factors	ALCCA Variables	Level 1	Level 2
Cruise Mach #	CMACH	2.0	2.6
Engine Cost	CTJI	$60 Million	$40 Million
% Composites	PWBODY	0%	60%
ROI Airline	RTRTNA	4%	12%
Payload	WPAYL	58,800 lbs. 280 passengers	67200 lbs. 320 passengers
Utilization	U	4,000 hrs.	6,000 hrs.
MTTR	ERR	5,000 hrs.	15,000 hrs.
Learning Curve	LEARN	90 %	75%
Turn Around Time	GRNDTM	2 hrs.	0.75 hrs.
Range	SL	5,000 nmi.	6,500 nmi.

Table VIII. Noise Factors as They Relate to the ALCCA Program

Factors	ALCCA Variables	Level 1	Level 2
Fuel Cost	COFL	$0.17 / lb.	$0.09 / lb.
Manufacturer's ROI	RTRTN	10%	14%
Production Rate	NV	400	700

2.1.4.5.1 Simulation Interpretation

Once the sixty-four (16 x 4 trials) simulation runs are completed, the results are extracted from ALCCA and are placed in the corresponding "simulation results" columns of the complete OA. Next, the influence of each factor on the quality characteristic is determined by evaluating the main effects and their influence in a qualitative way. Then, through an ANalysis Of VAriance (ANOVA) technique[19], the relative influence of the individual factors is identified to provide a measure of confidence in the Taguchi Method results. The Signal to Noise (S/N) ratio for each case is calculated to examine the variability associated with the multiple trial results. The S/N ratio is the variance index that is determined by the results obtained by repetition. Regardless of the type of quality characteristic selected, the transformations are such that the S/N ratio is always interpreted the same way: the larger the S/N ratio the better. The greater the Signal to Noise ratio, the smaller the variance around the target value. The Signal to Noise ratio is based on the mean square deviation (MSD) from the target value of the quality measure (i.e. yield/RPM). The MSD can be calculated several ways depending on the quality characteristic that is chosen[19]. For example if the quality characteristic is *smaller is better*, the MSD is calculated as follows:

$$MSD = \frac{(y_1^2 + y_2^2 + \ldots)}{n}$$

where y_is are the results of the experiments, and n is the number of repetitions. The S/N ratio can then be computed as follows:

$$S/N = -10 \log_{10}(MSD)$$

The three quality characteristics available for determining the *optimal* condition are:

- "smaller is better"
- "nominal is best"
- "bigger is better"

For a HSCT, the overall evaluation criterion selected was the average yield / RPM; therefore, smaller is better. The analysis will therefore answer the following questions:

- "What is the optimum condition?"
- "Which factors contribute to the results and by how much?"
- "What will be the expected results at the optimum condition?"[16]

2.1.4.5.2 The Experiment

In the first part of the project, ten control factors, one interaction between factors, and three noise factors were identified. The objective of this experiment was to find the control factor levels (see Table VII) that would be the least influenced by changes in the noise factors (see Table VIII), and would result in the "best" combination for the airline return on investment. Since this was the first time the experiment was attempted, no *a priori* knowledge was available as to which factors are the most important ones, and thus all of them were given equal importance and kept for further study. The control factors were tested using two levels instead of three in order to minimize the number of experiments and avoid the difficulty of creating interactions between three levels. The approach presented here is best suited for determining the effect that each of the control variables has on the evaluation criterion. It is therefore used for sensitivity analyses rather than the selection of an "optimum" configuration. Since the true optimum result will most likely lie somewhere between the two levels selected, the experiment can be repeated (once the number of control factors is reduced through this analysis) with more levels producing a real optimum. The noise factors were also varied between two levels.

Table IX. The Complete Orthogonal Array for the Design of Experiments

Experiment Number \ Column Number	1	2	3	4	5	6	7	8	9	10	11	12	13	14	15	R1	R2	R3	R4	S/N Ratio
1	1	1	1	1	1	1	1	1	1	1	1	1	1	1	1	0.1938	0.1867	0.1524	0.1679	15.0923
2	1	1	1	1	1	1	2	2	2	2	2	2	2	2	2	0.1672	0.1627	0.1241	0.1341	16.5851
3	1	1	1	2	2	2	1	1	1	2	2	2	2	2	2	0.1658	0.1592	0.1264	0.1411	16.5404
4	1	1	1	2	2	2	2	2	2	1	1	1	1	1	1	0.1582	0.1526	0.126	0.1367	16.8363
5	1	2	2	1	1	2	1	2	2	1	2	2	1	2	2	0.1853	0.1784	0.144	0.1577	15.5347
6	1	2	2	1	1	2	2	1	1	2	1	1	2	1	1	0.1332	0.1295	0.1006	0.1091	18.4974
7	1	2	2	2	2	1	1	2	2	2	1	1	2	1	1	0.1605	0.1529	0.1213	0.1375	16.8425
8	1	2	2	2	2	1	2	1	1	1	2	2	1	2	2	0.188	0.1819	0.1458	0.1582	15.4243
9	2	1	2	1	2	2	1	2	1	2	1	1	2	1	1	0.1669	0.1602	0.1306	0.144	16.4153
10	2	1	2	1	2	2	2	1	2	1	2	2	1	2	2	0.1531	0.149	0.1149	0.1243	17.3111
11	2	1	2	2	1	2	1	1	2	2	2	2	2	1	1	0.1655	0.1598	0.1234	0.1356	16.6484
12	2	1	2	2	1	2	2	2	1	1	1	1	1	2	2	0.1564	0.1518	0.1218	0.1311	17.0155
13	2	2	1	1	2	2	1	1	2	1	1	2	2	1	1	0.2056	0.1972	0.1573	0.1742	14.6773
14	2	2	1	1	2	2	2	2	1	2	2	1	1	2	2	0.1433	0.1389	0.1059	0.1156	17.9312
15	2	2	1	2	1	2	1	2	1	2	1	2	1	1	1	0.1325	0.1274	0.1006	0.1113	18.512
16	2	2	1	2	1	2	2	1	2	2	2	1	2	2	2	0.1478	0.1438	0.1126	0.1207	17.5839

Factor	Level 1	Level 2
Block Speed	2.00	2.60
Engine Cost	60M	40M
Interaction 8 x 11	N/A	-
% Composite	0	0.60
ROI Airline (%)	8	12
-	-	-
Payload	58,800	67,200
Utilization	4,000	6,000
-	-	-
-	-	-
MTTR	0.0002	0.000067
Learning Curve	0.90	0.75
Turn Around Time	2.00	0.75
Range (miles)	5,755	7,480
-	-	-

	Fuel Cost	Manufacture ROI	Production Rate
Level 1	0.17	10	400
Level 2	0.09	14	700
Columns	1	2	3
1	1	1	1
2	2	1	2
3	3	2	1
4	4	2	2

The OA selection was based on existing arrays found in Ref. 19. This selection process is significant in setting up the design of experiments. An L_{16} inner orthogonal array was selected for the control factors, since an L_{12} is not suitable for the analysis of interactions. The L_{16} orthogonal array calls for sixteen simulation runs to be conducted, which by definition is a set of trials equivalent to conducting $2^{15} = 32{,}768$ possible combinations that yield an indication of the "optimum" combination. Notice in Table IX that there is an interaction between Utilization and MTTR, which was placed in Column three.

The three selected noise factors were placed in the L_4 outer orthogonal array. The ones and twos in the inner and outer matrices represent the levels at which those factors should be set during the experiment. These two arrays have been combined in the manner shown in Table IX to form the complete design of experiments layout. The layout also includes a data matrix where the experiments ($/RPM) are recorded.

The four observations recorded for each simulation trial condition capture the effect that the noise factors have on the overall evaluation criterion. Once these probability distributions due to noise are computed, in addition to the mean responses, the combination of control factors that give the *optimal* result (while achieving robustness) was determined by performing an ANOVA on the results presented in Table IX.

2.1.4.5.3 Result Interpretation

In order to automate the evaluation process, a software package, Qualitek-4 (QT4)[20], developed by NUTEK, Inc. was used. Once the quality characteristic was decided (average yield / RPM) and the results were obtained from ALCCA, the next step was to evaluate the S/N ratio based on the MSD. The main effects of the S/N ratio on the control and noise factors were computed with the help of QT4, and an Analysis of Variance Analysis (ANOVA) was subsequently performed using this information to determine the *optimal* condition for the quality characteristic of "*smaller the better*", as well as their relative contributions. Since no *a priori* knowledge existed on the feasibility of a $0.10/RPM, a 20% increase was assumed to be a reasonable guess. Therefore, a target value of $0.12 dollars per RPM was used. Figure 41 illustrates the result distribution obtained by running the sixty-four experiments.

After the analysis was carried out, the control factor level combinations that yield the *optimal* configuration were obtained (see Table X). The control factors not listed in this chart were found to have a very small effect on the measure of quality, and were thus "pooled" together. The findings presented in Table X are best illustrated in Figure 42, where the relative importance of each factor is shown quantitatively. For example, the

manufacturer's learning curve was found to have the largest effect on the total system, which means that any improvements that can be made on reducing first unit cost (lean aircraft initiative) or simply lowering the learning curve for a given production lot will reduce significantly the aircraft acquisition cost, and consequently, the average yield per RPM. On the other hand, if a factor like the Mean Time To or Between Repairs (MTTR) is varied, a minimal variation of the overall evaluation criterion will be observed.

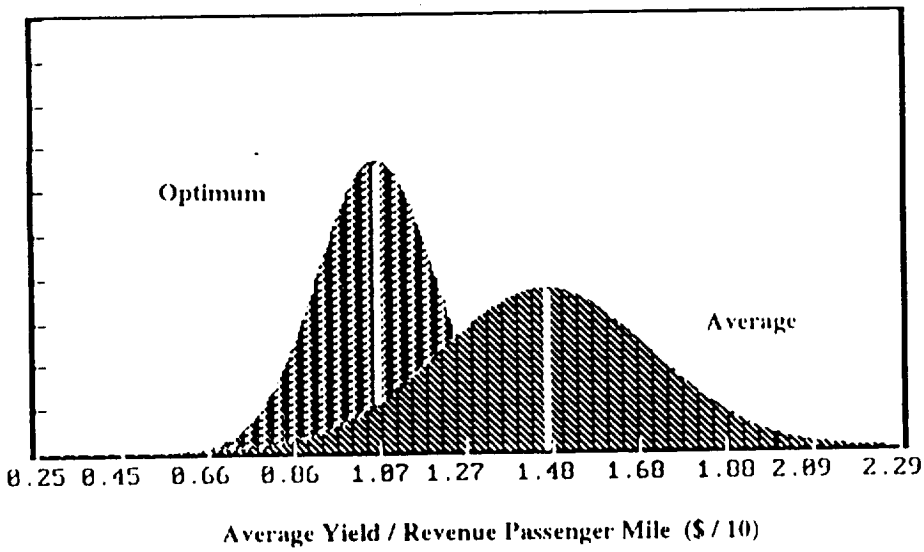

Figure 41: $/RPM Variations for All Experiments Performed Including the "Optimum" Distribution

Table X. The *Optimal* Configuration for the "Smaller the Better" Quality Characteristic Case

Control Factors	Level	Description	% Influence
Cruise Mach #	2	M=2.6 at cruise	7.25 %
Engine Cost	2	40M dollars	2.05 %
% Composites	2	60 %	3.59 %
ROI Airline	1	8%	3.89 %
Payload	2	67200 lbs.	16.01 %
Utilization	2	6000 hours	15.57 %
Mean Time to Repair	2	1/15,000 hrs	0.46 %
Learning Curve	2	75%	34.53 %
Range	1	5,000 naut. miles	15.19 %

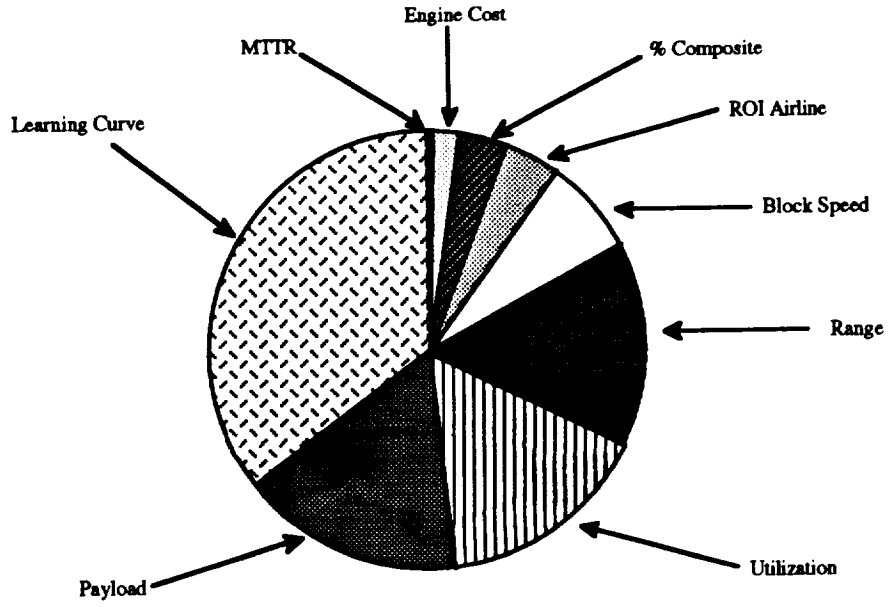

Figure 42: Control Factor Influences on Average Yield / Revenue Passenger Mile ($/RPM)

For the *optimal* condition, the analysis selected an airline ROI value of 8% and a payload of 67,200 lbs, which corresponds to a passenger count of 320. The learning curve level was assigned to be 75%, while the range was set at its lower value of 5,000 nautical miles.

The average signal to noise ratio was calculated to be 16.7157 for this "*smaller the better*" case. Using this ratio, the *optimal* configuration listed in Table X was obtained. The "minimum" expected average yield / RPM was found to be **$0.104**/RPM, which corresponds to an aircraft acquisition price of $227.85M (see Figure 43 for "best" and "worst" distributions) and an average ticket fare of $606.788 (Figure 44). This $/RPM result corresponds to just a four percent increase over the minimum assumed yield for the equivalent subsonic transports, and it corresponds to an expected improvement of **17.39%** with respect to the worst case scenario depicted in Figure 44.

In order to understand the influence that the various control factors have on the evaluation criterion, the levels were allowed to vary from the best level to the worst, one at a time. The results from this exercise are presented in Table XI. As can be seen from this table, the average yields are higher than the optimum, but within the acceptable range (compared to existing long range subsonic transport ticket fares) for most of the cases examined. For example, if the manufacturer's learning curve was allowed to vary from its *optimal* level of 75% to its highest allowable value of 90% (see Table XI), the overall evaluation criteria will vary from $0.104/RPM to $0.12/RPM. This example indicates how

variation with respect to a given control factor affects the *optimal* condition as it is determined by PDOMs. Since the noise factors can not be controlled, there are no set levels for these factors; thus, a variation from the target value will always occur. It is due to these noise effects that Figures 41, and 43-45 show variation rather than singular values.

The interaction between MTTR and Utilization that was incorporated into the inner array turned out to have a minimal effect and was pooled together with other small values. When transferring the factors into QT4, this interaction was thought to be significant. However, it turned out to be very weak due to the fact that the sizing program (FLOPS) and ALCCA did not take into account this relationship.

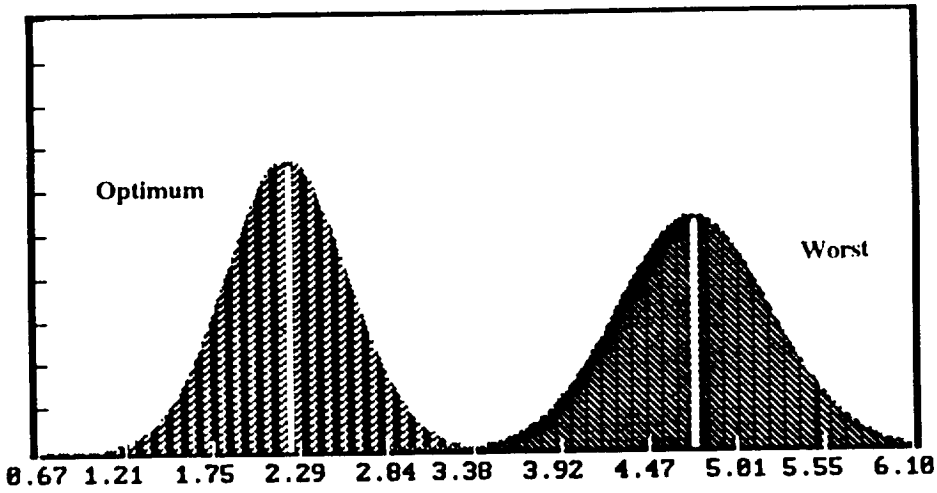

Figure 43: Aircraft Acquisition Price Variation for the "Optimum" and "Worst" Conditions

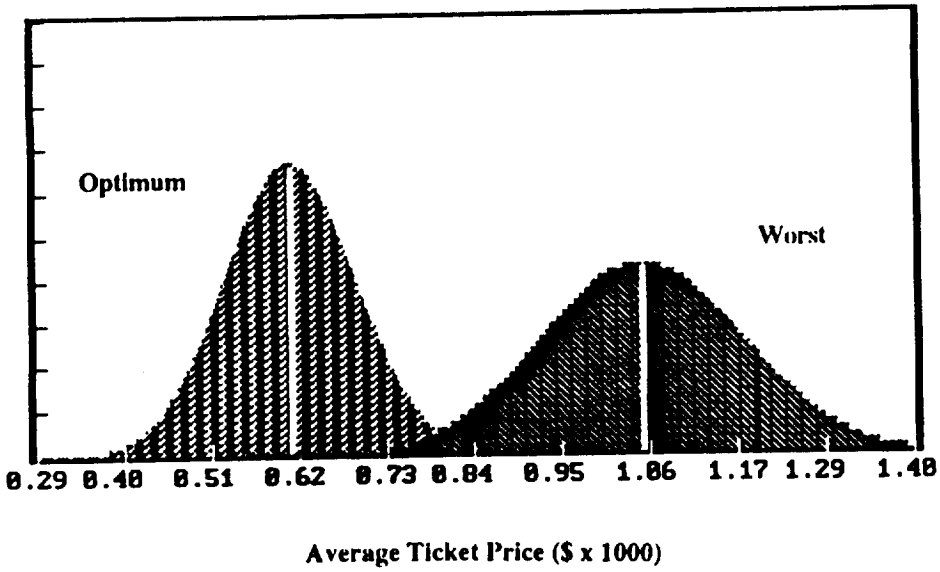

Figure 44: Average Ticket Price Variation for the "Optimum" and "Worst" Conditions

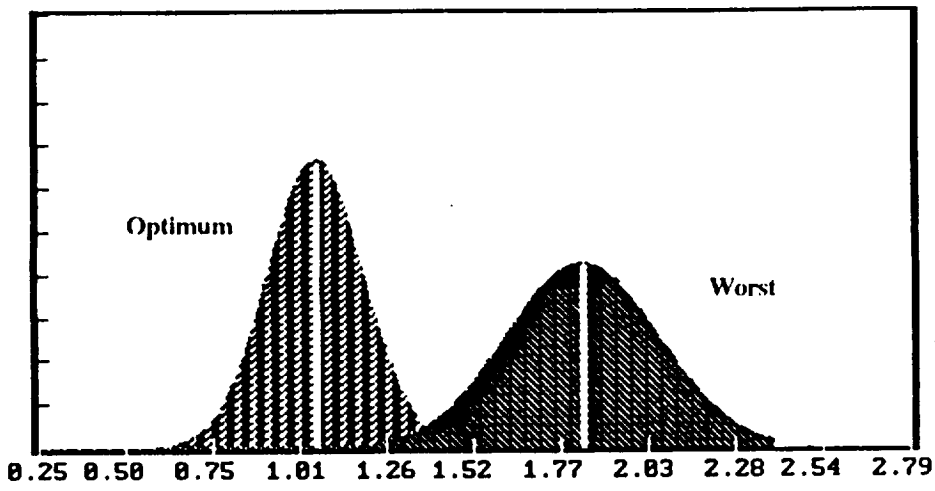

Figure 45: $/RPM Variation for the "Optimum" and "Worst" Conditions

Table XI. Change in Average Yield per RPM from the "Optimum" Condition

Control Factors	Levels	$/RPM
Learning Curve	2 to 1	0.120
Payload	2 to 1	0.115
Utilization	2 to 1	0.115
Range	1 to 2	0.114
Block Speed	2 to 1	0.111
ROI Airline	1 to 2	0.109
% Composites	2 to 1	0.109

2.1.4.5.4 Confirmation Test

The final step of the Taguchi PDOM is to run a test to confirm the "optimum" condition. Using the levels obtained for the *optimal* configuration as determined from the QT4 program, a confirmation test was executed using ALCCA. The results obtained from this test verified the optimum condition and are displayed for review in Table XII.

Table XII. The "Optimum" Condition Confirmation Results

	$/RPM
Result #1	0.1198
Result #2	0.1166
Result #3	0.0903
Result #4	0.0977

As previously mentioned, the average yield per RPM for the optimum condition was $0.104. The average of the four confirmation test cases gives a value of $0.106 per RPM. This variation is due to the noise factors, which is the reason why the confirmation run has four different values. The confirmation test verified that the *optimal* condition is viable.

2.1.4.6 Top Level Orthogonal Array

The first step in Georgia Tech's preliminary design methodology is the actual generation of feasible alternatives. This is done through Taguchi's PDOM. A top-level decision orthogonal array was defined with feasible configurations characterized by the type of engine (MFTF or TBE), cruise Mach number (2.2, 2.4, or 2.6), the type of mission (all supersonic or split subsonic/supersonic), the number of passengers (300 or 320), and the wing type (conventional or advanced technology, i.e., hybrid laminar flow control). The top-level feasible alternative OA can be seen in Table XIII.

Table XIII. Top-Level Decision OA

Factors	Level 1	Level 2	Level 3
Mach #	2.4	2.0	2.6
Engine Type	TBE	MFTF	
Mission	All Supersonic	25% Subsonic	
# Passengers	300	320	
Wing Type	Conventional	HLFC	

2.1.5 Evaluation of Alternatives

The decomposition and recomposition process for each of the feasible configurations presented in Table XIII can be best illustrated by Figure 46. The methodology developed is based on breaking down the various tasks of interest into their corresponding product and process characteristics, and all relevant design and manufacturing variables that should be considered were identified. The problem was then decomposed down to the individual disciplines where the optimization tradeoffs between the product and process design parameters take place at the component level. Once the "optimal" configuration is chosen at the component level, the information is passed back to the system level where tradeoffs take place with respect to the overall evaluation criterion selected for the system.

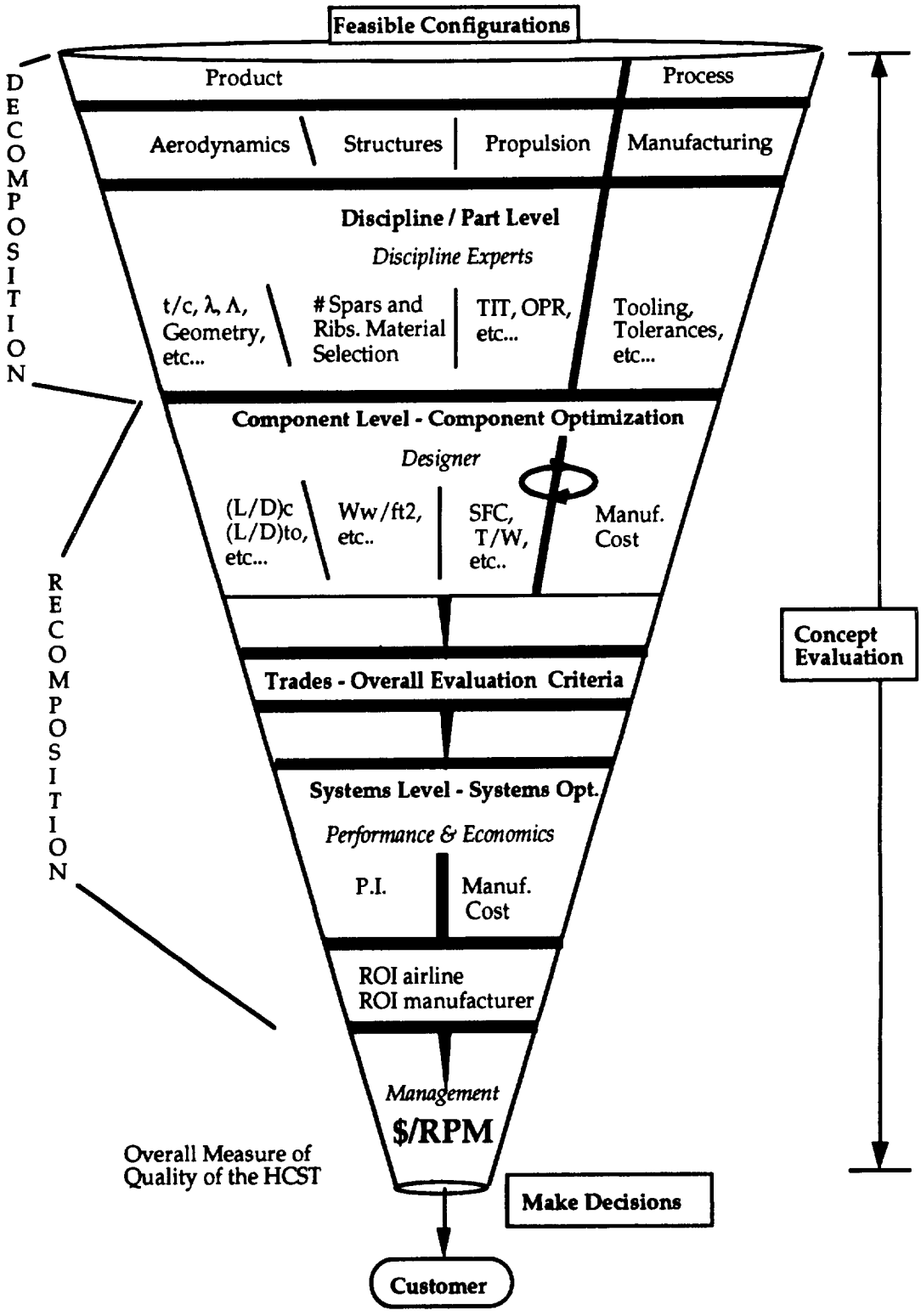

Figure 46: Feasible Alternative Evaluation Flowchart

A robust design assessment was conducted for each of these cases at the component level leading to the selection of a set of "optimal" wing/nacelle configurations. These

combinations were selected for a combined aerodynamic/structures and manufacturing point of view. Figure 47 illustrates this optimization procedure flow. Once the "optimum" wing geometry and characteristics are defined, the problem is recomposed back to the system level where the synthesis/economic analysis are performed, and the "optimum" overall configuration is chosen from an economics point of view. (Average Yield / Revenue Passenger Mile).

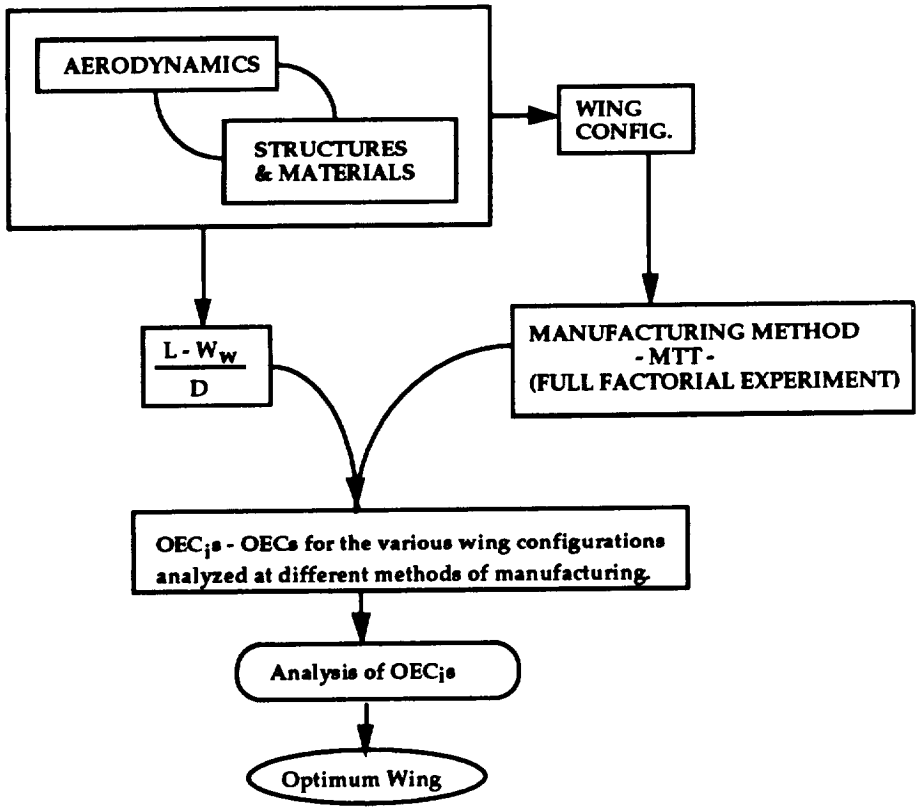

Figure 47: Wing Optimization Procedure

2.1.5.1 Aerodynamics Orthogonal Array

The following wing planform definition, displayed in Figure 48, was introduced to geometrically define both double delta and arrow wing configurations. From an aerodynamic design point of view, the performance criterion that best describes the quality of a design is the Lift to Drag ratio. In order to maximize this ratio, the "optimal" design variable settings must be determined. First, a list of key design variables for an integrated nacelle/wing configuration was composed. The control variables selected define the wing geometry, airfoil shapes, and fuselage attitude. The factors that the aerodynamicist does not have absolute control over were considered to be noise factors. The noise factors selected included the wing location, nacelle location, and nacelle size. These factors

account for the effects that handling qualities, aeroelasticity, structures, and propulsion sizing will have on the cruise L/D. Fifteen control factor variables were considered for further study. In order to reduce the size of the combined aero-structures experiment, the relative importance and influence of each of these variables was identified through a separate aerodynamics experiment (this aerodynamic study was carried out using the Boeing Design and Analysis Program (BDAP)[21]). Therefore, a preliminary Taguchi experiment was conducted to identify the factors that contribute/affect L/D the most in the chosen range of values. The control and noise variables selected for this experiment are presented in Table XIV and XV, while the relative control factor influences are illustrated in Figure 49. The results presented in Fig. 49 were obtained through an ANOVA by optimizing the Signal to Noise (S/N) ratio. The five most important design variables were: the longitudinal wing leading and trailing edge "kink" locations (X_1 and X_2 normalized by the chord root coordinate), the root t/c, maximum thickness location at the root, and the fuselage angle of attack. The average L/D ratio and corresponding standard deviation after the optimization turned out to be 8.62 and 0.30 respectively, while the average L/D ratio and corresponding standard deviation before the optimization were 8.02 and 0.30 respectively.

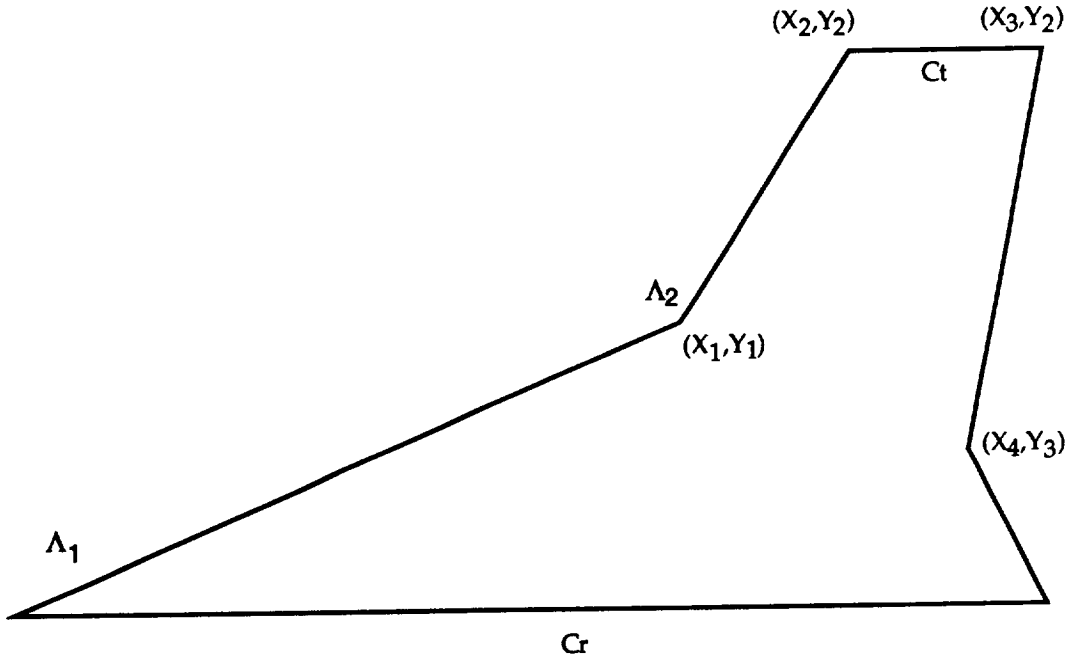

Figure 48: Wing Planform Configuration

Table XIV. Aerodynamic Experiment Control Factors

Factors	Level 1	Level 2
X1	0.667	0.767
X2	0.919	1.00
X3	1.0	1.10
X4	0.956	1.00
Y1	0.252	0.302
Y2	0.489	0.439
Y3	0.259	0.209
(t/c)r	2.9	2.7
(t/c)t	2.0	1.5
Max. Thick. @ Root	50%	60%
Max. Thick. @ Tip	50%	60%
nacelle height	-5	-7
Dist. btwn nacelles	14	18
Fuselage aoa	3°	6°
Wing Height	0%	-50%

Table XV. Aerodynamic Experiment Noise Factors

Factors	Level 1	Level 2
Scaling factor of Nacelle	1.0	1.2
Rel. Long. Loc. of wing wrt fuse.	0.289	0.239
Nacelle Placement	0.364	0.464

These most significant contributors were next used in the combined Aerodynamics-Structures-Materials OA experiment, while the rest of the aerodynamic design variables were held at the levels that yield the "optimum" L/D.

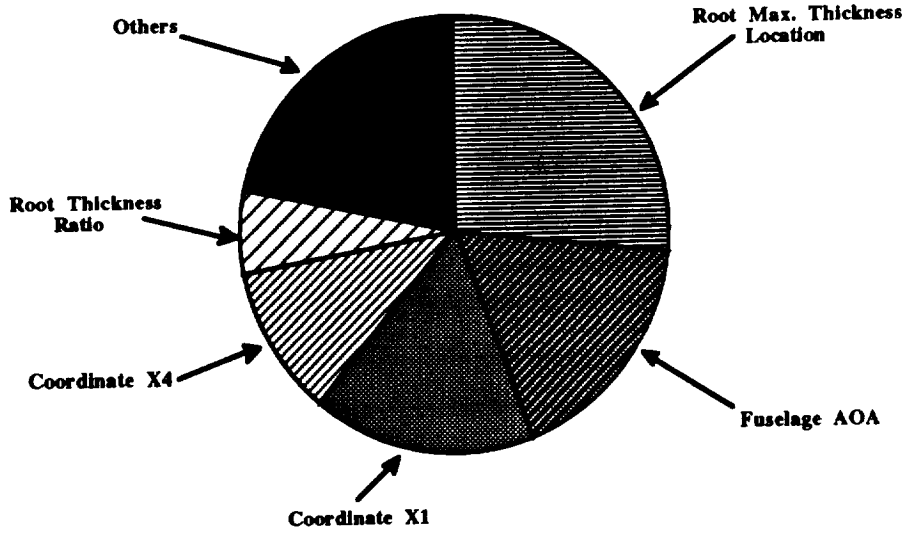

Figure 49: Control Factor Influences on the L/D Ratio for a Supersonic Mission

Table XVI shows the levels of the aerodynamic design variables that yield the best L/D. Furthermore, the design (cruise) C_L and the wing area were added as control variables to the combined aero-structures OA in order to quantify their effect on the Overall Evaluation Criterion (OEC) and account for the scaling in wing area during resizing.

Table XVI. Optimal Aerodynamic Control Factor Levels

Design Variables	Optimal Level
X1	2
X2	2
X3	2
X4	1
Y1	1
(t/c)root	2
(t/c)tip	2
(m)root	1
fuselage aoa	1
Wing Height	2

2.1.5.2 Aerodynamics, Structures, and Manufacturing Opt. Wing

Since the focus of the methodology implementation task was the design and optimization of a Nacelle-Wing configuration, an OEC function that captures the aerodynamic, structural, and manufacturing design aspects was selected. This chosen OEC (for the wing component) is presented below as:

$$OEC_i = \alpha \left[\frac{\frac{L\text{-}W_W}{D}}{\left(\frac{L\text{-}W_W}{D}\right)_{base}} \right] + \beta \left[1 - \frac{N^i_{rw}}{N^i_{rw_{base}}} \right]$$

where L and D in this equation represent the wing Lift and Drag, W_w denotes the wing weight, and N_{rw} corresponds to the manufacturing cost.

Finally, α and β are weighting factors selected by the team members to represent the relative importance of cost with respect to the performance criterion chosen. Since the two contributing factors (product and process side) have different units, the two quantities were normalized by their corresponding baseline values. The \$/RPM still remained the overall system criterion function.

2.1.5.2.1 Combined Array: Response-model/combined-array approach to Nacelle-Wing-Fuselage Integration

Assessing robustness through the use of the outer array concept increases the number of experiments significantly since the noise array has to be repeated for every row in the control array. Due to large computer run times associated with finite element methods (ASTROS), it became evident that a further reduction in the number of experiments conducted was necessary.

It has been proposed earlier that to generate an "optimum" Nacelle-Wing configuration, the aerodynamic, structural, and manufacturing design aspects need to be integrated together in the preliminary design stage. However, the integration of considerations from different disciplines is usually not an easy task. One of the many reasons is that more computational efforts would be involved during both design analysis and synthesis processes for an integrated design. It was introduced before that Taguchi's quality engineering method can be used to increase the efficiency of the simulation process, bring robustness into the design and generate the sensitivities of the factors, etc. Although the methods have been widely used, there is still much room for improvement. In this section, the response-model/combined array approach, a modification to the Taguchi method is applied to the integrated Nacelle-Wing-Fuselage design. The limitations of the

Taguchi method, the two part experimentation strategy, and the loss-model approach are presented in the proceeding sections. In addition to these limitations, the literature of response-model/combined array approach, some of the benefits of using this approach, and the procedure of implementing this combined aerodynamic, structures and manufacturing experiments are also provided.

2.1.5.2.2 Limitations of Taguchi Method

Taguchi provides a method supported by statistical techniques and metrics to assist engineers in establishing and improving a product's quality. His principles have been widely used to design quality into products and processes (Ref. 22-25). However, this method has also received criticisms from the American statistics community (Ref. 26-28). The major argument is that the statistical techniques proposed by Taguchi are not theoretically based or efficient enough and there is still room for improvement. Alternative experimental formats, design criteria, analysis techniques, graphical tools and optimization strategies therefore have been proposed by the American statistics community to overcome the difficulties.

Relevant to the application of Taguchi method in this work, i.e., the robust design optimization by simulating design models, the limitations of Taguchi method can be classified into two categories. The first category is related to Taguchi's two-part experimentation strategy, and the second one is associated with using the signal-to-noise-ratio as the performance criterion, sometimes called loss-model approach. Further explanation is provided as follows:

2.1.5.2.3 Limitations of Two-Part Experimentation Strategy

Taguchi recommends a two-part experimentation strategy to solve the robust design problem. Using his approach, the control factors (C) are varied according to a "control array", sometimes called inner array. For each row in the control array, the noise factors (N) are varied according to a "noise array", called outer array. This is schematically represented in Figure 50. There are two major limitations associated with this inner-outer array approach:

- Very large number of runs may be required because the noise array is repeated for every row in the control array.
- Because of the structure of using both inner and outer arrays, there is no flexibility to use some of the degrees of freedom to estimate interactions between control factors and noise factors (C x N). As the idea of robust design is to select the levels of control factors

to minimize the effects of the noise factors, it is necessary to examine the C x N interactions so that the control factors that have a dampening effect on individual noise factors can be identified.

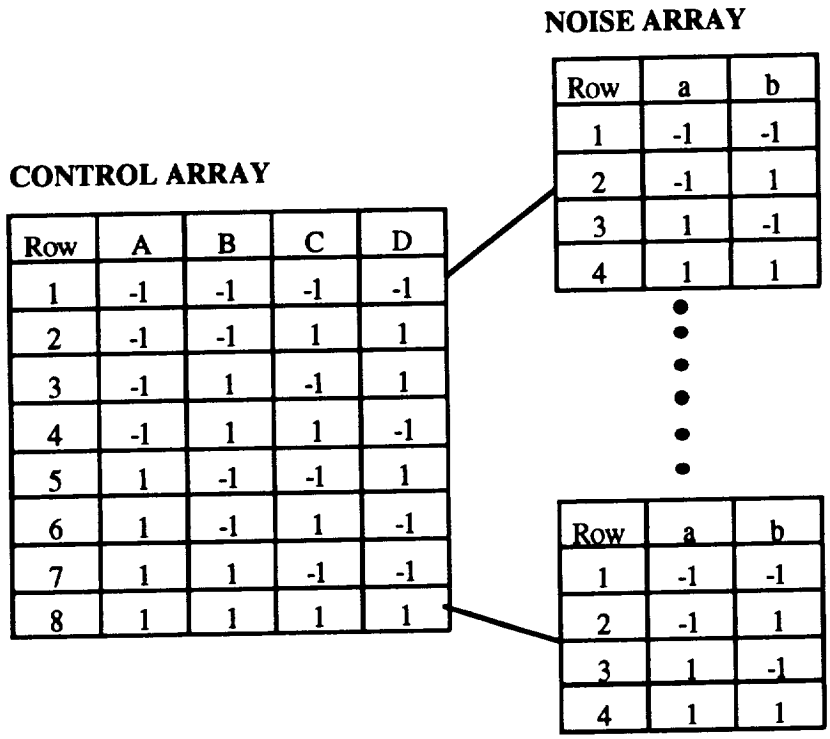

Figure 50: Two-Part Experimentation Strategy for Robust Design

2.1.5.2.4 Limitations of the Loss-Model Approach

In Taguchi's robust optimization, the objective function is to maximize the signal-to-noise ratio. Each noise array provides an estimate of this optimization criterion, represented by R, and new control-factor levels are identified by treating R as the dependent variable and examining control-factor main-effect and interaction plots and ANOVA. This approach to identifying new control-factor levels is called the loss-model approach because it is based on modeling the loss directly as a function of the control factors. There are several disadvantages of using this approach:

- The focus is on modeling R, which is often a nonlinear, many-to-one transformation of the response Y. It is less likely that R can be modeled well by a low-order linear model even if data transformations are employed.
- As the relationship between R and the control factors has not been quantified, in the case additional quality characteristics need to be considered, it is very difficult to do the

tradeoffs quantitatively. In the preliminary design of complex systems like aircraft, the considerations of multiple quality characteristics are always necessary.

2.1.5.2.5 The Use of Response-Model/Combined-Array Approach

To overcome the limitations of Taguchi method, a natural alternative is to model the response Y instead of modeling loss R and use the response model to discover control-factor values that help reduce variability. This approach is first proposed by Welch, et al. (Ref. 29) to remedy the aforementioned disadvantages in the context of computer experiments. The major elements of their approach are:

- combining control and noise factors in a single array,
- modeling the response itself rather than expected loss, and
- approximating a prediction model for loss based on the fitted-response model.

Shoemaker, et. al. (Ref. 30) further developed and strengthened this response-model/combined-array approach. They showed that run savings from using combined array are due to the flexibility that this formulation allows for estimation of effects.

Using the response-model/combined-array approach is effective in this project, due to the fact that there are large computer run times associated with finite element methods (ASTROS). It becomes evident that reduction in the number of experiments conducted is necessary. The computational time can be greatly saved by using the combined array approach (Instead of 16x4 experiments by inner-outer array approach, 16 experiments is needed using this method). Furthermore, there are several other benefits in using this approach:

- It is very easy to identify the control factors that have a dampening effect on individual noise factors by taking a look at the magnitude of the C x N coefficient in the response model equation.
- Since the response model is a low order math model, with some simple mathematical expansion, we can estimate the performance variation under different noise factor variations without running further experiments.
- The response model represents the mathematical behavior of the wing design. When later a HSCT design is integrated at the system design level, this equation can be used to estimate the wing weight value, instead of calling aerodynamic and structure analysis packages again and again.

2.1.5.2.6 Implementation Procedure of the Combined Array Experiment for the Nacelle-Wing-Fuselage Integration

To apply the response-model/combined-array approach to a HSCT Nacelle-Wing-Fuselage integration, an Overall Evaluation Criterion function that captures the aerodynamics, structural, and manufacturing design aspects will be taken as the overall quality characteristic to choose the "optimum" wing. The design objective in wing robust optimization is to maximize the mean value of OEC and minimize the variation caused by the noise factors around this mean. The eleven control factors (design parameters) are contributed by both major aerodynamic and structure design parameters, e.g., spar/rib number, material, coordinates, Nacelle placement, lift coefficient etc. Some of the noise factors include engine weight, wing area, fuel weight etc. Following the response-model/combined-array approach, we will go through the following procedure:

Step 1 Create a combined array including both control factors C and noise factors N. In this case, L_{16} standard array (16 experiments) is used for testing 11 control factors and 4 noise factors. The factors and their levels selected are presented in Table XVII.

For each of the 16 experiments, steps 2-4 are repeated:

Step 2 An aerodynamic analysis (using BDAP, WINGDES, and AWAVE) is performed to compute the corresponding L/D ratio for the wing, and the C_L distribution is used as an input to ASTROS.

Step 3 An ASTROS preprocessor is run to set up the finite element model.

Step 4 The ASTROS experiments are run to compute wing weights, etc.

Step 5 Based on the 16 experiment results, estimate control and noise main effects (C and N) and C x N interactions. During this process, normal distribution plots, interaction plots or other statistical analysis techniques will be used to identify the significance of different factors.

Step 6 The use of wing area as the response of the combined OA methodology adopted for the aero-structures experiment enables the determination of coefficients for a "wing area equation"; these coefficients will yield a more accurate wing weight for FLOPS when the aircraft is resized for a given mission.

Step 7 For each of these aero-structures combinations, a full factorial manufacturing experiment is conducted.

Step 8 A response model is fitted which represents the relationship between the response, OEC, and the significant C, N and CxN factors.

Step 9 Based on the equation obtained from step 8, the "optimum" control factors are chosen, which can maximize the mean value of OEC and reduce the variation caused by the noise factors around this mean.

Table XVII. Structure/Aerodynamic/Material/Manufacturing Combined Control and Noise Factors

Control Factors	Level 1	Level 2
# Spars/# ribs o/# ribs i	4/10	6/8
Material selection	Medium Risk	High Risk
Coordinate X1	0.667	0.767
Coodinate X4	0.956	1.00
Root (t/c)	2.9%	2.7%
Coordwise Location of Max. Thick. @ Root	50%	60%
Nacelle Placement	0.364	0.464
Fuselage aoa	3°	6°
Tip (t/c)	2.0	1.5
Lift Coefficient	0.09	0.11
Coordinate X3	1.00	1.10
Nac. Size / Eng. Wt.	35 ft / 17,000	42 ft. / 22,000
Wing Area	8,500 ft^2	10,000
Horiz. loc. of wing	0.289	0.239
Fuel Weight	350,000	500,000

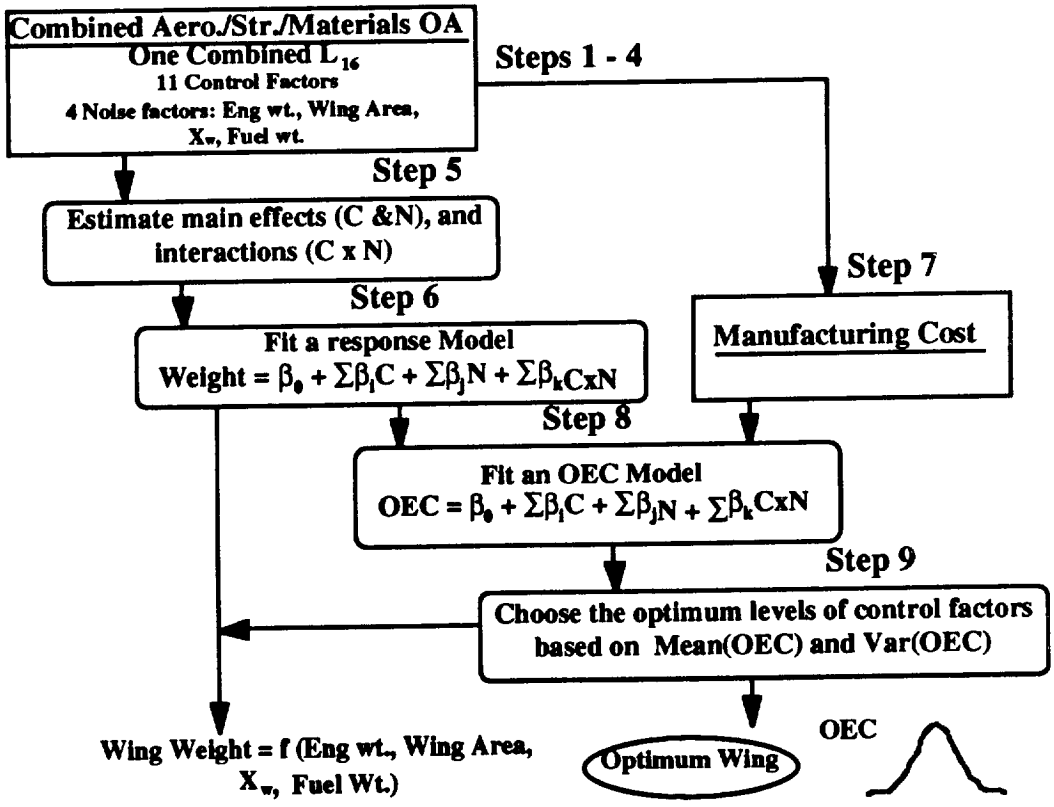

Figure 51: Combined Orthogonal Array

The steps are depicted graphically in Figure 51. The result from step 9 yields a robust "optimum" design for a HSCT wing. The wing weight equation, the optimum wing and the distribution of OEC will be brought as the input information to the next design stage.

A design of experiments was set up to determine the minimum wing weight and the corresponding variation distribution from this optimum. For this case, the wing taper ratio, sweep, t/c, wing area, nacelle placement, number of spars, beams, and ribs, the skin thicknesses, etc. were allowed to vary in order to obtain this "optimum" wing.

From the first case from the uppermost orthogonal array, which is for an all supersonic mission at Mach 2.4 using a turbine bypass engine as well as the information contained in the aerodynamics/structures orthogonal array, sixteen cases in ASTROS were run.

Two combinations of spars and ribs were considered in the design. The first combination included four main spars on the aft wing, ten ribs on the outboard portion of the wing and seven ribs along the inboard and forward section. The second spar and rib combination uses six main spars in the inboard section of the wing, eight ribs on the outer portion of the wing and seven ribs along the inboard and forward section.

To study the structural aspects of the design, a finite element code, ASTROS (Automated STRuctural Optimization System[31]), was used. ASTROS can be used to test the effect of different types of materials, structural concepts on wing weight, aeroelastic behavior, flutter, and manufacturing cost. It is uniquely suited for flight applications because performance considerations such as flutter can be addressed. ASTROS allows the user to input an initial design and then optimize it for weight by imposing constraints. For the cases considered in this project, the wings were analyzed at full and empty fuel conditions for a 2.5 g pull up maneuver, making sure that all flutter and material strength constraints were satisfied.

For each simulation run, the C_L distribution corresponding to the selected wing planform was provided to ASTROS from BDAP as well as the material(s) chosen. The actual materials were selected by carrying out a critical point design on the wing. According to this technique, three to four points were selected on the wing based on high load or stress concentration. The wing was then divided into regions as seen in Figure 52 that include these critical points, and it was assumed that the same material and manufacturing process will be used for every part in the region.

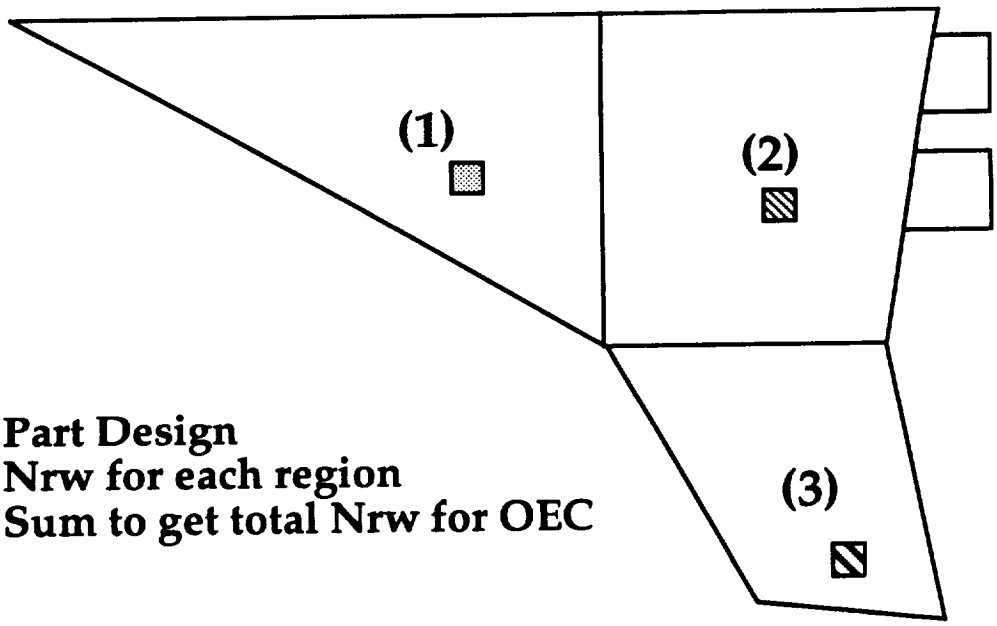

Figure 52: Wing Manufacturing Consideration, Three Point Design

All wing spars and ribs were assumed to be made of the titanium-aluminum alloy Ti-6Al-4V, while the material for the skin of the wing selected depended on the wing section location. As mentioned previously, three sections were chosen on the wing, and the materials were chosen for each section as shown below in Table XVIII:

Table XVIII. Material Selection

Section	Medium Risk	High Risk
Forward	IM7/520	MR50/5208
Inboard	Ti-6Al-4V	Ti-6Al-4V
Outboard	T650-35/R8320	Apollo-55-800/K111

ASTROS was run next to determine the corresponding wing weight for each of simulation cases that were set up. The results of each case were analyzed, and the most influential contributing factors were identified along with the optimum level combination and the risk associated with the design choices made. Next, the designer's production cost trade-off tool[32] were used to determine the cost of the wing structure, and the results of this investigation were then incorporated along with the wing weight distribution into FLOPS and ALCCA. The approach outlined in the previous two tasks was then repeated to obtain the configuration that yields the minimum $/RPM.

The Structural analysis (ASTROS) needed information about the aerodynamic characteristics of the wing in the form of aerodynamic load distributions. The spanwise lift variation on the wing was provided to ASTROS from BDAP, while the chordwise C_l was assumed to vary linearly.

Once again, appropriate ranges were selected for each of the selected control/noise factors (assuming two levels, minimum and maximum), and a suitable orthogonal array was chosen. The aerodynamic simulations were calculated using BDAP, WINGDES, AWAVE, etc. Once the combined nacelle-wing-fuselage configuration geometry was defined (fuselage geometry remained fixed throughout the study), BDAP was called upon to predict the pressure distribution over the wing accounting for nacelle-wing and fuselage-wing interactions. These pressure distributions were then integrated to yield lift and drag due to lift. WINGDES was called to provide the optimum twist and camber distributions for the computed lift value, while the overall wing drag was calculated based on the skin friction and wave drag contributions computed by BDAP and AWAVE, respectively. The most significant aerodynamic design parameters determined from the aerodynamic design of experiments were used for the combined aero/structures experiment, and the corresponding wing weight was calculated. The overall result of this design of experiments was an "optimum" wing geometry ("Optimum" in a linear sense; the true optimum exists somewhere in between the two levels selected), and a lift and drag distribution that is used by FLOPS and ALCCA (Aircraft Life-Cycle-Cost Analysis) to minimize gross weight and $/RPM distributions, respectively.

An ASTROS preprocessor was used to create the file for each of the sixteen cases of the L_{16} using geometric, aerodynamic, and material information. Once the ASTROS runs were obtained, a post processor was used, along with the database created by ASTROS, to calculate the weights of the different wing components. These weights were then given to the manufacturing members of the team to calculate the cost of manufacturing. The information from aerodynamics, structures, and manufacturing was then used to obtain the "optimum" wing.

2.1.5.3 Manufacturing Implementation

Once ASTROS has calculated the material thicknesses and area deformations that satisfy the static loads, dynamic loads and flutter, Georgia Tech will use the Manufacturer's Trade Off Tool. This is based on the following equation:

$$\text{Cost} = \text{Weight}^{a} \text{ X } b + (\text{Weight X } c)/Q$$

Cost: Manufacturing cost in $

a Material Cost for each material type & manufacturing method.

b Manufacturing complexity for the appropriate type, method, precision and number of fabricated parts in a component.

c Tooling cost based on material density and fabrication technique.

Q Quantity of a given part produced for the first 500 units.

The weights for each individual rib, spar and skin panel are received from the calculations of the ASTROS postprocessor. They are quickly summed using the a spreadsheet to get a weight for the entire wing.

The spreadsheet is then used to find the cost distribution for the three different areas and the associated cost for each candidate material. This process is repeated to account for the 16 combinations. This information will then be forwarded to be used in the ALCCA program for life cycle cost and into FLOPS for its impact on a HSCT performance.

As an example case, the first experiment of the top level orthogonal array was chosen. Due to the time constraints, one of the sixteen configurations was chosen rather than analyzed as the "optimum" configuration from an aerodynamics point of view. The configuration was then analyzed with the manufacturers trade-off tool in a full factorial experiment (eight manufacturing possibilities) as displayed in Table XIX. This process will yield 128 OEC_is, 16 for each run from the top level orthogonal array.

Table XIX. Manufacturing Full Factorial Experiment

	Level 1	Level 2
Tolerance	0.005	0.001
Process	Forging	Machining
Quantity	10	30

Experiment	1	2	3	4	5	6	7	8
Tolerance	1	2	2	1	1	1	2	2
Process	1	2	1	2	1	2	1	2
Quantity	1	2	1	1	2	2	2	1

2.1.5.4 Synthesis/Propulsion/Economic Analysis

For the propulsion downselection study, two engine cycles were considered, the Mixed Flow TurboFan engine, and the Turbine Bypass Engine concept. NASA Lewis and NASA Langley have carried out similar studies trying to optimize the SFC, NOx emissions, noise levels, and thrust produced for these engines. This study had similar objectives testing each engine cycle after they have been integrated on the various candidate configurations and mission profiles. Once again, the Taguchi orthogonal array (design of experiments) technique was used to determine the best combination of engine parameters that yield an "optimum" $/RPM.

Table XX. Propulsion/Sizing/Economic Experiment Control Factors

Control Factors	Level 1	Level 2
Overall PR	18	25
Fan PR (only for MFTF)	2	4
comp. exit airflow ratio (only for TBE)	0.07	0.10
Turb. Inlet Temp.	2800 deg. R	3400 deg. R
ROI Airline	10%	14%
Utilization	4,000 hr.	6,000 hr.
Turn Around Time	2.0 hr.	0.75 hr.
MTTR	1/5,000 hr.	1/15,000 hr.

The experiment setup started, once again, with the identification of the key engine design variables to be considered as well as the selection of the appropriate ranges for them (minima and maxima). These design variables included such parameters as the bypass ratio, the fan and compressor pressure ratios, the turbine inlet temperature, the combustion chamber temperature, the turbine cooling flow, etc. These variables were considered as control factors for the design of experiments. From an economic viability point of view, the factors selected included the ROI for the airline, the aircraft utilization rate, the turn around ground time, and the mean time between repairs. This short list was chosen based on prior experience that the team acquired while carrying out a similar study at the conceptual design phase. The noise factors selected included the fuel cost price, the number of aircraft produced, and the manufacturer's learning curve. The selected list of

control and noise factors is presented along with their corresponding levels in Table XX and XXI.

Table XXI. Propulsion/Sizing/Economic Experiment Noise Factors

Factors	Level 1	Level 2
Fuel Cost	$0.09/lb.	$0.17/lb.
Production Quantity	400	700
Learning Curve	82%	90%

For these factors, the ROI for the manufacturer was set at 12%, and the engine acquisition price was allowed to vary as a function of Mach number, thrust, and technology factor. The engine acquisition price fell between 2.5 to 4 times greater than the engine acquisition price for current subsonic transports.

The actual simulation results were obtained from QNEP/FLOPS (Quick NASA Engine Program/FLight OPtimization System) and ALCCA. It was essential that the control/noise factors selected matched those used as inputs by these programs. Qualitek-4, a Taguchi software package, was used to perform the analysis of variance and obtain the "optimum" results and assess the risk associated with obtaining these values. Although QNEP/FLOPS and ALCCA are not integrated together, only one design of experiment is necessary (using a much larger orthogonal array) with an overall evaluation criterion at the system level given by the yield per revenue passenger mile.

Table XXII. "Optimal" Control Factor Settings

Control Factors	Level	Description	% Effective
OPR	1	18	0.63%
Comp. Ex. Airflow	2	0.10	pooled
Turb. Inlet Temp.	1	2800 deg R	4.69%
ROI airline	1	10%	15.89%
Utilization	2	6,000 hr.	74.49%
Turn Around Time	2	0.75 hr.	0.16%
Mean Time to Repair	2	1/5,000 hr.	2.85%

For the first feasible alternative design combination (top array), the analysis yielded the "optimal" control factor settings presented in Table XXII and Figure 53. These figures also illustrate the relative importance that each control factor has on the $/RPM criterion. Figure 54 illustrates the result distribution obtained by running the 32 cases in FLOPS and ALCCA. For the case where all of the top level orthogonal array variables were set to level 1, the $/RPM was found to be in the order of $0.128 / RPM.

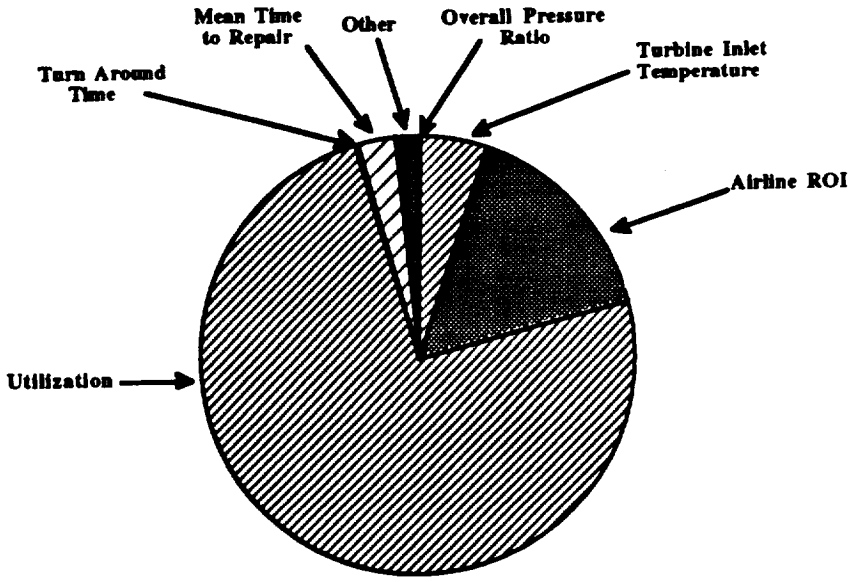

Figure 53: Significant Control Factor Influences on the System OEC, $/RPM

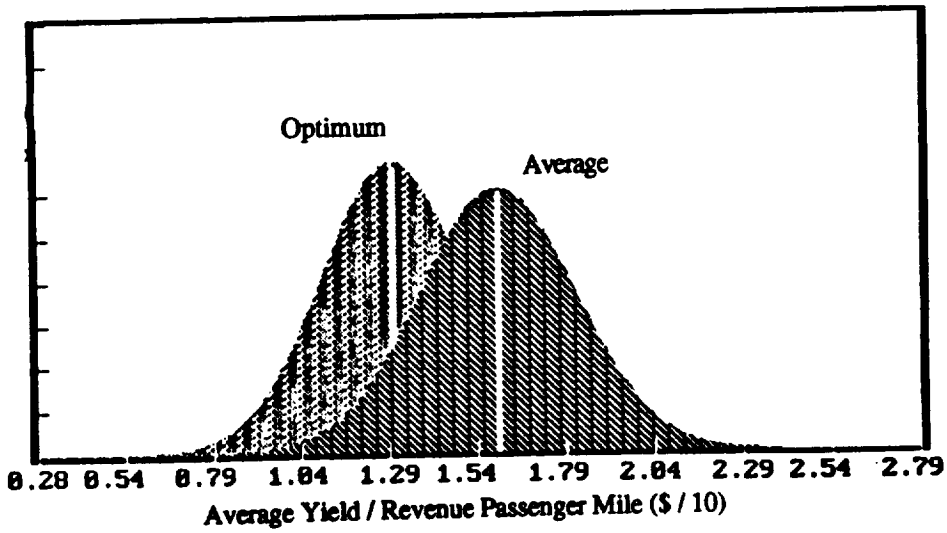

Figure 54: $/RPM Variations for the First Feasible Configuration of the Top Level Orthogonal Array Including the "Optimum" Distribution

2.1.6 Making a Decision

In order to design an experiment, it is necessary to select the most suitable orthogonal array, assign the factors to the appropriate columns, and describe the trial conditions. Through a series of brainstorming sessions, the various and relevant design variables that may be used as inputs by the selected simulation/analysis tools are determined. The next step is to design the experiments and choose the control and noise factor levels. Level 1 settings are chosen so as to represent low risk technologies, while level 2 settings correspond to medium risk technologies.

The feasible alternatives selected in step 4 of this methodology can now be evaluated through the use of a series of Taguchi experiments. The overall evaluation scheme is illustrated in Figure 55. Inspection of this figure indicates that all the feasible alternatives can be placed in a top decision matrix OA. For each and every one of the combinations identified from this array, an aerodynamics/structures and manufacturing example simulation is conducted to determine the "optimum" wing configuration, as well as the relative influence/importance that each of the design variables considered has on the wing OEC.

Once the "optimum" wing is selected, information related to its geometry, aerodynamic characteristics (C_L and C_D distributions, etc.), and weight (as a function of wing area) are passed to a synthesis/sizing code (FLOPS). Propulsion related (engine sizing) design variables are also selected to evaluate each of the feasible configurations at the system level. FLOPS sizes the aircraft and provides all the necessary aircraft related information to the ALCCA code, which computes the average yield per Revenue Passenger Mile. If noise factors are considered at this point (i.e. fuel price and production quantity), then a distribution of $/RPM is obtained, and the selection is based on obtaining a configuration that not only yields the minimum $/RPM but which also reduces the variation due to noise around this "optimum". Once all top level cases are calculated, an analysis of variance is conducted to determine which overall configuration yields the optimum $/RPM.

The new "optimum" design configuration, which will be identified once all experiments described in Figure 55 are performed, will then have to be subjected to a series of double-check tests to verify that all constraints are satisfied (NOx, noise, takeoff length, etc.) including a stability check. The stability and control check is essential since the empennage dimensions were selected based on chosen volume coefficients that may or may not be correct. Both the constraint and stability check will eventually include results obtained at takeoff, cruise, and landing.

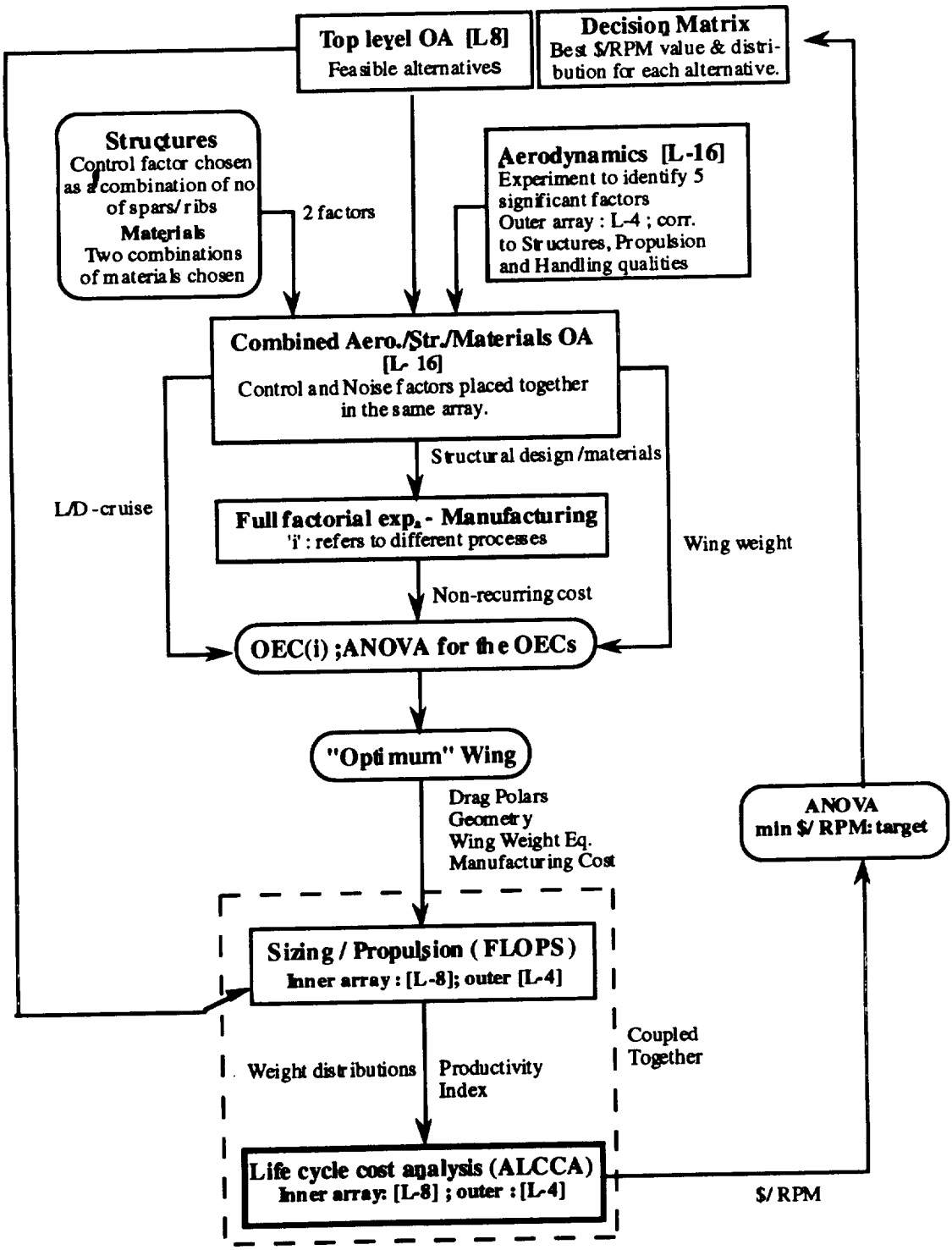

Figure 55: Concept Evaluation Experimental Schematic

The implementation of this methodology and the execution of all experiments presented for the determination of the "optimum" configuration will be the focus of next

year's design course sequence. The results will be presented at the annual ADP conference.

3.0 Conclusion - Future Work

The completion of the concept evaluation phase leads to the validation of the IPPD methodology, the shrinking of design space into 'optimal' regions, and the understanding of significant contributors and their effects. The knowledge obtained thus far can then be used in formal optimization schemes that have been developed for MultiDisciplinary Design Optimization. The use of Orthogonal Arrays (Taguchi Methods and the Combined Array method) make the extraction of sensitivities simpler. Future work shall focus on making use of the simplified model to derive Sensitivities and consequent application of Sobieski's Global Sensitivity Equation method and/or Response Surface Methodology. Since the methodology is well suited for the latter method, it will probably be explored to a greater extent.

The response-model/combined array approach has been used in this project to improve the computational efficiency for robust design by combining control and noise factors in a single array. Due to the scope of this project, the fitted response model only determines the coefficient of the main factors (control factors C and noise factors N) and the interactions between control factors and noise factors (CxN). Therefore, it is close to a first order polynomial approximation. Plus the fact that the experiment is only designed for 2 levels of each factor, it is difficult to capture the nonlinear behavior of the system, and, thus, the results obtained might not be an accurate one. To improve the accuracy of robust optimum, it is suggested to use second (or higher) order polynomial approximation for the response model in the future work. There is a formal technique called Response Surface Methodology (RSM) to support these activities[33].

Different from the traditional regression analysis, using RSM, a series of experiments are set up for measuring the response of interest. A model is then fitted based on the experiments results. In order to construct a second-order surface model, each design parameter must be analyzed at a minimum of three levels. The design for this experiment is called central composite design. Simply speaking, the central composite designs are the first order fractional factorial designs augmented by an additional "star" and "center"s which allow the estimation of a second order surface. Having obtained the response surface model, the mean and the variation of the response can be calculated, and the "optimum" design can be achieved based on the robust design criterion.

Overall, the benefit of using RSM in this work lies in the fact that this method allows for rapid exploration of the given parameter space and the determination of

sensitivities. In constrained robust optimization, it allows for easy modifications to the constraints bounds, without having to go back to perform additional experiment. This is very appropriate for the concept exploration of complex engineering systems such as aircraft.

Further work is also needed in each of the disciplinary contributing analysis to make the methodology more rigorous.

4.0 Appendix A

Strong Relations of the Product Planning Matrix & the Value Objectives Matrix

Product Planning Matrix

HOW	WHAT	WHY
Structural Life / Fatigue	Life Span	Obvious
High Lift / Drag Wing	Payload	More Lift allows for more payload.
Cruise Mach Number	T/O noise & Sonic Boom	The Higher the Mach #, the stronger the shock.
Cruise Mach Number	Low Fares	High the speed, the more Maintenance Needed - cost would be shifted to Pass.
Range / Gross Weight	Payload	Higher the GW, Higher the PL - Range Reduction.
Controlled Emissions	Exhaust Emissions	Obvious
Conventional Fuel	Low Total Operating Cost	Conventional Fuels - Less Expensive.
Engine Noise Suppressers	T/O noise & Sonic Boom	Obvious
Engine Noise Suppressers	Airport Regulations / ATC	Must meet FAR 36 Stage III
Engine Noise Suppressers	Comfort	Cabin Noise
Engine Choice	T/O noise & Sonic Boom	Higher Thrust means more Noise
Maintainability	Reliable Schedule	The easier it is to maintain, the more reliable the schedule will be.

Value Objectives Matrix

HOW	WHAT	WHY
Ticket Price	Cruise Mach Number	Higher the Speed, More Maintenance - Higher Fares.
Ticket Price	Conventional Fuel	Conventional Fuel Use - Lower Fares.
Resale Value	Advanced Materials	Use of Advanced Materials - Higher Resale Value.
Resale Value	Structural Life	Longer the Structural Life - Higher Resale Value.
Acquisition Cost	Advanced Materials	Advanced Materials - Higher Cost.
Acquisition Cost	Engine Choice	Engine Price greatly affects Total Cost.
Fuel Cost	High Lift / Drag Wing	Higher (L/D) - Less Fuel Needed.
Fuel Cost	Cruise Mach Number	Mach # < 2.6, Conventional Fuel use - lower cost.
Fuel Cost	Conventional Fuel Use	Conventional Fuels - Less Cost.
Fuel Cost	Low Specific Fuel Consumption	Higher the SFC - Higher the fuel Cost.
Maintenance Cost	Advanced Materials	Composites require more maintenance.
Maintenance Cost	Maintainability	Obvious
Payload	Range & Gross Weight	Higher the GW, Shorter the Range - Higher the PL.
Block Speed	Cruise Mach Number	Higher the Mach # - Higher the Block Speed.
Block Speed	Range & Gross Weight	Higher the GW, Shorter Range - Lower BS.
Empty Weight	Advanced Materials	Advanced Materials - Lower Empty Weight.
Empty Weight	Structural Life	Longer the Structural life - Higher the Empty Weight.
Empty Weight	Range & Gross Weight	Higher the GW, Shorter the Range - Higher Empty Weight.
Fuel Weight	High Lift / Drag	Higher L/D - Lower Wf
Fuel Weight	Cruise Mach Number	Higher Mach # - Higher Wf
Fuel Weight	Range & Gross Weight	Longer the Range - Higher the Fuel Weight.
Mean Time Between Failure	Structural Life	Longer the Structural Life - Longer the MTBF.
Mean Time Between Failure	Maintainability	Ease of Maintenance - Longer the MTBF.
Mean Time To Repair	Advanced Materials	Advanced materials - Greater the MTTR.

HOW	WHAT	WHY
Mean Time To Repair	High L/D wing	Thinner Wing - Greater the MTTR.
Mean Time To Repair	Serviceability	Greater Serviceability - Reduction in MTTR.
Maintenance Man Hour / Flight Hour	Serviceability	Greater serviceability - Decreased MMH/FH.
Turn Around Time	Serviceability	Greater serviceability - Decreased Turnaround Time

5.0 References

[1] Mavris, D., Brewer, J., and Schrage, D., *Economic Risk Analysis for a High Speed Civil Transport*, Presented at the 16th Annual Conference of the International Society of Parametric Analysts, Boston, MA, May 1994.

[2] *High Speed Civil Transport Study*, Boeing Commercial Airplanes, New Airplanes Development, NASA CR4233, 1989.

[3] Schrage, D. P., Mavris, D. N., *Integrated Design and Manufacturing for a High Speed Civil Transport*, AIAA93-3994, AIAA Aircraft Design, Systems and Operations Meeting, August 11-13, 1993, Monterey, CA.

[4] Mavris, D., Schrage, D., Marx, B., and Abel, R., *Integrated Design and Manufacturing for a High Speed Civil Transport*, Final Report for the NASA USRA ADP Program, June 1993.

[5] McCullers, L.A., *Flight Optimization System*, User's Guide, Version 5.41, NASA Langley Research Center, December 1993.

[6] Kusiak, A., *"Concurrent Engineering"*, John Wiley & Sons, Inc., 1993.

[7] Seidel, J., Haller, W., and Berton, J., *Comparison of Turbine Bypass and Mixed Flow Turbofan Engines for a High-Speed Civil Transport*, AIAA Aircraft Design Systems and Operations Meeting, Baltimore, MD, September 23-25, 1991.

[8] Schrage, D.P., & Rogan, J.E., *The Impact of Concurrent Engineering on Aerospace Systems Design:*, Introduction to Concurrent Engineering Course Notes, AE 8113, Fall Quarter, 1993, Georgia Institute of Technology.

[9] Alting, L., *Manufacturing Engineering Processes*, Second Edition, Revised and Expanded, Marcel Dekker, Inc, 1994.

[10] Alexander, J.M, Brewer, R.C., & Rowe, G.W., *Manufacturing Technology - Volume 2: Engineering Processes*, John Wiley & Sons, 1987.

[11] Crane, F.A.A, Charles, J.A., *Selection and Use of Engineering Materials*, Butterworths, 1984.

[12] Resetar, S.A., Curt Rogers, J., & Hess, R.W., *Advanced Airframe Structural MAterials - A Primer and Cost Estimating Methodology*, A Project Airforce Report, REF: R-4016-AF, RAND.

[13] Rogers, J. L., *DeMAID - A Design Manager's Aide for Intelligent Decomposition User's Guide*, NASA TM 101575, March 1989.

[14] Roskam, Jan, PhD., *Airplane Design - Part VIII: Airplane Cost Estimation: Design, Development, Manufacturing and Operation*, Roskam Aviation and Engineering Corporation, Ottawa, KS, 1990.

[15] Galloway, T.L. and Mavris, D.N., *Aircraft Life Cycle Cost Analysis (ALCCA) Program*, NASA Ames Research Center, September 1993.

[16] Bobick, J.C., Braun, R.L., and Denny, R.E., "Documentation of the Analysis of the Benefits and Costs of Aeronautical Research and Technology Models". Technical Report

submitted by SRI International to NASA Ames Research Center, Contract No. NAS2-10026, July 1979.

[17] Henderson, M., HSCT Project Manager, The Boeing Commercial Aircraft Group, *High Speed Civil Transport Program Review*, Seattle, WA.

[18] Bonner, E., Clever, W., and Dunn, K., *Aerodynamic Preliminary Analysis System II (APAS)*, Part I and II, NASA CR-182076, 1991.

[19] Roy, R., *A Primer on the Taguchi Method*, Van Nostrand Reinhold, New York, 1990.

[20] Roy, R., *Qualitek-4*, Automated Design and Analysis of Taguchi Experiments, NUTEK, Inc., Birmingham, MI, 1993.

[21] Middleton, W.D., Lundry, J.L., and Coleman, R.G., *A Computational System for Aerodynamic Design and Analysis of Supersonic Aircraft*, Boeing Commercial Airplane Company, NASA CR-2715-2717, Seattle, WA, 98124, August, 1976.

[22] Kachar, R.N., 1985, "Off-Line Quality Control, Parameter Design, and the Taguchi Method", *Journal of Quality Technology,* Vol. 17, 176-209.

[23] Phadke, M.S., 1986 "Design Optimization Case Studies", *AT&T Technical Journal,* Vol. 65, 51-84.

[24] Phadke, M.S., 1989, *Quality Engineering using Robust Design*, Prentice Hall, Englewood Cliffs, NJ.

[25] Yan, J., Rogalla, R. and Kramer, T., 1993, "Diesel Combustion and Transient Emissions Optimization using Taguchi Methods", Diesel Combustion Processes, SAE Special Publications, 89-102.

[26] Box, G., 1988, "Signal-To-Noise Ratios, Performance Criteria, and Transform-Actions", *Technometrics*, Vol. 30 no. 1, pp. 1-18.

[27] Tsui, K-L, 1992, "An Overview of Taguchi Method and Newly Developed Statistical Methods for Robust Design", *IIE Transactions*, Vol. 24 no. 5, 44-57.

[28] Nair, V.N., 1992 "Taguchi's Parameter Design: A Panel Discussion", *Technometrics,* May 1992, Vol. 34 no. 2), 127-161.

[29] Welch, W.J., Yu, T.K., Kang, S.M., and Sacks, J. (1990), "computer Experiments for Quality control by Parameter Design", *Journal of Quality Technology*, 22, 15-22.

[30] Shoemaker, A.C., Tsui, K_L, Wu, J. (1991), "Economical Experimentation Methods for Robust Design", *Technometrics*, 33(4), 415-427.

[31] ASTROS User Manuals, Flight Dynamics Laboratory, Wright-Patterson Air Force Base, December 1988.

[32] Request For Proposal for Student Design Competition, *Designer's Manufacturer's Trade Tool,* Appendix 2, 1992.

[33] Khuri, A., I. and Cornell, J.A., 1987, *Response Surfaces: Designs and Analysis*, Marcel Dekker Inc., New York, NY.

Additional References

Hoskin, Brian and Alan Baker. *Composite Materials for Aircraft Structures.* AIAA, New York, New York, 1986.

The Navy/NASA Engine Program - A User's Manual, NASA Lewis Research Center, August 1991.

Karbhari, V.M. and Kukich, D.S. (1994) "Debunking the Myth: Concurrent Engineering for Composites as a Reality and Not a Management Philosophy," *International Journal of Materials and Product Technology*, Vol. 9, Nos 1/2/3, pp 79-104.

Brookstein, D. (1994) "Concurrent Engineering of 3-D Textile Preforms for Composites," *International Journal of Materials and Product Technology*, Vol. 9, Nos 1/2/3, pp 116-124.

Cohen, S. E., Graves, C. T., Bernardon, E. and West, H. (1994) "Design of a New Composite Forming Process Using a Formal Design Methodology," *International Journal of Materials and Product Technology*, Vol. 9, Nos 1/2/3, pp 23-41.

Stubbs, N. and Diaz, M. (1994) "Impact of QFD utilization in the Development of a Nondestructive Damage Detection system for Aerospace Structures," *International Journal of Materials and Product Technology*, Vol. 9, Nos 1/2/3, pp 3-22.

Karbhari, V. M., Henshaw, J. M., Wilkins, D. J. and Munson-McGee, S. (1992) "Composites - Design, Manufacturing and Other Issues: a View Towards the Future," *International Journal of Materials and Product Technology*, Vol. 7, No 1, pp 13-37.

Merhar, C., Chong, C. and Ishii, K. (1994) "Simultaneous Design for Manufacturing Process Selection of Engineering Plastics," *International Journal of Materials and Product Technology*, Vol. 9, Nos 1/2/3, pp. 61-78.

Messimer, S. L. and Henshaw, J. (1994) "Composites Design and Manufacturing Assistant," *International Journal of Materials and Product Technology*, Vol. 9, Nos 1/2/3, pp. 105-115.

Barkan, Philip, and Hinckley, C. Martin, "The Benefits and Limitations of Structured Design Methodologies," *Manufacturing Review*, Vol. 6 No. 3, Sept., 1993.
"Industry Outlook - New High Temperature Resin," *Aviation Week and Space Technology*, April 11, 1994, p. 13.

"Composites May Cut Cost," *Aviation Week and Space Technology*, Jan. 24, 1994, p. 53.

Ayres, Robert U. and Butcher, Duane C., "The Flexible Factory Revisited," *American Scientist*, Vol. 81, Sept.-Oct. 1993, pp. 448-459.

Niu, Michael, C. Y., *Composite Airframe Structures: Practical Design Information and Data*, Conmilit Press Ltd., 1992.

Wells, James S. and Ward, Clay A., *HSR Task 23: High Speed Research Program Metrics, Final Report*, McDonnell Douglas Aerospace, NASA Contract NAS1-19345, Feb., 1994.

NASA, NAS2-5718, *OAST Advanced Concepts and Missions Division, Estimation of Airframe Manufacturing Costs: Final Report*, Vol. II, July, 1972.

"How to Build an Airliner," *Airlines*, Spring 1994, pp. 39-47.

Brunner, Michael D., and Velicki, Alex, *Study of Materials and Structures for High Speed Civil Transport*, NAS1-18862, McDonnell Douglas Aerospace Transport Aircraft, Long Beach, September 1993.

Resetar, Susan A., Rogers, J. Curt, and Hess, Ronald W., *Advanced Airframe Structural Materials: A Primer and Cost Estimating Methodology*, a United States Air Force Rand Report, R-4016-AF.

Niu, Michael C. Y., *Airframe Structural Design*, Burbank, CA, Conmilit Press Ltd., 1988.

Georgia Institute of Technology, School of Aerospace Engineering, *Design for Life Cycle Cost, AE 4353 Course Notes*, Winter Quarter 1994, Atlanta GA, 1994.

Jaikumar, Ramchandran, "Postindustrial Manufacturing," *Harvard Business Review*, November-December, 1986, pp. 69-75.

Hoskin, Brian C. and Baker, Alan A., *Composite Materials forAircraft Structures*, American Institute of Aeronautics and Astronautics, 1986.

Wiles, Greg, Georgia Tech CIMS/MOT Seminar, Manufacturing Research Center Auditorium, 4:30 p.m., May 2, 1994.

Nelson, R., *Flight Stability and Automatic Control* , McGraw-Hill Inc., New York, NY, 1989.

Etkin, B., *Dynamics of Flight - Stability and Control* , John Wiley and Sons, Inc., New York, NY, 1982.

Rogers, J. L., *A Knowledge-based Tool for Multilevel Decomposition of a Complex Design Problem*, NASA TP 2903, January 1989.

Kulfan, Robert M., *High Speed Civil Transport Opportunities, Challenges and Technology Needs*, 34th National Conference on Aeronautics and Astronautics, Nov. 1992.

Brunner, M.D., Velicki, A., *Study of Materials and Structures for High Speed Civil Transport*, McDonnell Douglas Aerospace, Contract NAS1-18862, September 1993.

Schrage, D.P., and Mavris, D.N., *Integrated Design andManufacturing for the High Speed Civil Transport*, Georgia Institute of Technology.

Autonomous Scout Rotocraft Testbed, Ref: GIT No: AERO-94-1033, Georgia Institute of Technology.

"nformation Technology and Manufacturing - A Preliminary Report on Research Needs, Computer Science and Telecommunications Board, Manufacturing Studies Board, National Research Council, 1993.

Calkins, D.E., et al, *Aerospace Systems Unified Life Cycle Engineering Producibility Measurement Issues*, Institute of Defense Analyses, IDA Paper P - 2151, May 1989.

Konig, I.W, *Applied research on the Machinability of Titanium and its Alloys*, Advanced Fabrication Processes, AGARD Conference Proceedings No. 256, 1978.

Stacher, G.W., & Weisert, E.D., *Concurrent Superplastic Forming/Diffusion Bonding on B-1 Components*, Advanced Fabrication Processes, AGARD Conference Proceedings No. 256, 1978.

Marx, W.J., Mavris, D.N., & Schrage, D.P., *Integrating Design and Manufacturing for a High Speed Civil Transport Wing*, Georgia Institute of Technology, 1994.

Technology for Affordability, The National Center for Advanced Technologies, January 1994.

Tien, J.K., et al, *Advances in Superalloys and High Temperatures Intermetallics*, Advanced Topics in Materials Science and Engineering, Edited by Lopez, J.L., & Sanchez, J.M., 1993.

Sakata, I.F., Davis, G.W., *Arrow-Wing Supersonic Cruise Aircraft Structural Design Concepts Evaluation*, NASA Contract No. NAS1-12288, October 1975.

Hollowell, S.J., Beeman II, E.R., & Hiyama, S.J., *Conceptual Design Optimization Study*, NASA Contract NAS1-18015, 1990.